

# Automated Algorithmic Discovery for Gravitational-Wave Detection Guided by LLM-Informed Evolutionary Monte Carlo Tree Search

He Wang<sup>1,2\*</sup> and Liang Zeng<sup>3\*</sup>

<sup>1</sup>International Centre for Theoretical Physics Asia-Pacific,  
University of Chinese Academy of Sciences, 100190, Beijing,  
China.

<sup>2</sup>Taiji Laboratory for Gravitational Wave Universe, University of  
Chinese Academy of Sciences, 100049, Beijing, China.

<sup>3</sup>Tsinghua University, 100084, Beijing, China.

\*Corresponding author(s). E-mail(s): [hewang@ucas.ac.cn](mailto:hewang@ucas.ac.cn);  
[zengliangcs@gmail.com](mailto:zengliangcs@gmail.com);

## Abstract

Gravitational-wave signal detection with unknown source parameters buried in dynamic detector noise remains a formidable computational challenge. Existing approaches face core limitations from restrictive assumptions: traditional methods rely on predefined theoretical priors, while neural networks introduce hidden biases and lack interpretability. We propose Evolutionary Monte Carlo Tree Search (Evo-MCTS), the first integration of large language model (LLM) guidance with domain-aware physical constraints for automated gravitational wave detection. This framework systematically explores algorithmic solution spaces through tree-structured search enhanced by evolutionary optimization, combining MCTS for strategic exploration with evolutionary algorithms for solution refinement. The LLM component provides domain-aware heuristics while maintaining interpretability through explicit algorithmic pathway generation. Experimental validation demonstrates substantial performance improvements, achieving a 20.2% improvement over state-of-the-art

gravitational wave detection algorithms on the MLGWSC-1 benchmark dataset and a remarkable 59.1% improvement over other LLM-based algorithm optimization frameworks. Beyond performance improvements, our framework establishes a transferable methodology for automated algorithmic discovery across computational science domains.

## 1 Introduction

The pursuit of scientific discovery increasingly demands computational approaches that can navigate complex, high-dimensional data spaces while maintaining physical interpretability [1–4]. In gravitational wave astronomy, this computational challenge manifests as a fundamental algorithmic problem: detection systems must identify faint astrophysical signals buried in detector noise while leveraging theoretical predictions from general relativity [5, 6], yet remain adaptable to unexpected signal morphologies that could reveal new physics beyond current theoretical models.

Gravitational wave detection serves as an exemplary case study for automated algorithm discovery, embodying the fundamental tension between model-driven precision and data-driven flexibility [7]. Current methodologies represent three complementary yet insufficient paradigms: Matched filtering techniques [8, 9] achieve optimal sensitivity under Gaussian stationary noise assumptions but critically depend on accurate prior knowledge of signal morphologies. Non-template methods [10] offer model-independent detection but sacrifice sensitivity for generality. Deep neural networks [11–13] provide computational efficiency but operate as black-box architectures that obscure decision-making logic and introduce hidden biases [14]. Each paradigm represents different trade-offs between sensitivity, generality, and interpretability, yet none adequately addresses the challenge of discovering novel algorithmic approaches that could transcend these traditional limitations.

The fundamental bottleneck in modern scientific computing is algorithmic sophistication rather than computational power or data availability [3, 4]. Current gravitational wave detection pipelines represent decades of manual engineering yet still miss potentially discoverable signals due to three critical limitations: (i) *combinatorial explosion* of possible signal processing combinations that exceeds human exploration capacity [15, 16], (ii) *cognitive biases* that constrain designers to familiar paradigms [17], and (iii) *local optimization traps* where manual refinement leads to incremental improvements while missing global optima [18]. These limitations necessitate automated algorithm discovery approaches that can navigate vast design spaces while maintaining scientific rigor.

Automated algorithm discovery in scientific domains presents unique challenges requiring simultaneous navigation of *semantic coherence* (algorithms must respect physical laws), *exploration efficiency* (vast search spaces with

expensive evaluations), and *interpretability preservation* (discoverable and validatable by experts). The interdependent nature of these challenges suggests effective solutions must address all three simultaneously. Large Language Models (LLMs) emerge as natural candidates for semantic coherence, having been trained on scientific literature and capable of incorporating domain knowledge directly into code generation [19, 20]. Monte Carlo Tree Search (MCTS) provides structured exploration framework, creating hierarchical memory while balancing exploration with exploitation [21–23]. Their synergy creates a self-reinforcing cycle: LLMs provide semantic understanding and domain knowledge integration, MCTS provides structured exploration and cumulative learning, enabling evolutionary operations that preserve algorithmic coherence while systematically exploring scientific algorithm spaces.

Existing approaches to algorithm discovery span multiple paradigms. Traditional approaches including genetic programming [24], neural architecture search [15], and evolutionary computation [16] suffer from critical limitations: generating syntactically invalid code, lacking domain knowledge integration, or focusing on network topology rather than algorithmic logic. Recent advances have integrated LLMs with structured search and evolutionary methods, including FunSearch [25], EoH [26], AEL [27], ReEvo [28], and MCTS-AHD [29] for algorithm discovery, which combine LLMs’ code generation capabilities with systematic optimization frameworks. However, the existing LLM-based frameworks focus on combinatorial optimization tasks with discrete decision sequences and well-defined mathematical formulations. Scientific signal processing problems like gravitational wave detection present fundamentally different challenges, requiring continuous parameter optimization, domain-specific physical constraints, and interpretable algorithmic pathways that can be validated against theoretical predictions.

We propose Evo-MCTS (Evolutionary Monte Carlo Tree Search), a framework that realizes synergistic integration through three key innovations: (i) *Reflective Code Synthesis* that leverages LLM domain knowledge for performance-driven algorithm generation, adapting to optimization landscapes while maintaining scientific validity, (ii) *Multi-Scale Evolutionary Operations* (Parent/Sibling/Path-wise Crossover, Point Mutation) that operate on structured code representations through MCTS tree traversal, enabling semantic-aware algorithmic transformations, and (iii) *Interpretable Algorithm Pathways* that emerge naturally from the tree structure, enabling post-hoc analysis of algorithmic evolution while providing cumulative learning for future discoveries. The framework addresses interdependent challenges through architectural design—each element enhances others’ capabilities while compensating for individual limitations.

We demonstrate Evo-MCTS effectiveness through comprehensive evaluation on gravitational wave detection benchmarks, achieving a 20.2% improvement over state-of-the-art algorithms on the MLGWSC-1 benchmark dataset and a remarkable 59.1% improvement over other LLM-based algorithm optimization frameworks. The framework demonstrates systematic breakthrough

discoveries across independent executions, with high-performing variants consistently incorporating sophisticated signal processing techniques including Multi-resolution Thresholding, Continuous Wavelet Transform with Ricker wavelets, Tikhonov Regularization, and Curvature Boosting, among others. These discoveries generate human-interpretable algorithmic pathways that reveal distinct performance patterns organized by functional categories, identifying novel algorithmic combinations that human designers might overlook while providing empirical guidance for component selection in complex signal processing pipelines.

Beyond gravitational wave astronomy, this work establishes a general paradigm for AI-guided algorithmic discovery in scientific computing. The Evo-MCTS framework’s ability to generate interpretable algorithmic pathways while maintaining high performance makes it particularly valuable for scientific applications where understanding algorithmic reasoning is as important as achieving optimal performance. Our approach opens new avenues for automated scientific discovery across physics, chemistry, biology, and engineering disciplines, providing a transferable methodology that respects domain-specific constraints while systematically exploring algorithmic possibilities beyond human intuition.

## 2 Results

### 2.1 Framework Architecture for Automated Algorithm Discovery

**Algorithmic Discovery Pipeline.** The Evo-MCTS framework systematically transforms raw time-series data into a comprehensive catalog of optimized detection algorithms through an automated discovery pipeline that integrates domain knowledge encoded in large language models (Figure 1a, see Methods Section 4.1 for formal problem definition). To understand this automated transformation process, the framework can be conceptualized through two complementary perspectives (Figure 1b): as an MCTS-guided tree search where nodes represent complete algorithmic implementations and edges encode LLM-driven transformations (detailed implementation in Methods Section 4.2), or as an evolutionary algorithm where populations of algorithms undergo sophisticated selection, crossover, and mutation operations guided by domain knowledge (detailed implementation in Methods Section 4.3).

**MCTS-Guided Evolutionary Exploration.** The core innovation of our Evo-MCTS framework lies in reformulating algorithm design as a tree search problem, where each node represents an executable algorithm and edges correspond to code transformations (Figure 1c). Starting from a seed algorithm, the framework employs four specialized evolutionary operations to expand the search tree:

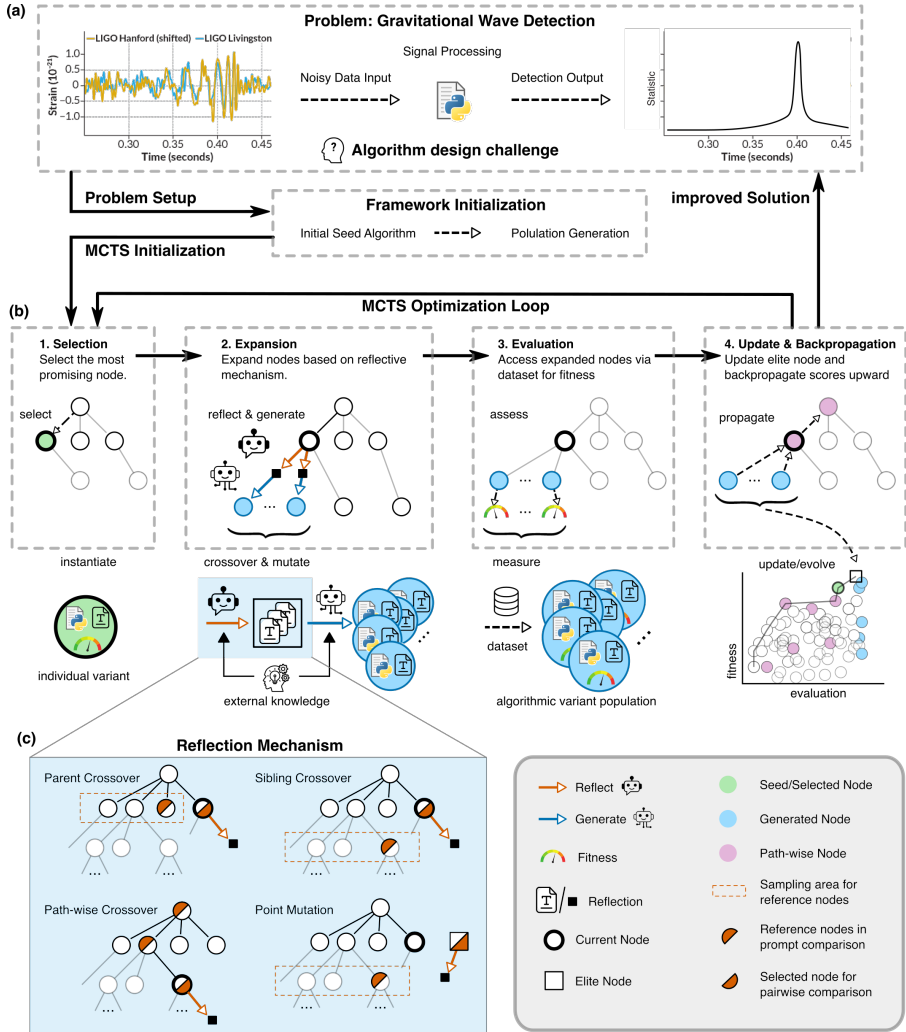


**Fig. 1 LLM-Informed Evolutionary Monte Carlo Tree Search Framework for Automated Algorithm Discovery.** (a) Overview of the algorithm discovery pipeline. Starting from raw gravitational wave strain data (left), the framework applies automated algorithmic transformations through LLM-generated code synthesis (center) to produce optimized detection statistics (right). (b) Core architectural components showing the integration of MCTS exploration with evolutionary optimization through dual perspectives of tree search and population evolution. (b.1) UCT-based node selection from initial algorithmic variants including seed algorithms and individual variants, each represented as nodes containing baseline signal processing code. (b.2) MCTS expansion phase where new algorithmic variants are generated through evolutionary operations. Each node contains executable Python code implementing specific detection strategies. (b.3) Algorithm evaluation phase where generated variants are tested against benchmark data to compute fitness scores, determining performance-based selection for subsequent iterations. (b.4) MCTS backpropagation and elite node updates after multiple evolutionary cycles, propagating performance feedback through the tree structure and maintaining diverse high-performing detection strategies. (c) Detailed view of the reflection mechanism during MCTS expansion, showing four evolutionary operations: Parent Crossover, Sibling Crossover, Path-wise Crossover, and Point Mutation.

- *Parent Crossover (PC)*: Combines algorithmic features from parent nodes to generate offspring that inherit successful detection strategies while exploring new combinations.
- *Sibling Crossover (SC)*: Enables horizontal knowledge transfer between algorithms at the same tree depth, promoting diversity while maintaining comparable complexity levels.
- *Path-wise Crossover (PWC)*: Synthesizes information across complete root-to-leaf trajectories, capturing long-range dependencies and enabling global optimization strategies.
- *Point Mutation (PM)*: Introduces targeted modifications to individual algorithms based on performance analysis, leveraging insights from elite algorithms to enable fine-grained optimization of specific components.

These operations are fundamentally different from traditional genetic algorithms because they operate on structured code representations rather than abstract encodings, and modifications are guided by LLM-based reasoning rather than random perturbations (see Methods Section 4.3 and Supplementary Material A.1 for operation details).

**Reflection-Driven Code Synthesis.** Central to the Evo-MCTS framework’s effectiveness is the reflection mechanism that analyzes algorithm performance patterns and guides subsequent explorations (Figure 1b-(2) and Figure 1c). This dual-component system comprises: (i) a performance reflection module that identifies strengths and weaknesses in current algorithms through systematic evaluation across diverse signal conditions, and (ii) a code synthesis module that leverages these insights to generate improved implementations (An example is shown in Figure 2). The reflection process operates at multiple scales—from individual algorithmic components to complete detection pipelines—ensuring both local optimization and global coherence (detailed prompts and examples in Supplementary Information Section A.1).

## 2.2 Performance Benchmarking on MLGWSC-1 Dataset

We evaluated our Evo-MCTS framework’s algorithmic discovery capabilities using the first official Machine Learning Gravitational-Wave Search Mock Data Challenge (MLGWSC-1) benchmark dataset [30]—an internationally recognized and rigorous evaluation standard established by the gravitational wave detection community. The MLGWSC-1 benchmark represents a comprehensive and challenging assessment framework that includes mock detector data with simulated gravitational wave signals embedded in realistic detector noise, enabling systematic comparison of detection algorithms across diverse signal morphologies and noise conditions.

**Framework Adaptation for Domain-Specific Evaluation.** Figure 3a illustrates the Evo-MCTS framework’s adaptation to the MLGWSC-1 evaluation protocol, showcasing the critical integration between automated algorithm generation and standardized performance assessment. The system transforms

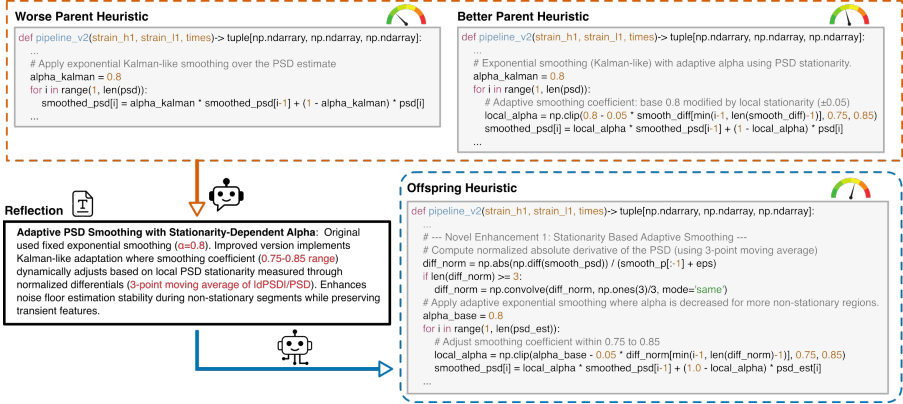


**Fig. 2 LLM-Driven Algorithmic Evolution Through Reflective Code Synthesis.** Demonstration of a single Parent Crossover evolutionary step showing the transformation from two parent algorithms to an enhanced offspring algorithm. **(Top row)** Code segments from two parent nodes highlighting complementary algorithmic components that will be combined through the crossover operation. **(Bottom left, black box)** Reflective analysis process showing how the LLM identifies strengths and limitations in the parent algorithms, synthesizing insights about their respective detection strategies and potential synergies. **(Bottom right)** Generated offspring algorithm code incorporating successful elements from both parents while addressing identified limitations through domain-aware synthesis. This example illustrates the framework’s capability to generate physically-motivated algorithmic improvements through automated reasoning, demonstrating how LLM-guided reflection enables discovery of sophisticated signal processing techniques by combining and enhancing existing algorithmic components without manual intervention. The complete reflection prompts and additional evolution examples are provided in Supplementary Material A.1.

raw dual-channel strain data through our evolved algorithms, producing detection catalogs that are evaluated against the ground truth signal catalog. The evaluation pipeline incorporates the area under the curve (AUC) metric as the primary performance indicator, computed from sensitivity distance versus false alarm rate curves spanning 4-1000 events per month. This comprehensive metric balances detection sensitivity against false alarm rates—a critical trade-off in gravitational wave detection applications—ensuring that algorithmic optimization targets practical deployment requirements rather than narrow performance metrics (detailed experimental configuration provided in Methods Section 4.5).

### Progressive Complexity and Performance Improvements.

Figure 3b presents the comprehensive optimization trajectory across 877 total evaluations from five independent Evo-MCTS runs, revealing systematic algorithmic discovery with progressive increases in both algorithmic sophistication and detection performance. The optimization process exhibits four distinct phase transitions (PT 1-4), each marking algorithmic breakthroughs that represent the discovery of increasingly sophisticated algorithmic components building upon previous innovations. The combined fitness trajectory demonstrates the framework’s capability to navigate the complex algorithmic design space while maintaining consistent improvement patterns across multiple

independent runs, systematically exploring and integrating complex detection strategies (detailed analysis of algorithmic evolution patterns provided in Supplementary Material A.3).

**Maintaining Solution Diversity while Converging toward Optimal Performance.** The diversity analysis reveals sophisticated exploration patterns that balance algorithmic variety with performance optimization throughout the search process. Peak diversity occurs during the intermediate optimization phase between PT 2 and PT 3, where both Shannon diversity index and Complexity Index of Diversity reach maximum values, indicating the framework maintains diversity in both component selection and structural complexity while systematically exploring combinations of successful components before converging on optimal configurations. Fitness-stratified analysis demonstrates systematic convergence: diversity decreases progressively from broad initial exploration in lower-performing variants to focused refinement in highest-performing configurations, confirming effective balance between exploration and exploitation (diversity metric definitions and computational details provided in Methods Section 4.5).

**Superior Performance Against State-of-the-Art Methods.**

Figure 3c demonstrates the Evo-MCTS framework’s superior sensitivity performance against seven benchmark gravitational wave detection algorithms on MLGWSC-1, Set 4 dataset. The PT-4 configuration achieves a 20.2% improvement over state-of-the-art methods including Sage [14], Virgo-AUTH [30, 31], PyCBC [30, 32], TPI FSU Jena [30, 33], cWB [30, 34], MFCNN [30, 35], and CNN-Coinc [30, 36, 37]. Most significantly, at the stringent low false alarm rate of approximately 4 events per month—the regime most critical for confident astrophysical detection—PT-4 achieves a 23.4% performance improvement over the highest-performing benchmark (Sage), with progressive algorithmic sophistication demonstrated through four milestone configurations (PT-1 through PT-4) across the false alarm rate range of 4-1000 events per month (detailed performance metrics provided in Supplementary Material A.3).

**Interpretable Nonlinear Algorithm Discovery.** The systematic improvement from PT-1 to PT-4 demonstrates our framework’s capability to discover sophisticated nonlinear filtering algorithms that surpass traditional approaches across different algorithmic paradigms. While traditional matched filtering pipelines like PyCBC [32] represent the theoretical optimum for Gaussian stationary noise conditions [9, 38], real detector noise exhibits non-Gaussian and non-stationary characteristics that limit the effectiveness of linear correlation operations despite incorporating nonlinear post-processing stages [39, 40]. Our evolved algorithms achieve superior performance through intrinsically nonlinear transformations that adapt dynamically to these realistic noise conditions, effectively addressing the fundamental limitations of matched filtering in practical detector environments [5, 6].

Compared to coherent WaveBurst (cWB) [10, 41], which shares our template-free philosophy and employs nonlinear wavelet-based detection methods, our framework demonstrates the effectiveness of systematic algorithmic

exploration over heuristic design approaches. Both methods recognize that optimal detection strategies must transcend linear processing assumptions, but our automated discovery process identifies algorithmic configurations that cWB’s manually-designed heuristics cannot achieve. The performance gains reflect the fundamental advantage of exhaustive exploration over expert intuition in complex optimization landscapes [26, 42].

Furthermore, our framework achieves a 20.2% performance improvement over state-of-the-art AI-based methods despite their inherent nonlinear processing capabilities, demonstrating that interpretable algorithmic discovery can achieve superior detection performance while maintaining complete transparency in decision logic. Unlike deep learning approaches that operate as black boxes with millions of parameters [43], our evolved algorithms provide explicit mathematical formulations that enable physical interpretation of detection mechanisms [44, 45]. This interpretability advantage, combined with the progressive complexity enhancement observed across phase transitions, establishes the framework’s capability to discover sophisticated yet transparent algorithmic solutions that bridge the gap between model-driven precision and data-driven flexibility (detailed quantitative analysis and algorithmic specifications provided in Supplementary Material A.3).

## 2.3 Interpretability Analysis

### 2.3.1 Algorithm Performance and Generalization Analysis

**Generalization capability and robustness of optimized algorithms.** We evaluated 877 algorithmic configurations on an independent 1-day test dataset, distinct from the 7-day training corpus, under a 0.2-second trigger arrival time uncertainty constraint to assess robustness and interpretability (data specifications in Supplementary Material A.2).

Figure 4a demonstrates strong training-test performance correlation ( $r = 0.84$ ) across all algorithms, with each point representing AUC-based fitness scores for individual configurations. This correlation validates robust generalization despite significant domain shift between datasets, with performance variation reflecting the non-stationary, non-Gaussian noise characteristics inherent in realistic gravitational wave detection environments. The 0.2-second timing constraint ensures temporal precision essential for astrophysical parameter estimation while preserving detection sensitivity, empirically determined through systematic constraint-correlation analysis (Supplementary Material A.4). These results confirm that optimized algorithms achieve genuine performance improvements transferable to independent datasets, validating our evolutionary framework’s practical utility for real-world gravitational wave detection applications.

**MCTS Depth-Stratified Performance Analysis.** We analyzed the relationship between MCTS tree depth and algorithm fitness across optimization phases. Figure 4b reveals systematic evolution patterns in performance and generalization capability.

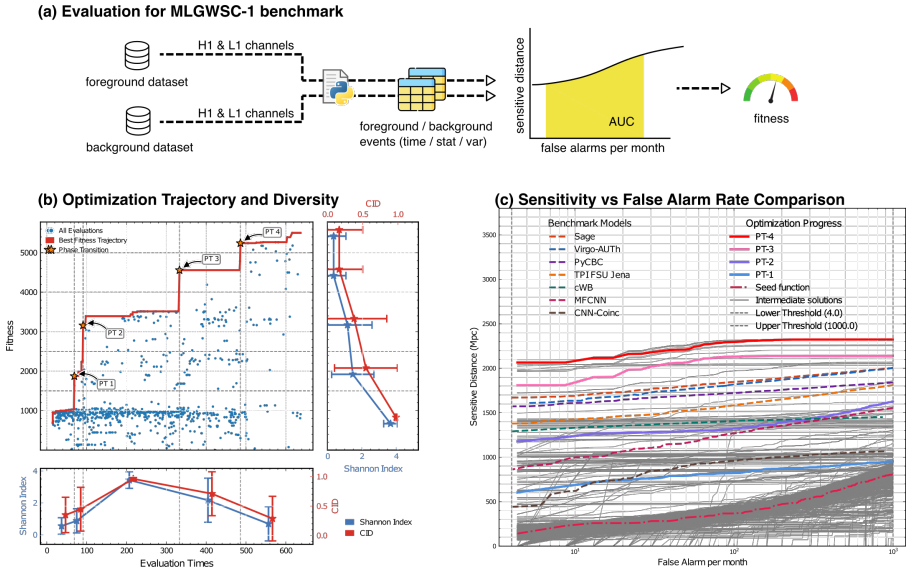


**Fig. 3 Comprehensive Performance Analysis on MLGWSC-1 Benchmark Dataset.** (a) Evo-MCTS framework adaptation pipeline showing domain-specific fitness evaluation using area under the curve (AUC) metric for sensitivity distance versus false alarm rate curves, demonstrating integration with standardized gravitational wave detection evaluation protocols. The pipeline processes dual-channel strain data from Hanford(H1) and Livingston(L1) detectors through evolved algorithms to produce detection statistics evaluated against ground truth catalogs. (b) Objective optimization trajectory and diversity analysis across 877 evaluations from 5 independent Evo-MCTS runs. Combined fitness trajectory (blue dots) with best objective envelope (red line) showing four phase transitions (PT 1-4, orange stars) marking algorithmic breakthroughs with fitness gains  $\geq 400$  units. Maximum fitness of 5,241 units achieved, representing 6-fold improvement from baseline. Diversity metrics include Shannon diversity index (blue, left axis) and Complexity Index of Diversity (CID, red, right axis) with error bars showing standard deviation across runs. Right panel shows fitness-stratified diversity analysis revealing systematic exploration patterns across performance levels. (c) Sensitivity versus false alarm rate comparison on MLGWSC-1, Set 4 dataset. Optimization milestones PT-1 through PT-4 show progressive improvement, with PT-4 achieving AUC of 5,241 units outperforming seven benchmark algorithms (Sage, Virgo-AUTh, PyCBC, TPI FSU Jena, cWB, MFCNN, CNN-Coinc). Grey curves represent intermediate solutions explored during optimization, while red dotted line shows seed function baseline. Vertical dashed lines indicate evaluation range boundaries (4-1000 events per month). Results demonstrate systematic algorithmic discovery with superior sensitivity performance, controllable thresholds, and clear interpretability through progressive complexity enhancement. The optimization process systematically explored diverse parameter spaces while converging toward optimal configurations, integrating nonlinear transformations, adaptive parameter selection, and sophisticated statistical analysis methods that remain fully interpretable throughout the discovery process.

The analysis demonstrates clear progression in algorithmic quality through successive phase transitions. During PT1, algorithms are predominantly in shallow depth groups with modest fitness values ( $< 2,000$ ). As optimization progresses to PT2 and PT3, high-performing algorithms (fitness  $> 3,000$ ) increasingly emerge in deeper tree layers, indicating successful identification and refinement of promising algorithmic directions.

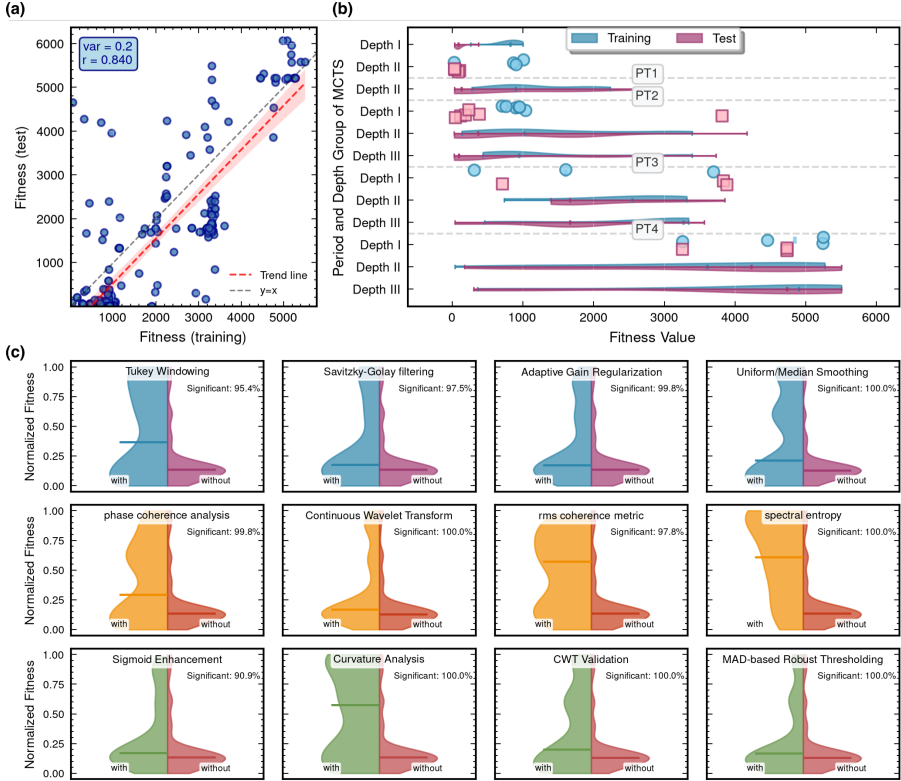


**Fig. 4 Comprehensive Algorithm Performance Analysis.** (a) Training versus test performance correlation for 877 algorithmic configurations evaluated under 0.2-second trigger arrival time uncertainty constraint. Each point represents an individual algorithm’s AUC-based fitness scores on training (7-day dataset) and test (1-day independent dataset) data. Linear correlation coefficient  $r = 0.840$  indicates strong generalization capability, while variance reflects expected performance variation due to non-stationary, non-Gaussian noise characteristics. Red dashed line shows the empirical trend relationship, while grey dashed line represents perfect correlation ( $y=x$ ). High-performing algorithms (fitness  $> 4000$ ) demonstrate particularly robust generalization across different noise realizations and signal parameters. (b) MCTS depth-stratified performance analysis across optimization phases. Fitness distribution of algorithms organized by MCTS tree depth groups (Depth I: depths 1-4, Depth II: depths 5-7, Depth III: depths 8-10) and phase transitions (PT1-PT4). Training performance (teal) and test performance (pink) are shown with violin plots for sample sizes  $n \geq 10$  and scatter plots (circles/rectangles) for  $n < 10$ . The analysis reveals systematic migration of high-fitness algorithms toward deeper tree layers as optimization progresses, with elite algorithms (fitness  $> 5,000$ ) emerging exclusively in deeper layers during PT4. Enhanced generalization capability is observed in deeper layers during later optimization phases, as evidenced by improved training-test performance alignment in Depth III compared to shallower depth groups. (c) Algorithmic component impact analysis. Violin plots comparing normalized fitness distributions between algorithms with specific techniques (left) versus without (right). Techniques categorized as conditioning methods (teal), time-frequency analysis (orange), and trigger detection (green). Technique effectiveness is determined by distributional separation: wider gaps between left and right distributions indicate stronger performance impact. Conditioning techniques (Savitzky-Golay filtering, Adaptive Gain Regularization) and trigger detection methods (Curvature Analysis, Continuous Wavelet Transform Validation) demonstrate the most substantial improvements through clear distributional shifts toward higher fitness values. Statistical validation across 1,000 resampling iterations confirms significance ( $p < 0.001$ ) and practical importance.

Elite algorithms (fitness  $> 5,000$ ) emerge exclusively in deeper tree layers during PT4, suggesting sophisticated solutions require extensive refinement through multiple decision levels. Training (teal) and test (pink) performance distributions show robust generalization across all depth groups, with algorithms maintaining relative performance rankings regardless of tree depth.

High-performing algorithms become increasingly rare but more consistent in deeper layers, reflecting natural convergence toward superior solutions. Critically, deeper layers exhibit superior generalization capability during later optimization phases, with training-test performance gaps narrowing significantly in Depth III compared to shallower groups. This improved generalization suggests extensive algorithmic refinement enhances both performance and robustness across different observational conditions, confirming the MCTS framework effectively balances exploration breadth with exploitation depth.

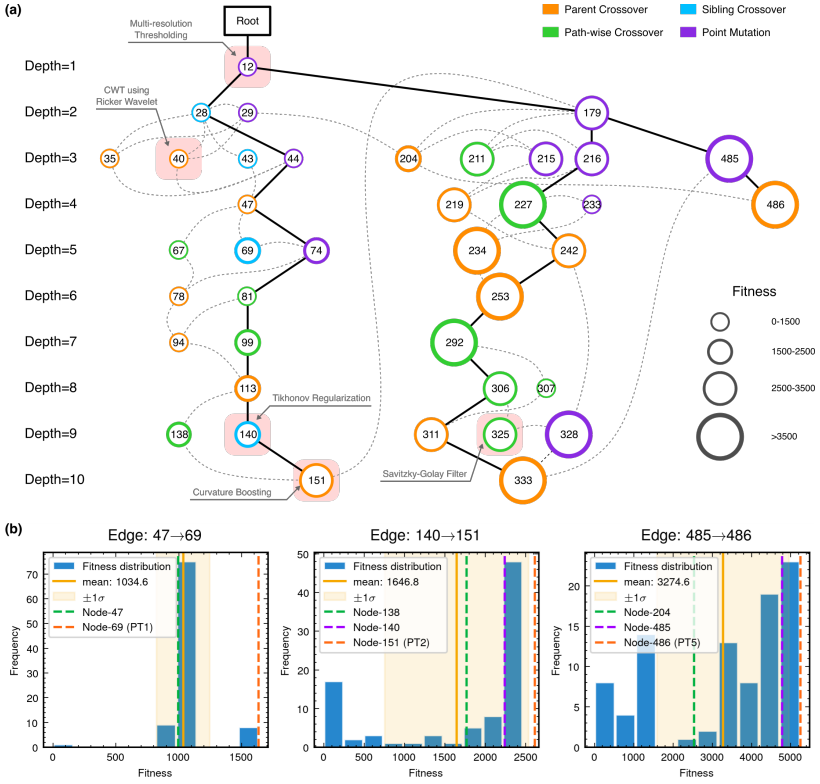
**Algorithmic Component Impact Analysis.** We conducted comprehensive technique impact analysis using controlled comparative methodology, systematically evaluating algorithms with specific signal processing techniques against matched controls. (details in Supplementary Material A.5).

Figure 4c reveals distinct performance impacts across algorithmic components. Conditioning techniques demonstrate the most pronounced positive effects, with Savitzky-Golay filtering showing clear distributional separation and asymmetric violin plots shifted toward higher fitness values. This technique has been applied in gravitational wave counterpart studies for smoothing two-dimensional dispersed images from the Hubble Space Telescope, effectively removing high-frequency structure while preserving underlying emission patterns [46]. These findings establish quantitative benchmarks for algorithmic component selection in automated gravitational wave detection systems.

### 2.3.2 Algorithmic Evolution Pathway and Discovery Mechanism Analysis

**MCTS Tree Structure and Knowledge Propagation.** To understand the mechanistic basis of algorithmic discovery, we conducted comprehensive analysis of the complete MCTS exploration pathway leading to the PT4 algorithm (node 486, fitness = 5241.4). Figure 5a presents the full tree structure encompassing all nodes associated with the selected algorithm, revealing systematic patterns in knowledge accumulation and technique integration across multiple optimization phases (full MCTS tree data and visualization available in Supplementary Information Section S6).

Critical to understanding the framework’s discovery mechanism is the identification of five key algorithmic breakthroughs that emerge at specific nodes and propagate through subsequent generations. These innovations demonstrate systematic knowledge accumulation, with breakthrough techniques subsequently incorporated into descendant algorithms through evolutionary operations. The propagation patterns reveal progressive sophistication through iterative refinement and technique combination, with superior algorithmic components showing robust inheritance and integration capabilities



**Fig. 5 MCTS Algorithmic Evolution Pathway and Edge Robustness Analysis.** (a) Complete MCTS tree structure showing all nodes associated with the PT4 algorithm (node 486, fitness=5241.4) discovered in an optimization run. Node sizes encode fitness values (larger circles = higher performance), with evaluation times displayed inside circles. Node colors indicate expansion operation types: Parent Crossover (orange), Sibling Crossover (cyan), Path-wise Crossover (green), and Point Mutation (purple). Solid black lines represent the selected MCTS exploration path, while dashed gray lines indicate nodes referenced in expansion prompts for knowledge synthesis. Five key algorithmic breakthroughs are annotated: Multi-resolution Thresholding (first appearing at node 12), CWT using Ricker Wavelet (node 28), Tikhonov Regularization (node 140), Curvature Boosting (node 151), and Savitzky-Golay Filter (node 333). These techniques propagate through subsequent generations, demonstrating systematic knowledge accumulation and refinement. The tree visualization reveals how sophisticated detection algorithms emerge through progressive technique integration across multiple MCTS depth levels. (b) Edge robustness analysis for three critical evolutionary transitions. Each subplot shows fitness distributions from 100 independent re-executions of specific edges: Edge 47→69 (early breakthrough, mean fitness 1034.6, 89.25% variants exceeding preceding node performance), Edge 140→151 (intermediate advancement, mean fitness 1646.8, 52.81% achieving superior fitness with 100% regularization technique inheritance), and Edge 485→486 (final optimization stage, mean fitness 3274.6, 70.65% variants outperforming node 204, 25.00% surpassing node 485). Vertical reference lines indicate the original node fitness values and key ancestral nodes. The distributions demonstrate the stochastic nature of LLM-driven code generation while confirming consistent discovery of high-performance algorithmic variants with robust knowledge transfer across independent executions.

that directly influence fitness improvements across generations. The complete tree structure demonstrates effective LLM-guided exploration that balances exploitation of promising directions with exploration of novel algorithmic territories, leading to high-performance detection strategies significantly exceeding conventional approaches.

**Edge Robustness and Stochastic Validation.** Through comprehensive re-execution analysis of three pivotal evolutionary transitions using 100 independent runs each, we validated the consistency of breakthrough innovations in Figure 5b. These analyses confirm that breakthrough algorithmic innovations emerge through systematic discovery processes rather than fortuitous random variations, demonstrating stable technique inheritance and high-probability performance improvements across all re-executions despite increased algorithmic complexity, validating the framework’s reliability for automated algorithm discovery and providing confidence in the generalizability of discovered techniques to broader gravitational wave detection challenges.

## 2.4 Framework Mechanism Analysis

To validate Evo-MCTS’s effectiveness, we conducted systematic mechanism analysis across three critical dimensions: integrated optimization architecture, LLM model selection, and domain knowledge incorporation. These analyses reveal that superior performance emerges from synergistic component interactions rather than simple additive effects - addressing the vast search space problem through MCTS-guided reflection structuring, ensuring code generation quality via optimal LLM selection, and maintaining scientific relevance through domain knowledge integration. This multi-faceted approach demonstrates that successful automated discovery requires intelligent integration of search strategy, reasoning capability, and domain expertise beyond mere computational power.

**Integrated Architecture Validation.** Figure 6a demonstrates the substantial benefits of combining evolutionary optimization with Monte Carlo Tree Search in LLM-guided algorithm discovery. Evo-MCTS achieves superior performance compared to its constituent components operating in isolation - pure MCTS-AHD [29] and pure evolutionary optimization (ReEvo [28]), all of which leverage LLMs for code generation and algorithmic reasoning.

The performance hierarchy reveals critical insights about LLM-based optimization strategy effectiveness. Pure evolutionary approaches struggle with the vast search space and become trapped in local optima despite LLM guidance, exhibiting high variance with frequent suboptimal exploration in the LLM-generated algorithm space. MCTS-AHD provides improvement through systematic search space organization but with limited diversity in LLM-generated solutions. The full Evo-MCTS combines the best of both worlds: maintaining population diversity through evolutionary mechanisms while focusing computational resources on promising algorithmic directions through tree search guidance, all while maximizing the utilization of LLM reasoning capabilities. This integration achieves a remarkable 59.1% improvement over

MCTS-AHD alone, demonstrating that combining population-based diversity maintenance with tree-structured exploitation creates emergent optimization capabilities that exceed the sum of individual LLM-powered components.

**LLM Model Selection and Robustness Analysis.** Figure 6b investigates the impact of different foundation models on algorithmic discovery performance, revealing significant variations in code generation capability across state-of-the-art language models. The analysis establishes `o3-mini-medium` as our fiducial model configuration.

The performance hierarchy reveals insights about the relationship between model architecture and scientific code generation capability. Particularly intriguing is the superior performance of `claude-3-7-sonnet-20250219-thinking` over `o1-2024-12-17`, despite both being reasoning-enhanced models. This suggests that Claude’s specific training methodologies and architectural choices may be better suited for sustained algorithmic reasoning tasks in gravitational wave detection algorithm development. The substantial performance gap between reasoning-enhanced models and general-purpose models underscores the critical importance of model architecture selection for scientific code generation tasks.

This demonstrates that framework effectiveness depends not merely on having access to large language models, but on selecting models with appropriate reasoning architectures for complex scientific applications. The robustness analysis shows consistent performance rankings across multiple runs, validating our model selection strategy while revealing that different LLM architectures exhibit distinct strengths in algorithmic reasoning and code synthesis.

**Domain Knowledge Integration Impact.** Figure 6c presents one of the most striking results: the dramatic impact of domain knowledge integration on algorithmic discovery performance. The comparison between frameworks with and without external knowledge reveals a performance difference of 115%, demonstrating that domain-specific guidance is essential for effective automated algorithm discovery in specialized scientific domains.

The framework without external knowledge exhibits relatively flat optimization trajectories, while domain knowledge integration demonstrates sustained improvement by serving as a constraint mechanism that guides the vast search space toward physically meaningful solutions. The emphasis on non-linear processing significantly enhances gravitational wave signal detection in real-world non-Gaussian, non-stationary noise environments, successfully leveraging scientific expertise to accelerate discovery beyond pure computational search (domain knowledge templates and integration methodology detailed in Supplementary Material A.1).

### 3 Discussion

The Evo-MCTS framework demonstrates that automated algorithm discovery can achieve substantial performance improvements in gravitational wave detection through systematic exploration of algorithmic spaces. Our results establish

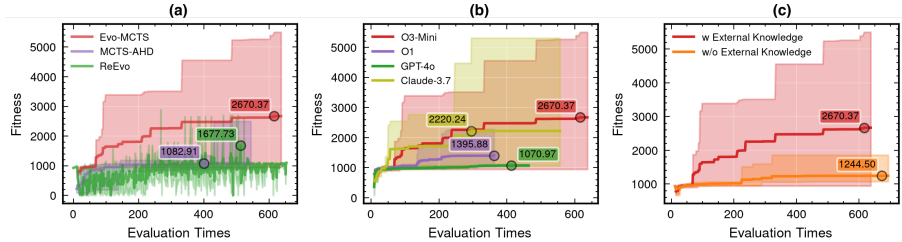


**Fig. 6 Framework Mechanism Analysis and Component Contributions.** (a) Integrated architecture validation comparing Evo-MCTS (red) against constituent components: MCTS-AHD (purple, 1,677.73 fitness) and ReEvo (green, 1,082.61 fitness). Evo-MCTS achieves superior performance (2,670.37 fitness) through synergistic combination of evolutionary population dynamics and tree-structured search. (b) LLM model selection analysis showing performance variation across foundation models: `o3-mini-medium` (red, 2,670.37), `claude-3-7-sonnet-20250219-thinking` (yellow, 2,220.24), `o1-2024-12-17` (purple, 1,395.88), and `gpt-4o-2024-11-20` (green, 1,070.97). Results demonstrate the superior performance of reasoning-enhanced models, with `o3-mini-medium` achieving 150% improvement over general-purpose models. (c) Domain knowledge integration impact comparing frameworks with external knowledge (red, 2,670.37) versus without domain-specific guidance (orange, 1,244.50). The 115% performance improvement demonstrates the essential role of scientific domain expertise in automated algorithm discovery. All curves represent averages over at least five independent runs with shaded regions indicating standard deviation. Results validate the framework’s three core design principles: integrated optimization architecture, optimal model selection, and domain knowledge incorporation.

key insights extending beyond gravitational wave detection to broader scientific algorithm discovery applications.

**Physical Insights and Algorithmic Discovery.** The evolved algorithms reveal nonlinear processing strategies that effectively address fundamental limitations of both template-based and non-template approaches in realistic detector environments. The discovered multi-scale wavelet decompositions, adaptive thresholding mechanisms, and sophisticated statistical analysis methods dynamically adapt to non-Gaussian and non-stationary noise characteristics [5, 40]. These algorithmic discoveries provide new perspectives on optimal gravitational wave detection, demonstrating that theoretical optimality of template-based methods under idealized conditions [9, 38] can be substantially enhanced through interpretable nonlinear transformations that bridge template and non-template paradigms in practical scenarios.

**Current Limitations.** The framework focuses on static optimization scenarios and requires extensions for dynamic environments involving real-time parameter estimation. MLGWSC-1’s simplified testing environment, limited evaluation metrics, and potential overfitting risks do not fully capture operational detector complexity, as analyzed in the Supplementary Material A.7. The framework’s reliance on large language models introduces dependencies on model architecture and prompt engineering, with 150% performance variation across implementations requiring expert validation modules for physical reasonableness verification. Our approach provides a novel framework for algorithmic optimization rather than a complete production-ready pipeline, with

discovered algorithms serving as proof-of-concept demonstrations requiring further validation before operational deployment.

**Future Directions.** The evolutionary MCTS approach demonstrates broad potential for scientific algorithm discovery beyond gravitational waves. As Browne et al. note, MCTS “can be used with little or no domain knowledge, and has succeeded on difficult problems where other techniques have failed” [21]. The framework’s domain-agnostic architecture suggests applications in molecular optimization for drug discovery, materials design algorithms, and signal detection across astrophysical domains. The demonstrated interpretability advantages enable hybrid human-AI systems where algorithmic discoveries inform theoretical understanding while domain insights guide optimization, potentially accelerating scientific algorithm development across multiple disciplines.

## 4 Methods

### 4.1 Problem Formulation

This section formalizes gravitational wave algorithm discovery as a constrained optimization problem and introduces the LLM-guided evolutionary framework architecture.

**Gravitational Wave Detection Problem.** Given dual-detector strain data  $\mathbf{d}(t) \in \mathbb{R}^{2 \times N}$ , where  $\mathbf{d}(t) = [d_H(t), d_L(t)]^T$  represents the strain data from Hanford and Livingston interferometers sampled at  $f_s = 2048$  Hz over finite observation windows of length  $N$  samples, we seek to discover an optimal detection algorithm that maximizes performance while satisfying operational constraints.

**Optimization Objective.** The algorithm discovery problem is formulated as:

$$a^* = \arg \max_{a \in \mathcal{A}} \mathcal{F}(a, \mathbf{d}) \quad (1)$$

$$\text{subject to } \|\Delta t_{\text{arrival}}\| \leq 0.2 \text{ seconds} \quad (2)$$

$$T_{\text{comp}}(a) \leq T_{\text{max}} \quad (3)$$

$$E(a) \leq E_{\text{max}} \quad (4)$$

$$a : \mathbb{R}^{2 \times N} \rightarrow \mathbb{R}^3 \quad (5)$$

where:

- $\mathcal{A} = \{a \mid a \text{ is executable and satisfies constraints}\}$  represents the space of executable detection algorithms
- $\mathcal{F}(a, \mathbf{d}) = \int_{FAR_{\text{min}}}^{FAR_{\text{max}}} d_L(FAR; a, \mathbf{d}) d(FAR)$  measures detection performance as the area under the sensitive distance versus false alarm rate curve following the MLGWSC-1 protocol [30]
- $\Delta t_{\text{arrival}}$  denotes trigger arrival time uncertainty for astrophysical parameter estimation

- $T_{\text{comp}}(a)$  and  $E(a)$  represent computational time and error handling trial count constraints with thresholds  $T_{\text{max}}$  and  $E_{\text{max}}$
- Each algorithm  $a$  maps dual-detector strain data to a three-column detection catalog table containing peak times, signal ranking statistics, and timing uncertainties

The fitness function  $\mathcal{F}$  evaluates algorithms against ground truth labels  $\mathbf{y}_{\text{true}}$  using the area under the curve (AUC) of sensitive distance versus false alarms per month, where  $d_L(FAR; a, \mathbf{d})$  represents the sensitive distance at a given false alarm rate  $FAR$ , providing more physically meaningful performance assessment than traditional Receiver Operating Characteristic curves for gravitational wave detection applications.

**Algorithm Discovery Framework.** We model the discovery process as an iterative search procedure that combines Monte Carlo Tree Search exploration with evolutionary population dynamics:

$$\mathbf{P}_{t+1} = \text{Evolve}(\mathbf{P}_t, \mathcal{L}, \mathcal{K}_{\text{GW}})$$

where  $\mathbf{P}_t = \{a_1^{(t)}, a_2^{(t)}, \dots, a_k^{(t)}\}$  represents the algorithm population at iteration  $t$ .

**Key Components:**

- **LLM Code Generation:**  $\mathcal{L} : (\text{prompt}, \text{context}) \rightarrow \text{code}$  represents the language model for code generation, with operation-specific prompting strategies  $\sigma : \mathcal{O} \rightarrow \mathcal{P}$  mapping evolutionary operations  $\mathcal{O} = \{\text{PC}, \text{SC}, \text{PWC}, \text{PM}\}$  to specialized prompt templates  $\mathcal{P}$
- **Domain Knowledge:**  $\mathcal{K}_{\text{GW}} = (\mathcal{K}_{\text{physics}}, \mathcal{K}_{\text{signal}}, \mathcal{K}_{\text{constraint}})$  encapsulates gravitational wave detection expertise including physical principles, signal processing techniques, and computational constraints
- **MCTS Selection:** Node selection follows Upper Confidence bounds applied to Trees (UCT) with adaptive exploration:

$$\pi_{\text{UCT}}(n) = \arg \max_{c \in \text{children}(n)} [\text{normalized\_fitness}(c) + \text{adaptive\_exploration}(c)]$$

where the complete implementation with fitness normalization, adaptive exploration constants, and epsilon regularization is detailed in Section 4.4.

**Evolutionary Operations.** The framework employs four evolutionary operations for algorithmic transformation, each utilizing operation-specific prompting strategies with the same underlying language model:

$$\text{PC}(\mathbf{P}_t) : a_{\text{new}} = \mathcal{L}(\text{prompt}_{\text{PC}}(a_p, a_r), \mathcal{K}_{\text{GW}}) \quad (6)$$

$$\text{SC}(\mathbf{P}_t) : a_{\text{new}} = \mathcal{L}(\text{prompt}_{\text{SC}}(a_c, \{a_{s_i}\}), \mathcal{K}_{\text{GW}}) \quad (7)$$

$$\text{PWC}(\mathbf{P}_t) : a_{\text{new}} = \mathcal{L}(\text{prompt}_{\text{PWC}}(\{a_{d_i}\}), \mathcal{K}_{\text{GW}}) \quad (8)$$

$$\text{PM}(\mathbf{P}_t) : a_{\text{new}} = \mathcal{L}(\text{prompt}_{\text{PM}}(a_c, a_e), \mathcal{K}_{\text{GW}}) \quad (9)$$

where PC = Parent Crossover, SC = Sibling Crossover, PWC = Path-wise Crossover, PM = Point Mutation. Here,  $a_p$  and  $a_r$  denote parent and reference algorithms,  $a_c$  represents the current algorithm,  $\{a_{s_i}\}$  are sibling algorithms,  $a_e$  is an elite algorithm, and  $\{a_{d_i}\}$  are distant algorithm sets.

Each operation employs tailored prompt templates  $\text{prompt}_{\text{op}}(\cdot)$  that guide the language model to generate appropriate algorithmic variants: Parent Crossover prompts emphasize combining successful features from parent algorithms, Sibling Crossover focuses on lateral exploration within similar algorithmic families, Path-wise Crossover promotes paradigm shifts by integrating distant algorithmic approaches, and Point Mutation targets localized refinements of existing implementations. Domain knowledge  $\mathcal{K}_{\text{GW}}$  ensures adherence to gravitational wave detection principles and physical constraints across all operations.

**Reflection and Adaptation.** The system incorporates analytical reasoning through specialized reflection using the DeepSeek-R1 model:

$$\mathcal{K}_{\text{GW}}^{(t+1)} = \mathcal{K}_{\text{GW}}^{(t)} \cup \{\text{insights}(R(\text{history}_t, \text{performance}_t, \mathcal{K}_{\text{physics}}))\}$$

where  $R : \mathcal{H} \times \mathcal{F}^* \times \mathcal{K}_{\text{physics}} \rightarrow \mathcal{I}$  represents the reflection function mapping MCTS history  $\mathcal{H}$ , fitness evaluations  $\mathcal{F}^*$ , and physical knowledge to actionable insights  $\mathcal{I}$ .

This reflection mechanism analyzes performance patterns across the MCTS tree to identify successful algorithmic principles and guide subsequent evolutionary operations toward promising regions of the solution space.

**Population Management.** At each iteration, the algorithm population is updated through elite preservation with selection pressure  $\beta$ :

$$\mathbf{P}_{t+1} = \text{Elite}(\mathbf{P}_t \cup \{a_{\text{new}}\}, k, \beta) \quad (10)$$

where  $\text{Elite}(\cdot, k, \beta)$  selects the top- $k$  algorithms based on fitness scores  $\mathcal{F}(a_i, \mathbf{d})$  with selection probability:  $p_{\text{select}}(a_i) = \exp(\beta \cdot \mathcal{F}(a_i, \mathbf{d})) / \sum_{j=1}^{\mathbf{P}''} \exp(\beta \cdot \mathcal{F}(a_j, \mathbf{d}))$ . This formulation establishes gravitational wave algorithm discovery as a constrained optimization problem in the space of executable detection algorithms, solved through LLM-guided evolutionary search with MCTS exploration and domain knowledge integration.

## 4.2 LLM Integration for Code Generation

The framework leverages state-of-the-art language models to transform algorithmic concepts into executable code, implementing a multi-model strategy that capitalizes on the complementary strengths of different architectures. This subsection details the model selection, prompting strategies, and error handling mechanisms that enable robust algorithmic discovery.

**Model Architecture and Task Allocation.** The framework employs a heterogeneous ensemble of four language models:

o3-mini-medium, o1-2024-12-17, gpt-4o-2024-11-20, and claude-3-7-sonnet-20250219-thinking for code generation tasks. For reflection operations, we utilize deepseek-r1-250120 exclusively due to its analytical reasoning capabilities.

**Prompting Strategy and Temperature Control.** All models operate with temperature 1.0 to optimize the trade-off between algorithmic diversity and code validity.

The prompting framework employs depth-aware adaptation mechanisms. Task descriptions clarify optimization objectives, while depth information guides exploration scope: shallow nodes emphasize paradigm shifts, deeper nodes focus on parameter optimization. External domain knowledge integration provides optimization directives referencing established signal processing principles and computational constraints. This adaptive architecture enables systematic solution space exploration while maintaining gravitational wave detection coherence (complete templates in Supplementary Material A.1).

**Error Handling and Iterative Refinement.** The framework implements a robust error recovery mechanism to handle code generation failures. When syntax errors or runtime exceptions occur during algorithm evaluation, the system captures detailed error information including stack traces and execution context. This diagnostic information is then incorporated into subsequent conversation rounds with the LLM to generate corrected implementations. The system attempts up to three correction iterations per failed algorithm. If all correction attempts fail, the corresponding node expansion is skipped to maintain computational efficiency. This approach ensures that the majority of generated algorithms remain executable while preventing infinite correction loops that could stall the evolutionary process (complete templates in Supplementary Material A.1).

**Post-Generation Analysis** Following successful code generation, each algorithm undergoes a post-thought analysis phase that extracts key design principles and compresses algorithmic representations. This reflection process creates human-readable summaries while reducing token consumption to prevent context window overflow in subsequent LLM interactions.

The analysis captures algorithmic innovations, signal processing techniques, performance expectations, and computational characteristics in compressed form. This enables efficient reference to previous discoveries without overwhelming the LLM context, facilitating continued exploration while maintaining algorithmic memory across generations (complete templates in Supplementary Material A.1).

**Domain Knowledge Integration.** The framework incorporates gravitational wave domain expertise through three structured prompt categories: initialization prompts defining matched filtering principles and noise characteristics, evolution prompts encouraging nonlinear transformations and adaptive thresholding, and reflection prompts evaluating sensitivity and computational efficiency (complete templates in Supplementary Material A.1).

The knowledge base prioritizes nonlinear processing techniques including adaptive thresholds, phase space reconstruction, and robust estimators. Implementation emphasizes adaptive parameters over fixed values while maintaining computational efficiency.

This approach ensures physical constraint compliance while enabling exploration beyond conventional linear methods.

### 4.3 Evolutionary Operations Design and Seed Algorithm

**Baseline Algorithm Architecture.** The optimization process begins with a deliberately simple, linear seed function that establishes a baseline for algorithmic improvement (detailed implementation in Supplementary Material A.1). This seed algorithm implements a conventional signal processing pipeline consisting of three sequential operations that represent standard approaches in gravitational wave data analysis.

The first operation performs frequency-domain whitening to normalize the detector noise characteristics:

$$X_{\text{white}}(f) = \frac{X(f)}{\sqrt{S(f)}} \quad (11)$$

where  $X(f)$  represents the Fourier transform of the input strain data, and  $S(f)$  is the power spectral density estimate obtained via Welch’s method using a 4096-sample window with 50% overlap and Hann windowing. This whitening operation ensures that all frequency components contribute equally to subsequent analysis, compensating for the detector’s frequency-dependent noise characteristics.

The second operation applies time-frequency decomposition using the short-time Fourier transform (STFT) to capture transient signal characteristics:

$$S_{xx}(f, \tau) = \left\| \sum_{n=0}^{N-1} x(n + \tau) w(n) e^{-j2\pi f n/N} \right\|^2 \quad (12)$$

where  $w(n)$  is a window function (256 samples with 128-sample overlap),  $\tau$  is the time shift, and  $N$  is the window length. The algorithm independently processes both Hanford (H1) and Livingston (L1) detector data, then combines the resulting spectrograms using simple averaging:

$$\text{TF}_{\text{metric}} = \frac{1}{2} \langle S_{xx}^{\text{H1}} + S_{xx}^{\text{L1}} \rangle_f$$

where  $\langle \cdot \rangle_f$  denotes averaging over frequency bins.

The final operation identifies candidate events through basic peak detection with fixed thresholds. The algorithm estimates background levels using the median and applies simple peak finding with predetermined height and prominence criteria. This approach represents a minimalist detection strategy

that lacks the sophistication necessary for robust gravitational wave identification, particularly in the presence of non-Gaussian noise transients and weak signals.

**Initial Population Generation.** The evolutionary framework initializes with a single seed algorithm, then generates 8 diverse variants through systematic prompting variations (Figure 1a). Each variant maintains identical input-output interfaces while implementing distinct signal processing approaches: alternative whitening schemes, varied time-frequency decomposition methods, and different peak detection strategies. Following initial generation, two Point Mutation operations are applied to create additional variants, resulting in a total population of 10 algorithms that form the depth-1 initial population for MCTS exploration.

**Elite Preservation Strategy.** The framework maintains an elite individual representing the best-performing algorithm discovered throughout evolution. This elite serves as a performance benchmark for new variants and provides genetic material during Point Mutation operations, which specifically leverage elite characteristics to guide targeted algorithmic improvements (Figure 1c). The elite is updated whenever a new algorithm demonstrates superior performance, ensuring monotonic progress while maintaining access to the current best solution (Figure 1b.4).

**Evolutionary Operation Framework.** Each MCTS expansion level follows a structured sequence of evolutionary operations: Parent Crossover (PC) executes 5 times, Path-wise Crossover (PWC) executes 2 times, Sibling Crossover (SC) executes once, and Point Mutation (PM) executes twice. As observed in Figure 5a, this sequence balances four distinct algorithmic improvement mechanisms: (i) vertical knowledge transfer through PC operations that combine features from algorithms at different tree depths, (ii) long-range dependency capture via PWC operations that synthesize information along complete evolutionary trajectories, (iii) horizontal exploration using SC operations that facilitate exploration between algorithms of similar complexity based on nodes already generated at the same tree level, and (iv) fine-grained optimization through PM operations that introduce targeted modifications based on performance analysis. The systematic application of these operations ensures comprehensive exploration of the algorithmic solution space while maintaining computational efficiency through controlled expansion rates.

## 4.4 Monte Carlo Tree Search Implementation

**MCTS Framework and Tree Policy.** The framework implements a standard Monte Carlo Tree Search algorithm adapted for algorithmic discovery, where each node represents an executable algorithm and tree expansion corresponds to algorithmic evolution (Figure 1b). The MCTS operates through four canonical phases: selection, expansion, simulation, and backpropagation. However, our implementation modifies the traditional simulation phase by replacing random rollouts with direct algorithm evaluation on the gravitational wave detection task.

The selection phase traverses the tree from root to leaf using the Upper Confidence Bound applied to Trees (UCT) policy, balancing exploitation of high-performing algorithms with exploration of under-visited branches (Figure 1c). Unlike traditional MCTS applications where leaf nodes represent terminal game states, our leaf nodes represent algorithms that can be further evolved through the four evolutionary operations (PC, SC, PWC, PM).

**UCT Score Calculation and Adaptive Exploration.** The UCT score for each node combines exploitation and exploration terms with an adaptive exploration strategy that accounts for the finite evaluation budget:

$$\text{UCT}(n) = \frac{Q(n) - Q_{\min}}{Q_{\max} - Q_{\min} + \epsilon} + c \cdot \sqrt{\frac{\ln(N(p) + 1)}{N(n) + \epsilon}} \quad (13)$$

where  $Q(n)$  represents the normalized fitness value of node  $n$ ,  $Q_{\min}$  and  $Q_{\max}$  are the minimum and maximum fitness values observed across all nodes,  $N(p)$  and  $N(n)$  are the visit counts of the parent and current node respectively,  $\epsilon$  is a small constant preventing division by zero, and  $c$  is the exploration constant.

The exploration constant  $c$  adapts dynamically based on the remaining evaluation budget:

$$c = c_0 \cdot \max\left(1 - \frac{t}{T}, 0\right) \quad (14)$$

where  $c_0$  is the initial exploration constant,  $t$  is the current evaluation count, and  $T$  is the maximum evaluation budget. This adaptive mechanism ensures that the algorithm emphasizes exploration early in the search when the budget is abundant, then gradually shifts toward exploitation as evaluations are consumed.

**Fitness Normalization and Q-Value Management.** The fitness values (corresponding to the objective function in MCTS) are normalized to the range  $[0, 1]$  to ensure consistent UCT calculations regardless of the absolute scale of performance metrics. The normalization uses running minimum and maximum values:

$$Q_{\text{normalized}} = \frac{Q_{\text{raw}} - Q_{\min}}{Q_{\max} - Q_{\min} + \epsilon} \quad (15)$$

This normalization is crucial for maintaining meaningful exploration-exploitation balance, as it prevents algorithms with vastly different performance scales from skewing the selection process.

**Backpropagation and Value Updates.** The backpropagation phase updates node values along the path from the newly evaluated leaf to the root. Our implementation uses a discount factor approach that balances immediate performance with long-term potential:

$$Q(p) = Q(p) \cdot (1 - \gamma) + \max_{c \in \text{children}(p)} Q(c) \cdot \gamma \quad (16)$$

where  $Q(p)$  is the parent node’s Q-value,  $\gamma$  is the discount factor, and the maximum is taken over all child nodes. This update rule ensures that parent

nodes reflect the performance of their best children while maintaining some memory of their previous estimates.

The backpropagation also maintains global statistics by updating the minimum and maximum Q-values across the entire tree, enabling consistent normalization for future UCT calculations. Additionally, the algorithm maintains a ranked list of all observed fitness values to support advanced selection strategies and performance analysis.

**Tree Expansion Strategy.** Node expansion occurs when the UCT selection phase reaches a leaf node that has been visited multiple times, indicating sufficient confidence in its potential. The expansion strategy creates one new child node per expansion operation, chosen through the evolutionary operations framework. This conservative expansion approach prevents explosive tree growth while ensuring thorough exploration of promising regions.

Each newly created node inherits structural information from its parent, including the algorithmic context and performance history. The initial Q-value for new nodes is set to the parent’s Q-value, providing a reasonable starting estimate that will be refined through subsequent evaluations.

**Memory Management and Tree Pruning.** To maintain computational efficiency with limited memory resources, the implementation includes mechanisms for selective tree pruning. Nodes that demonstrate consistently poor performance relative to their siblings are marked for potential removal, while maintaining sufficient diversity to avoid premature convergence.

The tree structure also maintains subtree references that enable efficient traversal and analysis of evolutionary pathways. These references support the PWC operation by providing access to complete root-to-leaf trajectories without requiring expensive tree traversals.

**Convergence Detection and Termination.** The MCTS continues until either the evaluation budget is exhausted or convergence is detected through analysis of the Q-value distribution. Convergence is identified when the top-performing algorithms show minimal improvement over a specified number of iterations, indicating that the search has reached a local optimum within the current exploration strategy.

This MCTS implementation creates a systematic framework for exploring the algorithmic space while maintaining computational efficiency and ensuring reproducible results. The combination of adaptive exploration, normalized fitness values, and efficient tree management enables the discovery of high-performing algorithms within reasonable computational budgets.

## 4.5 Experimental Setup

**MLGWSC-1 Dataset and Evaluation Framework.** We evaluated our Evo-MCTS framework using the first Machine Learning Gravitational-Wave Search Mock Data Challenge (MLGWSC-1) benchmark, which provides a standardized evaluation environment for gravitational wave detection algorithms [30]. The benchmark includes four datasets with increasing complexity,

of which we utilized Dataset 4 for our primary evaluation as it represents the most realistic scenario using actual detector noise from the O3a observing run.

Dataset 4 incorporates real noise from both Hanford (H1) and Livingston (L1) detectors, filtered to include only segments with the DATA data-quality flag active while excluding problematic categories (CBC\_CAT1, CBC\_CAT2, CBC\_HW\_INJ, and BURST\_HW\_INJ). Overlapping segments span a minimum duration of 2 hours, with signal injection parameters specifically designed to ensure that at least 33% of injected signals have an optimal network SNR  $< 4$  and thus cannot be detected, creating a challenging evaluation scenario that includes both detectable and sub-threshold events.

**Algorithm Input/Output Interface.** Following the MLGWSC-1 specification, each algorithm processes HDF5 files containing raw detector data from both H1 and L1 detectors. The input files contain grouped datasets organized by integer start times, with each dataset including strain data and metadata attributes (`start_time`, `delta_t`). Our evolved algorithms output HDF5 files containing exactly three datasets of equal length: (i) `time` - GPS times of suspected gravitational wave events, (ii) `stat` - ranking statistics where larger values indicate higher detection confidence, and (iii) `var` - timing accuracy tolerance representing the maximum allowed separation between predicted and true event times.

**Evaluation Metrics and Performance Assessment.** The framework employs two primary evaluation metrics consistent with MLGWSC-1 standards. The false-alarm rate (FAR) measures the expected frequency of false-positive events exceeding a given ranking statistic threshold, calculated by applying algorithms to pure noise data and dividing event counts by total analyzed time. The sensitive distance quantifies detection capability at specified false-alarm rates, representing the maximum distance at which sources can be reliably detected. For uniformly distributed signals in volume, this reduces to the fraction of detected signals multiplied by the volume of a sphere with radius equal to the maximum injected distance. The area under the curve (AUC) metric integrates sensitive distance across the false-alarm rate range, providing a comprehensive performance indicator that balances detection sensitivity against false-alarm tolerance.

**Training and Test Set Configuration.** To ensure efficient optimization while maintaining statistical rigor, we partitioned the MLGWSC-1 Dataset 4 into training and test subsets. The training set comprises the first 7 days of data from early injection indices, enabling rapid algorithmic evaluation during the optimization process. This temporal partitioning ensures that the minimum false-alarm rate boundary is set at 4 events per month, corresponding to the statistical requirements for meaningful AUC calculation. The test set consists of 1 day of data selected from later temporal segments, providing independent validation of optimized algorithms (detailed data partitioning specifications provided in Supplementary Material A.2).

**Diversity Metrics in Evolutionary Computation.** We implemented sophisticated diversity measurement following established practices in evolutionary computation [47]. Population encoding involves three preprocessing steps: (i) removing comments and docstrings using abstract syntax tree parsing to focus on functional algorithmic content, (ii) standardizing code snippets into common coding style following PEP 8 conventions to eliminate stylistic variations, and (iii) converting normalized code snippets to vector representations using the CodeT5+ embedding model to enable quantitative similarity analysis.

We employ two complementary diversity metrics: the Shannon Diversity Index, calculated as  $H = -\sum_{i=1}^n p_i \log p_i$  where  $p_i$  represents the frequency of the  $i$ -th unique algorithmic variant in the population, and the Complexity Index of Diversity (CID), computed as  $CID = \frac{1}{n} \sum_{i=1}^n \frac{x_i - \bar{x}}{\bar{x} + \epsilon}$  where  $x_i$  represents the embedding vector of the  $i$ -th algorithm,  $\bar{x}$  is the population centroid, and  $\epsilon$  prevents division by zero. These metrics provide complementary perspectives on population diversity: Shannon index captures algorithmic variety while CID measures structural complexity differences.

**LLM API Configuration and Model Selection.** Our framework integrates multiple state-of-the-art language models through official APIs from OpenAI, Anthropic, and DeepSeek [48–51]. For code generation tasks, we employ thinking-enhanced models including `o3-mini-medium`, `o1-2024-12-17`, `gpt-4o-2024-11-20`, and `claude-3-7-sonnet-20250219-thinking`, selected for their demonstrated capabilities in multi-step reasoning and code synthesis [19, 52]. For reflection mechanisms, we exclusively utilize `deepseek-r1-250120` due to its superior performance in analytical reasoning tasks [51], particularly its ability to identify subtle performance patterns and propose targeted algorithmic improvements based on empirical observations. We designate `o3-mini-medium` as our fiducial model configuration, providing the baseline reference for performance comparisons and ensuring consistency across experimental runs. All models operate with temperature parameter set to 1.0 to balance creative exploration with syntactic reliability [53].

**Hyperparameter Configuration and Experimental Design.** The Evo-MCTS framework employs carefully tuned hyperparameters optimized for gravitational wave detection algorithm discovery. Initial population size is set to 10 algorithms, balancing computational efficiency with adequate diversity for effective exploration. MCTS depth is limited to 10 levels, providing sufficient hierarchical structure for complex algorithmic development while maintaining computational tractability. Each experimental configuration undergoes 5 independent runs with different random seeds to ensure statistical robustness and enable confidence interval estimation.

The 5-run experimental design serves multiple purposes: (i) quantifying algorithmic discovery reliability across different initialization conditions, (ii) enabling statistical analysis of optimization trajectories and convergence patterns, and (iii) providing robust diversity measurements that account for

stochastic variations in the evolutionary process. Comprehensive results from all individual runs are documented in Supplementary Material A.3, enabling detailed analysis of inter-run variability and optimization consistency.

**Ablation Studies and Comparative Analysis.** To validate the effectiveness of our integrated Evo-MCTS approach, we conduct comprehensive ablation studies comparing against two established frameworks: ReEvo [28] (pure evolutionary mechanism) and MCTS-AHD [29] (pure MCTS mechanism). These comparisons isolate the contributions of different algorithmic components while maintaining consistent evaluation protocols.

ReEvo represents the evolutionary optimization baseline, employing genetic algorithms with traditional crossover and mutation operations powered by large language models but without tree-structured exploration. The framework implements population-based optimization through iterative code generation and selection, focusing on evolutionary diversity maintenance and fitness-driven selection pressure. MCTS-AHD implements pure Monte Carlo Tree Search for automated heuristic design without evolutionary population dynamics or reflection mechanisms. This approach emphasizes tree-based exploration with UCT-guided node selection but lacks the multi-generational insight synthesis and population diversity maintenance that characterizes evolutionary approaches.

By comparing Evo-MCTS against these component frameworks using identical LLM integration protocols and evaluation budgets, we quantify the synergistic benefits of combining evolutionary population dynamics with structured tree search exploration. The experimental design maintains consistent evaluation metrics, hardware configurations, and statistical analysis procedures across all three frameworks, with computational fairness ensured through equivalent LLM evaluation counts as the unified iteration metric. This approach enables direct performance comparison while isolating the specific contributions of different optimization strategies under identical resource constraints. The comprehensive multi-run analysis results across all frameworks are presented in Figure A2, demonstrating the statistical robustness of our comparative evaluation.

**Edge Robustness Analysis Protocol.** To validate the consistency of algorithmic breakthroughs, we developed a systematic edge re-execution protocol. For each selected evolutionary transition, we perform 100 independent re-executions using identical prompt templates while maintaining all experimental conditions constant except for the LLM sampling parameters. Each re-execution employs the same parent algorithms, evolutionary operation type, and external knowledge integration templates used in the original optimization run.

The re-execution protocol preserves all deterministic components (fitness evaluation, data preprocessing, statistical analysis) while allowing natural variation in LLM-generated code through different random seeds. This approach enables quantification of discovery mechanism robustness while accounting for the inherent stochasticity in large language model outputs. Statistical

analysis employs standard descriptive metrics (mean, standard deviation) combined with confidence interval estimation to characterize the reliability of breakthrough discovery patterns, as illustrated in Figure 5(b).

**Computational Resources and Parallelization.** The numerical calculations in this study were carried out on the ORISE Supercomputer, equipped with 32-core x86 processors operating and 4 GPGPU accelerators per node, enabling efficient parallel execution of LLM API calls and algorithm evaluations. The Evo-MCTS framework employs asynchronous parallelization to maximize resource utilization, allowing multiple LLM requests to be processed concurrently while maintaining synchronization for tree updates and performance analysis. This parallelization strategy significantly reduces overall computational time while ensuring that all evaluations are performed under consistent conditions.

## 5 Data availability

The MLGWSC-1 Dataset 4 used in this study is publicly available at <https://github.com/gwastro/ml-mock-data-challenge-1/>. The dataset includes real detector noise from LIGO Hanford (H1) and Livingston (L1) observatories during the O3a observing run.

The ReEvo framework implementation is available at <https://github.com/ai4co/reevo> with the original codebase and documentation. The MCTS-AHD framework can be accessed through its official repository at <https://github.com/zz1358m/MCTS-AHD-master>. Both frameworks were used for comparative analysis following their original specifications and hyperparameter configurations.

Training and test data partitions, along with detailed preprocessing specifications, are provided in the Supplementary Material A.2. All experimental results and algorithm performance metrics are available upon reasonable request to the corresponding author.

## 6 Code availability

The complete source code for the Evo-MCTS framework is publicly available at <https://github.com/iphysresearch/evo-mcts>. The repository includes all implementation details, experimental configurations, and reproducibility instructions. Additionally, a permanent archived version is available through the Zenodo repository at <https://zenodo.org/record/10000000000000000000>. The code is written in Python and is fully reproducible with the provided environment and dependencies. The repository contains comprehensive documentation, example usage scripts, and all necessary configuration files to replicate the experimental results presented in this study.

## Acknowledgments

We thank the LIGO Scientific Collaboration for providing the MLGWSC-1 dataset and establishing the evaluation framework that enabled this research. We acknowledge the computational resources provided by the ORISE Supercomputer facility, which were essential for the large-scale LLM-based optimization experiments.

We are grateful to OpenAI, Anthropic, and DeepSeek for providing API access to their language models, which formed the core of our algorithmic discovery framework. We also thank the developers of the ReEvo and MCTS-AHD frameworks for making their implementations publicly available for comparative analysis.

H.W. is supported by the National Key Research and Development Program of China (Grant No. 2021YFC2203004), the National Natural Science Foundation of China (NSFC) (Grant Nos. 12405076, 12247187, 12147103), the National Astronomical Data Center (Grant No. NADC2023YDS-01), and the Fundamental Research Funds for the Central Universities.

**Supplementary information.**

## Appendix A Supplementary Material

### A.1 LLM Prompting Templates

This section provides comprehensive details of the prompting strategies employed across different phases of the algorithmic discovery process. The templates are designed to guide language models through systematic reasoning while incorporating domain-specific knowledge and maintaining consistency across evolutionary operations.

**System Context and Task Definition.** All interactions with the LLM ensemble begin with a standardized system prompt that establishes the expert role and problem context:

You are an expert in gravitational wave signal detection algorithms. Your task is to design heuristics that can effectively solve optimization problems. The task involves constructing a pipeline for gravitational wave signal detection. This pipeline will encompass data conditioning and time-frequency transformations as part of the signal processing workflow. The input will consist of raw, finite-length dual-channel gravitational wave data from the H1 and L1 detectors. The pipeline will be tested on segmented data spanning several weeks, with each segment having variable length (7000s -30000s). Each segment's dual-channel data will be directly used as input. The ultimate goal is to produce a catalog of potential gravitational wave signals, where each trigger includes information such as GPS time, ranking statistic, and the timing accuracy of the prediction. This systematic approach is essential for effectively identifying and cataloging candidate gravitational wave signals.

This system prompt serves multiple purposes: (i) establishing domain expertise expectations, (ii) defining the specific optimization context, (iii) specifying input data characteristics, and (iv) clarifying the expected output format and evaluation criteria.

### A.1.1 Initial Algorithm Generation Prompts

**Seed Function Template and Analysis Framework.** The initial algorithm generation process begins with a structured analysis of the seed function to establish baseline understanding. The seed function analysis template guides the LLM through systematic examination of the foundational algorithm:

```
## Seed Function Analysis Task
Analyze the foundational algorithm's design strategy to establish baseline understanding
for Monte Carlo Tree Search (MCTS) exploration. This first-level analysis will guide
subsequent optimization directions.

## Seed Function Implementation
```python
{prompt_seed_func}
```

- Technical implementation details: {prompt_other_inf}
- Performance impact rationale: {prompt_inout_inf}

## Context for Analysis
This initial analysis at MCTS depth first-level should:
- Identify core algorithmic mechanisms
- Extract fundamental processing stages
- Surface high-level optimization opportunities
- Establish baseline for diversity generation
{external_knowledge}

## Analysis Requirements
1. Characterize the seed's core approach in one sentence containing:
  - Primary computational strategy
  - Key transformation stages
  - Fundamental signal processing techniques
  - Overall optimization philosophy

2. Focus on architectural-level characteristics rather than implementation details

3. Description must fit within single braces and avoid:
  - Code references
  - Parameter-level details
  - Performance assessments
  - Comparative statements

## Output Format Rules
- Return optimization strategies within SINGLE BRACE
- Ensure entire response can be parseable by regex: \\{{{(.*)\\}} with DOTALL flag
```

**Seed Algorithm Specification.** The seed function implements a three-stage linear signal processing pipeline that serves as the evolutionary starting point:

- Stage 1: Data Conditioning and Whitening

---

```
1  def data_conditioning(strain_h1: np.ndarray, strain_l1: np.ndarray, times: np.ndarray) -> tuple[np.ndarray, np.ndarray,
↳ np.ndarray]:
2      window_length = 4096
3      dt = times[1] - times[0]
4      fs = 1.0 / dt
5
6      def whiten_strain(strain):
7          strain_zeromean = strain - np.mean(strain)
8          freqs, psd = signal.welch(strain_zeromean, fs=fs, nperseg=window_length,
9                                  window='hann', noverlap=window_length//2)
10         smoothed_psd = np.convolve(psd, np.ones(32) / 32, mode='same')
11         smoothed_psd = np.maximum(smoothed_psd, np.finfo(float).tiny)
12         white_fft = np.fft.rfft(strain_zeromean) / np.sqrt(np.interp(np.fft.rfftfreq(len(strain_zeromean), d=dt), freqs,
↳ smoothed_psd))
13         return np.fft.irfft(white_fft)
```

```

14         whitened_h1 = whiten_strain(strain_h1)
15         whitened_l1 = whiten_strain(strain_l1)
16
17     return whitened_h1, whitened_l1, times
18

```

---

### • Stage 2: Time-Frequency Decomposition

---

```

1  def compute_metric_series(h1_data: np.ndarray, l1_data: np.ndarray, time_series: np.ndarray) -> tuple[np.ndarray,
↳ np.ndarray]:
2      fs = 1 / (time_series[1] - time_series[0])
3      f_h1, t_h1, Sxx_h1 = signal.spectrogram(h1_data, fs=fs, nperseg=256, noverlap=128, mode='magnitude', detrend=False)
4      f_l1, t_l1, Sxx_l1 = signal.spectrogram(l1_data, fs=fs, nperseg=256, noverlap=128, mode='magnitude', detrend=False)
5      tf_metric = np.mean((Sxx_h1**2 + Sxx_l1**2) / 2, axis=0)
6      gps_mid_time = time_series[0] + (time_series[-1] - time_series[0]) / 2
7      metric_times = gps_mid_time + (t_h1 - t_h1[-1] / 2)
8
9      return tf_metric, metric_times

```

---

### • Stage 3: Peak Detection and Trigger Generation

---

```

1  def calculate_statistics(tf_metric, t_h1):
2      background_level = np.median(tf_metric)
3      peaks, _ = signal.find_peaks(tf_metric, height=background_level * 1.0, distance=2, prominence=background_level * 0.3)
4      peak_times = t_h1[peaks]
5      peak_heights = tf_metric[peaks]
6      peak_deltat = np.full(len(peak_times), 10.0) # Fixed uncertainty value
7      return peak_times, peak_heights, peak_deltat

```

**Template Variables and Customization.** The prompting template incorporates several customizable variables that enable systematic variation generation:

- `prompt_seed_func`: Complete seed function implementation
- `prompt_other_inf`: Technical implementation details including sampling rates, window parameters, and algorithmic constraints
- `prompt_inout_inf`: Performance impact rationale explaining the relationship between input characteristics and expected output quality
- `external_knowledge`: Domain-specific knowledge injection including gravitational wave physics, detector characteristics, and signal morphology constraints

**Output Format Requirements.** All generated algorithms must conform to the standardized interface:

---

```

1  def pipeline_v(N)(strain_h1: np.ndarray, strain_l1: np.ndarray, times: np.ndarray) -> tuple[np.ndarray, np.ndarray,
↳ np.ndarray]:
2      # Algorithm implementation for seed function
3      # ...
4      # Stage 1: Data Conditioning and Whitening
5      whitened_h1, whitened_l1, data_times = data_conditioning(strain_h1, strain_l1, times)
6      # Stage 2: Time-Frequency Decomposition
7      tf_metric, metric_times = compute_metric_series(whitened_h1, whitened_l1, data_times)
8      # Stage 3: Peak Detection and Trigger Generation
9      peak_times, peak_heights, peak_deltat = calculate_statistics(tf_metric, metric_times)
10     return peak_times, peak_heights, peak_deltat

```

---

This interface consistency ensures that all generated algorithms can be evaluated within the same framework while enabling diverse internal implementations.

### A.1.2 Parent Crossover Implementation

The Parent Crossover (PC) operation represents a sophisticated genetic operation that combines algorithmic components from two reference implementations at different levels of the MCTS hierarchy. This operation is designed to preserve successful characteristics from both parent algorithms while introducing novel enhancements that exceed simple interpolation.

**Template Structure and Crossover Strategy.** The PC operation employs a structured template that guides the LLM through systematic analysis and synthesis of two parent algorithms:

```

## Task Overview
Develop a novel algorithm that strategically combines components from two reference
implementations while introducing innovative enhancements. The solution must demonstrate
measurable improvements beyond simple interpolation of existing approaches.
Current Depth Level: [Level {depth}]

## Implementation Analysis
### Code Comparison
1. VERSION A (Baseline Implementation):
```python
{worse_code}
```

2. VERSION B (Enhanced Implementation):
```python
{better_code}
```

### Strengths to Combine
```text
{reflection}
```

Key Synthesis Requirements:
- Preserve 2 distinct advantages from Version A
- Incorporate 3 critical enhancements from Version B
- Identify 1 synergistic improvement opportunity

## Architecture Strategy
{external_knowledge}

### Depth-Specific Synthesis Guidelines (Depth={depth})
1. Structural Synthesis (Depth 1-2):
  - Create hybrid control flow combining best elements from both versions
  - Example: "Combine Version A's iteration structure with Version B's termination
  conditions"
  - Forbid direct replication of either version's architecture

2. Implementation Fusion (Depth 3-4):
  - Develop novel parameter hybridization techniques
  - Example: "Blend Version A's exploration mechanism with Version B's exploitation
  strategy"
  - Require at least one innovative combination per functional module

3. Mathematical Innovation (Depth 5+):
  - Derive new computational operators through version synthesis
  - Example: "Fuse Version A's approximation method with Version B's error correction"
  - Mandate 10-20% computational complexity reduction

```

This template structure ensures that the crossover operation is not merely concatenative but involves intelligent analysis and strategic combination of algorithmic strengths.

**Depth-Adaptive Synthesis Guidelines.** The PC operation implements depth-specific strategies that adapt the crossover complexity based on the current position in the MCTS tree:

- Structural Synthesis (Depth 1-2):
  - Focuses on combining high-level architectural elements from both parent algorithms
  - Creates hybrid control flow structures that merge the best organizational patterns
  - Example directive: “Combine Version A’s iteration structure with Version B’s termination conditions”
  - Explicitly forbids direct replication of either parent’s complete architecture
- Implementation Fusion (Depth 3-4):
  - Emphasizes parameter hybridization and functional module integration
  - Develops novel approaches to blend algorithmic strategies
  - Example directive: “Blend Version A’s exploration mechanism with Version B’s exploitation strategy”
  - Requires at least one innovative combination per functional module
- Mathematical Innovation (Depth 5+):
  - Derives new computational operators through sophisticated version synthesis
  - Focuses on mathematical justification for algorithmic improvements
  - Example directive: “Fuse Version A’s approximation method with Version B’s error correction”
  - Mandates 10-20% computational complexity reduction alongside performance gains

**Innovation Requirements and Quality Assurance.** The PC operation enforces strict innovation standards to ensure that generated algorithms represent genuine improvements:

- Core Innovation Targets:
  - Synthesize 3+ novel elements not present in either parent version
  - Resolve 2 fundamental limitations identified through comparative analysis
  - Introduce 1 breakthrough enhancement with rigorous mathematical justification
  - Demonstrate non-trivial performance gains over both parent algorithms
  - Prohibit direct replication of complete code blocks from either parent

**Reflection Generation Process.** Before conducting the crossover synthesis, the system generates analytical insights through a depth-adaptive reflection template:

## Task Objective

Analyze optimization patterns across algorithm versions and generate depth-specific improvement strategies. Current MCTS Depth: depth/max\_depth={depth}/{max\_depth}

```

## Depth-Specific Focus
- Shallow (Depth 1-2): Structural patterns & control flow
- Medium (Depth 3-4): Implementation techniques & parameterization
- Deep (Depth 5+): Mathematical formulations & computational primitives

## Algorithm Comparison
- Original (Suboptimal)
  ```python
{code_worse}
  ```
- Improved (Optimized)
  ```python
{code_better}
  ```

## Depth-Adaptive Analysis
### 1. Core Pattern Extraction
For {depth}-level analysis:
- Shallow: Compare control structures/algorithmic paradigms
- Medium: Analyze parameter configurations/function compositions
- Deep: Examine mathematical operators/numerical methods

### 2. Optimization Principle Generation
Generate 3-5 transferable rules that:
- Directly address {depth}-specific limitations
- Contain concrete parameter values from improved version
- Maintain functional equivalence

## Output Format Rules
- Return optimization strategies within SINGLE BRACE
- Ensure entire response can be parseable by regex: \{\{(.*)\}\} with DOTALL flag

```

This reflection generation produces the `reflection` variable used in the main crossover template.

**Reflection-Guided Analysis.** The crossover process incorporates a reflection component that analyzes the strengths and weaknesses of both parent algorithms:

```

## Requirements
1. Core Innovation Targets:
  - Synthesize 3+ novel elements not present in either version
  - Resolve 2 fundamental limitations identified in analysis
  - Introduce 1 breakthrough enhancement with mathematical justification
  - Demonstrate non-trivial performance gain over both versions
  - Prohibit direct replication of complete code blocks

```

This reflection analysis is generated through the `deepseek-r1-250120` model and provides crucial insights that guide the synthesis process. The reflection identifies:

- Computational advantages in each parent algorithm
- Structural design patterns that contribute to performance
- Potential synergistic combinations that could yield emergent benefits
- Limitation patterns that should be addressed in the offspring

**Output Format and Validation.** The PC operation enforces a standardized output format that ensures both human readability and automated processing:

2. Output Format:

- Place the core design idea in a sentence within a brace BEFORE the function definition
- For the core design idea format: `\{\{A hybrid gravitational wave detection pipeline...\}\}`
- Implement as Python function: `{func_name}`
- Inputs: `{input_count}` parameter(s) (`{joined_inputs}`)
- Outputs: `{output_count}` return value(s) (`{joined_outputs}`)
- Follow: `{inout_inf}`
- Constraints: `{other_inf}`
- IMPORTANT: All output code MUST be valid Python syntax. Do not place description text inside curly braces within the function body.
- Example of correct format:
 

```

\{\{Core design description here\}\}
-- python
def pipeline_v2(strain_h1: np.ndarray, strain_l1: np.ndarray, times: np.ndarray) ->
tuple[np.ndarray, np.ndarray, np.ndarray]:
    """Core design description can alternatively be placed here as a docstring"""
    # Function implementation...
...


```

### A.1.3 Sibling Crossover Implementation

The Sibling Crossover (SC) operation implements a sophisticated two-phase approach that leverages peer algorithm insights to generate improved offspring. Unlike Parent Crossover, which combines algorithms from different hierarchical levels, SC focuses on horizontal knowledge transfer between algorithms at the same MCTS depth, promoting diversity while maintaining comparable complexity levels.

**Two-Phase Architecture.** The SC operation employs a unique two-stage process: first generating optimization hints through multi-level reflection analysis (Phase 1), then implementing concrete algorithmic improvements based on these insights (Phase 2). This separation enables more targeted optimization by allowing the system to first identify improvement opportunities before implementing solutions.

**Phase 1: Multi-Level Reflection Analysis.** The first phase generates depth-specific optimization hints by synthesizing insights from sibling algorithms and parent-level analysis:

```

## Task Overview
Generate depth-specific optimization hints for gravitational wave detection algorithms by synthesizing multi-level reflections.
Current Optimization Depth: {parent_depth}/{max_depth} (shallow: structural patterns, medium: implementation techniques, deep: mathematical details)

## Contextual Insights
1. Peer Algorithm Reflections (Depth {parent_depth}):
  - Formatted as performance-annotated entries: [No.N Brother Reflection Score: X] <reflection>
  - Time-ordered weighting (newest=highest priority) with objective score-based ranking
  - Includes full technical post-mortems from immediate ancestors
{parent_reflections}

2. Father Algorithm Analysis (Depth {father_depth}):
{father_reflection}

## Hint Generation Requirements
1. Produce 3-5 executable optimization directives that:
  - Integrate cross-depth insights from peer implementations
  - Target {parent_depth}-level (shallow: structural patterns, medium: implementation techniques, deep: mathematical details) components for improvement
  - Formulate mathematically sound enhancements

```

- Align with gravitational wave data processing objectives
2. Output Format Rules
- Return optimization strategies within SINGLE BRACE
  - Ensure entire response can be parseable by regex: `\\{\\{(.*)\\}\\}` with DOTALL flag
  - Focus on {parent\_depth}-appropriate modifications
  - Emphasize time-domain processing optimizations
- ## Critical Constraints
- Each directive must correspond to concrete code changes
  - Explicitly connect to reflection insights where applicable
  - Maintain strict {parent\_depth}-level focus in all suggestions
  - Exclude explanatory text within the hint brace
  - Prioritize modifications matching current depth's optimization type

**Sibling Selection and Weighting Strategy.** The SC operation employs a sophisticated parent selection mechanism that prioritizes high-performing sibling algorithms:

---

```

1 # Select parents based on objective value weights
2 other = [ind for ind in pop if ind['code'] != father['code']]
3 weights = [1.0 / (-ind['fitness'] + 1e-10) for ind in other] # Lower objective = higher weight
4 normalized_weights = [w / sum(weights) for w in weights]
5 parents = random.choices(other, weights=normalized_weights, k=min(self.m, len(other)))

```

---

This weighting strategy ensures that successful algorithmic patterns from high-performing siblings are more likely to influence the offspring generation process.

**Depth-Adaptive Optimization Focus.** The first phase implements depth-specific optimization strategies that adapt to the current position in the MCTS tree:

- Shallow Depth (1-2): Focuses on structural patterns and control flow restructuring
- Medium Depth (3-4): Emphasizes implementation techniques and numerical optimizations
- Deep Depth (5+): Concentrates on mathematical details and advanced computational methods

**Phase 2: Concrete Algorithm Implementation.** The second phase transforms the optimization hints into executable algorithms:

```

## Algorithm Optimization Task
Develop an enhanced gravitational signal processing algorithm for interferometer data
analysis by implementing concrete improvements from multi-level code analysis.

## Technical Context
1. Optimization Depth Specifications:
- Current Focus Level: {depth} (max_depth={max_depth})
  (1-2: Control flow restructuring, 3-4: Numerical computation optimizations, 5+:
  Advanced linear algebra methods)
- Code Analysis Insights from Prior Level:
```text
{reflection}
```

2. Base Implementation Details:
[Functional Purpose] {algorithm_description}
[Core Implementation]
```python
{algorithm_code}

```

```

...

## Implementation Directives (Depth {depth}):
- Shallow (1-2): Restructure control flow using reflection suggestion (e.g., split data
conditioning/analysis phases)
- Medium (3-4): Apply numerical optimizations from reflection (e.g., FFT window size
optimization)
- Deep (5+): Implement matrix computation improvements from reflection (e.g., regularized
inverse covariance)

{external_knowledge}

## Output Format
- Place the core design idea in a sentence within a brace BEFORE the function definition
- For the core design idea format: \\{A hybrid gravitational wave detection pipeline...}
- Implement as Python function: {func_name}
- Inputs: {input_count} parameter(s) ({joined_inputs})
- Outputs: {output_count} return value(s) ({joined_outputs})
- Follow: {inout_inf}
- Constraints: {other_inf}
- IMPORTANT: All output code MUST be valid Python syntax. Do not place description text
inside curly braces within the function body.
- Example of correct format:
  \\{Core design description here}
  ```python
  def pipeline_v2(strain_h1: np.ndarray, strain_l1: np.ndarray, times: np.ndarray) ->
  tuple[np.ndarray, np.ndarray, np.ndarray]:
      """Core design description can alternatively be placed here as a docstring"""
      # Function implementation...
  ...

## Important Notes
- Focus on algorithmic improvements rather than code style changes
- Ensure the new implementation directly addresses the reflection insights

```

**Reflection Processing and Template Variables.** The SC operation processes multiple sources of algorithmic insight through structured template variables:

- `parent_reflections`: Performance-annotated reflections from peer algorithms, formatted as ranked entries with objective scores
- `father_reflection`: Analysis from the immediate parent algorithm at depth-1
- `reflection`: Synthesized optimization hints generated in Phase 1
- `algorithm_description`: Functional description of the base algorithm
- `algorithm_code`: Complete implementation of the parent algorithm

**Quality Assurance and Validation.** The two-phase approach enables comprehensive quality control:

- Phase 1 Validation:
  - Ensures reflection insights are depth-appropriate
  - Validates mathematical soundness of optimization suggestions
  - Confirms alignment with gravitational wave processing objectives
- Phase 2 Validation:
  - Verifies syntactic correctness of generated code
  - Confirms interface compliance with standardized function signatures

- Tests algorithmic improvements against reflection insights
- Validates computational efficiency claims

**Temporal Weighting and Performance Ranking.** The SC operation implements sophisticated temporal weighting that prioritizes recent algorithmic discoveries while maintaining objective score-based ranking:

- Time-ordered weighting: Newer algorithms receive higher priority in the reflection synthesis
- Performance-based ranking: Algorithms with better objective scores contribute more heavily to the optimization hints
- Cross-depth integration: Insights from both peer algorithms and parent-level analysis are systematically combined

This comprehensive approach ensures that SC operations generate algorithms that not only improve upon their immediate ancestors but also incorporate the collective intelligence of high-performing siblings, leading to more robust and efficient gravitational wave detection strategies.

#### A.1.4 Point Mutation Implementation

Point Mutation (PM) operations introduce targeted modifications to individual algorithms based on performance analysis, implementing two distinct approaches that offer different levels of sophistication and computational investment. The framework provides both single-stage direct improvement and two-stage reflection-driven enhancement strategies.

##### Single-Stage Point Mutation: Direct Algorithm Improvement.

The operation implements a straightforward approach that directly compares an original algorithm with a high-performing elite algorithm to generate improvements. This method prioritizes computational efficiency while maintaining effective algorithmic enhancement.

Template Structure:

```
## Task Overview
You will analyze an original algorithm, an improved version of it, and create a new
enhanced algorithm. Below are the key components:

## Algorithm Details
1. ORIGINAL ALGORITHM:
  - Description: {original_algorithm_description}
  - Code:
  ```python
  {original_algorithm_code}
  ```
  - Objective Value: {original_objective_value}

2. BETTER ALGORITHM (Reference Implementation):
  - Description: {better_algorithm_description}
  - Code:
  ```python
  {better_algorithm_code}
  ```
  - Objective Value: {better_objective_value}
  - Improvement Insights:
  ```text
  {better_algorithm_reflection}
```

...

```

## Implementation Requirements
1. Analyze the differences between the original and better algorithms
2. Create a new algorithm that:
  - Incorporates successful elements from the better algorithm
  - Addresses limitations revealed in the improvement insights
  - Produces better results than the original algorithm
3. Output format requirements:
  - Place the core design idea in a sentence within a brace BEFORE the function
  definition
  - For the core design idea format: \\{{A hybrid gravitational wave detection pipeline
  ...}}
  - Implement as Python function: {func_name}
  - Inputs: {input_count} parameter(s) ({joined_inputs})
  - Outputs: {output_count} return value(s) ({joined_outputs})
  - Follow: {inout_inf}
  - Constraints: {other_inf}
  - IMPORTANT: All output code MUST be valid Python syntax. Do not place description text
  inside curly braces within the function body.
  - Example of correct format:
    \\{{Core design description here}}
    ```python
    def pipeline_v2(strain_h1: np.ndarray, strain_l1: np.ndarray, times: np.ndarray) ->
      tuple[np.ndarray, np.ndarray, np.ndarray]:
        """Core design description can alternatively be placed here as a docstring"""
        # Function implementation...
    ```
{external_knowledge}

## Important Notes
- Focus on algorithmic improvements rather than code style changes
- Ensure the new implementation directly addresses the reflection insights

```

**Two-Stage Point Mutation: Reflection-Driven Enhancement.** The operation implements a sophisticated two-phase approach that mirrors the sibling crossover methodology but focuses on individual algorithm improvement rather than horizontal knowledge transfer.

**Phase 1: Strategic Reflection Generation.** The first phase synthesizes insights from multiple sources to generate comprehensive optimization guidelines:

```

## Task Overview
Generate optimized technical guidelines for gravitational wave detection algorithms through
systematic analysis of multi-generational reflection insights. Focus on enhancing data
conditioning pipelines, time-frequency analysis methods, noise suppression techniques, and
H1-L1 detector coherence optimization. Produce executable directives addressing: waveform
recognition precision, computational complexity management, and non-stationary noise
differentiation while maintaining strict API compliance.

## Input Context
1. NEW INSIGHTS FROM RECENT ITERATIONS:
  - Formatted as performance-annotated entries: [Parent N Reflection Score: X]<
  reflection>
  - Time-ordered weighting (newest=highest priority) with objective score-based ranking
  - Includes full technical post-mortems from immediate ancestors
{parent_reflections}

2. LONG-TERM REFLECTION REPOSITORY:
  - Contains battle-tested insights from top 1% performers
  - 3x weighting factor for architectural-level insights
  - Curated through 3-stage filtration:
    1. Statistical significance validation
    2. Cross-generational effectiveness verification
    3. Compatibility check with current detector configurations

```

```

{elite_reflection}

## Implementation Requirements
1. Perform weighted synthesis of reflections
2. Generate 3-5 technically-grounded optimization directives
3. Prioritize:
  - Mitigation of historical implementation flaws
  - Amplification of proven effective patterns
  - Weighted integration of multi-generational insights

## Output Format
- Return all guidelines within SINGLE BRACE
- Ensure entire response can be parseable by regex: \\{{{(.*)\\}} with DOTALL flag
- Concrete technical directives only
- No explanatory text or formatting

Phase 2: Concrete Algorithm Implementation. The second phase
transforms the strategic insights into executable algorithmic improvements:

## Task Overview
Leverage insights from prior strategic reflection to architecturally enhance the
gravitational wave detection algorithm. Develop improvements that directly address
identified limitations in CRITICAL REFLECTION INSIGHTS while preserving core functionality
through:

1. Stage-level architectural modifications informed by reflection analysis
2. Reflection-driven noise reduction and coherence enhancement strategies
3. Time-frequency analysis variations targeting specific weaknesses identified
4. H1-L1 synthesis improvements based on cross-detector insights

Generate architecturally distinct variants that implement reflection-derived concepts
through fundamental structural changes.

## Input Context
1. CRITICAL REFLECTION INSIGHTS (Improvement Basis):
...text
{reflection}
...

2. REFERENCE IMPLEMENTATION:
[Description] {elite_algorithm_description}
[Baseline Code]
...python
{elite_algorithm_code}
...

## Implementation Requirements
1. Execute reflection-guided analysis:
  - Map reflection insights to specific code components
  - Identify 2-3 architectural limitations in current implementation
2. Propose improvements that directly convert reflection insights into:
  - Enhanced signal path architecture
  - Novel noise handling structures
  - Optimized computational patterns
  - Advanced detector synergy mechanisms
3. Maintain strict interface compatibility with existing system integration

{external_knowledge}

## Output Format
- Place the core design idea in a sentence within a brace BEFORE the function definition
- For the core design idea format: \\{{A hybrid gravitational wave detection pipeline...}}
- Implement as Python function: {func_name}
- Inputs: {input_count} parameter(s) ({joined_inputs})
- Outputs: {output_count} return value(s) ({joined_outputs})
- Follow: {inout_inf}
- Constraints: {other_inf}

```

```

- IMPORTANT: All output code MUST be valid Python syntax. Do not place description text
inside curly braces within the function body.
- Example of correct format:
  \{\{Core design description here\}\}
  ```python
  def pipeline_v2(strain_h1: np.ndarray, strain_l1: np.ndarray, times: np.ndarray) ->
  tuple[np.ndarray, np.ndarray, np.ndarray]:
  """Core design description can alternatively be placed here as a docstring"""
  # Function implementation...
  ...

## Important Notes
- Focus on algorithmic improvements rather than code style changes
- Ensure the new implementation directly addresses the reflection insights

```

**Selection Strategies and Elite Integration.** Both PM operations leverage the elite offspring as a performance benchmark and source of successful algorithmic patterns. The key distinction lies in their selection strategies:

- Single-Stage Selection Strategy:
  - Selects a single parent algorithm from the population (excluding the elite)
  - Directly compares parent performance with elite offspring
  - Implements immediate improvement through direct analysis
- Two-Stage Selection Strategy:
  - Selects multiple parent algorithms for comprehensive reflection analysis
  - Incorporates both recent algorithmic insights and long-term elite patterns
  - Implements sophisticated multi-generational knowledge synthesis

**Computational Efficiency Considerations.** The two PM approaches offer different computational trade-offs:

- Single-Stage Advantages:
  - Single-stage processing reduces computational overhead
  - Direct comparison enables rapid algorithm improvement
  - Simplified prompting reduces LLM token consumption
- Two-Stage Advantages:
  - Two-stage processing enables more sophisticated optimization
  - Multi-generational insight integration leads to more robust improvements
  - Reflection-driven approach produces more interpretable algorithmic modifications

**Template Variable Integration.** Both PM operations incorporate comprehensive template variables that enable systematic algorithmic improvement:

- Common Variables:
  - `func_name`, `input_count`, `output_count`: Interface specification
  - `joined_inputs`, `joined_outputs`: Parameter documentation
  - `better_algorithm_description`, `better_algorithm_code`: Elite algorithm details

- `original_objective_value`, `better_objective_value`: Performance metrics
- `better_algorithm_reflection`: Elite algorithm insights
- Two-Stage Variables:
  - `parent_reflections`: Multi-parent reflection synthesis
  - `elite_reflection`: Long-term elite insights
  - `reflection`: Generated optimization guidelines

**Quality Assurance and Validation.** Both PM operations implement rigorous validation procedures:

- Single-Stage Validation:
  - Direct performance comparison with both parent and elite algorithms
  - Verification of improvement insight integration
  - Confirmation of interface compliance
- Two-Stage Validation:
  - Two-stage validation covering both reflection generation and implementation
  - Cross-generational consistency checking
  - Architectural improvement verification

The dual PM approach provides flexibility in algorithmic improvement strategies, enabling the framework to adapt to different optimization scenarios while maintaining consistent quality standards and interface compliance.

### A.1.5 Path-wise Crossover Implementation

Path-wise Crossover (PWC) operations synthesize information along complete root-to-leaf trajectories in the MCTS tree, capturing long-range dependencies and enabling global optimization strategies. The framework implements two distinct PWC approaches that differ in their analytical methodologies: reflection-based synthesis and comprehensive algorithm analysis.

**Reflection-Based Path-wise Crossover: Multi-Algorithm Insight Synthesis.** The operation implements a two-stage process that analyzes reflection patterns across multiple algorithms in a complete MCTS path to identify generalizable optimization principles.

**Phase 1: Cross-Algorithm Pattern Analysis.** The first phase extracts recurring technical strategies from multiple algorithm reflections:

```
## Task Overview
Analyze and synthesize technical reflections from multiple algorithm iterations to identify
cross-algorithm optimization patterns and guide next-generation algorithm design.
Prioritize extraction of generalizable technical principles over implementation-specific
details.
Current Optimization Depth: depth/max_depth={depth}/{max_depth} (shallow: structural
patterns, medium: implementation techniques, deep: mathematical details)

## Input Context
```

Analyzing {num\_algorithms} algorithm reflections from MCTS exploration trajectories. Technical reflections follow depth-specific analysis requirements. Structural format: [No.N algorithm's reflection (depth: X)]<reflection> {algorithm\_reflections}

#### ## Reflection Requirements

- Pattern Identification** (Key Observed Patterns):
  - Extract 2-3 recurring technical strategies (e.g. "Multi-scale wavelet decomposition" not "used Morlet wavelet")
  - Categorize by analysis level:
    - Structural: Component architecture (e.g. "Parallel filter banks")
    - Implementation: Algorithmic choices (e.g. "Adaptive thresholding")
    - Mathematical: Core transforms (e.g. "Orthogonal matching pursuit")
- Technical Pathway Analysis** (Promising Technical Pathways):
  - Identify under-utilized but theoretically sound approaches (e.g. "Sparse representation in frequency domain")
  - Specify required technical components without code details (e.g. "Requires: Overcomplete basis construction")
- Optimization Principles** (Strategic Optimization Principles):
  - Formulate depth-specific guidelines (e.g. "At mathematical level: Maximize time-frequency product  $\leq 0.5$ ")
  - Relate physical constraints to algorithmic parameters (e.g. "Wavelet duration should match typical glitch durations")
- Specificity Balance**:
  - Technical specificity: Name mathematical concepts (e.g. "Gabor uncertainty") and signal processing domains
  - Implementation avoidance: Omit code structures (e.g. "Avoid: 'Use 3 nested loops'")

#### ## Output Format Rules

- Return optimization strategies within SINGLE BRACE
- Ensure entire response can be parseable by regex: `\{\{(.*)\}\}` with DOTALL flag
- Do not include markdown formatting or additional explanations

**Phase 2: Algorithm Implementation.** The second phase transforms the synthesized insights into concrete algorithmic improvements:

#### ## Task Overview

Develop an enhanced gravitational wave detection algorithm through targeted modifications addressing specific technical shortcomings identified in the reflection analysis.

#### ## Input Context

```
[Critical Reflection Insights]
```text
{reflection}
```
```

```
[Baseline Implementation]
[Functional Description] {algorithm_description}
[Current Codebase]
```python
{algorithm_code}
```
```

```
{external_knowledge}
```

#### ## Output Format

- Place the core design idea in a sentence within a brace BEFORE the function definition
- For the core design idea format: `\{\{A hybrid gravitational wave detection pipeline...\}\}`
- Implement as Python function: `{func_name}`
- Inputs: `{input_count} parameter(s) ({joined_inputs})`
- Outputs: `{output_count} return value(s) ({joined_outputs})`
- Follow: `{inout_inf}`
- Constraints: `{other_inf}`
- IMPORTANT:** All output code MUST be valid Python syntax. Do not place description text inside curly braces within the function body.

```
- Example of correct format:
\\{{Core design description here}}
```python
def pipeline_v2(strain_h1: np.ndarray, strain_l1: np.ndarray, times: np.ndarray) -> tuple
[np.ndarray, np.ndarray, np.ndarray]:
    """Core design description can alternatively be placed here as a docstring"""
    # Function implementation...
...

## Important Notes
- Focus on algorithmic improvements rather than code style changes
- Ensure the new implementation directly addresses the reflection insights
```

**Comprehensive Algorithm Analysis Path-wise Crossover: Multi-Level Technical Synthesis.** The operation implements a more sophisticated analytical approach that examines complete algorithm implementations across different depth levels.

**Phase 1: Multi-Level Technical Analysis.** The first phase conducts comprehensive analysis of algorithms along the complete MCTS path:

```
## Task Objective
Synthesize technical insights from algorithm evolution MCTS path to guide targeted
improvements. Current Analysis Level: depth/max_depth={depth}/{max_depth} (1-2: structural,
3-4: implementation, 5+: mathematical)

## Depth-Specific Focus
- Shallow (Depth 1-2): Structural patterns & control flow
- Medium (Depth 3-4): Implementation techniques & parameterization
- Deep (Depth 5+): Mathematical formulations & computational primitives

## Input Context
Analyzing {num_algorithms} algorithm reflections from MCTS exploration trajectories.
Technical reflections follow depth-specific analysis requirements. Structural format: [No.N
algorithm's reflection (depth: X)]<description><objective><code>
{parent_info}

## Synthesis Process
1. Cross-Level Insight Integration:
  - Identify key recurring technical strategies across abstraction levels
  - Note level-specific constraints affecting current implementations

2. Domain Compliance Verification:
  - Validate approaches against gravitational wave signal characteristics
  - Check numerical reliability across different implementation levels

3. Improvement Planning:
  - Structural: Adjust data processing pipelines
  - Implementation: Optimize critical parameter relationships
  - Mathematical: Enhance core transformation components

## Technical Workflow
### 1. Multi-Level Technical Analysis
Structural -> Compare module composition and interaction patterns
Implementation -> Assess parameter sensitivity and adaptation logic
Mathematical -> Examine transformation kernels and precision handling

### 2. Level-Appropriate Optimization
For current depth={depth}:
  - Select 2-4 improvement focus areas with technical rationale
  - Define implementation requirements for each focus area
  - Establish verification criteria with domain constraints

## Output Format Rules
- Return optimization strategies within SINGLE BRACE
- Ensure entire response can be parseable by regex: \\{{(.*?)\\}} with DOTALL flag
- Do not include markdown formatting or additional explanations
```

**Phase 2: Algorithm Implementation.** The operation shares the same implementation phase as the reflection-based path-wise crossover, utilizing the reflection-based PWC template for consistent output formatting and algorithmic generation.

**Methodological Distinctions.** The key differences between the reflection-based path-wise crossover and the comprehensive algorithm analysis PWC lie in their analytical strategies:

- Reflection-Based PWC:
  - Focuses on synthesizing existing reflection insights from multiple algorithms
  - Emphasizes pattern recognition across previously analyzed algorithmic behaviors
  - Prioritizes extraction of generalizable technical principles over implementation details
  - Categorizes insights by structural, implementation, and mathematical analysis levels
- Comprehensive Algorithm Analysis PWC:
  - Conducts direct analysis of complete algorithm implementations
  - Examines algorithmic components across multiple depth levels simultaneously
  - Integrates cross-level insights through systematic technical workflow
  - Emphasizes domain compliance verification and improvement planning

**Depth-Adaptive Processing.** Both PWC operations implement depth-specific analysis strategies that adapt to the current position in the MCTS tree:

- Shallow Depth Focus (1-2):
  - Structural patterns and component architecture analysis
  - Control flow restructuring and module composition optimization
  - Data processing pipeline adjustments
- Medium Depth Focus (3-4):
  - Implementation techniques and algorithmic parameter optimization
  - Critical parameter relationship assessment
  - Numerical computation enhancement strategies
- Deep Depth Focus (5+):
  - Mathematical formulation analysis and computational primitive optimization
  - Transformation kernel examination and precision handling
  - Advanced linear algebra method integration

**Path Trajectory Analysis.** Both operations process algorithms along complete MCTS paths, with depth tracking that enables comprehensive evolutionary analysis:

- Reflection-Based PWC Path Processing:
  - Analyzes reflection patterns from algorithms at decreasing depth levels
  - Tracks depth-specific insights through structured format annotations
  - Synthesizes cross-depth technical strategies for optimization guidance
- Comprehensive Algorithm Analysis PWC Path Processing:
  - Examines complete algorithm implementations with performance metrics
  - Integrates algorithmic descriptions, objective values, and code analysis
  - Conducts multi-level technical synthesis across the entire path trajectory

**Template Variable Integration.** Both PWC operations incorporate sophisticated template variables that enable comprehensive path analysis:

- Common Variables:
  - `depth`, `max_depth`: Depth-specific processing parameters
  - `num_algorithms`: Path length and analysis scope
  - `func_name`, `input_count`, `output_count`: Interface specifications
  - `external_knowledge`: Domain knowledge integration
- Reflection-Based PWC Variables:
  - `algorithm_reflections`: Multi-algorithm reflection synthesis
  - `reflection`: Generated optimization insights
- Comprehensive Algorithm Analysis PWC Variables:
  - `parent_info`: Complete algorithm implementation details
  - `current_algorithm_description`, `current_algorithm_code`: Baseline algorithm specifications
  - `current_objective_value`: Performance reference metrics

**Quality Assurance and Validation.** Both PWC operations implement comprehensive validation procedures:

- Reflection-Based PWC Validation:
  - Pattern identification verification across multiple algorithm reflections
  - Technical pathway analysis consistency checking
  - Optimization principle formulation validation
- Comprehensive Algorithm Analysis PWC Validation:
  - Multi-level technical analysis coherence verification
  - Domain compliance checking across different implementation levels
  - Cross-level insight integration validation

The dual PWC approach provides complementary strategies for capturing long-range dependencies in the MCTS tree, enabling the framework to synthesize insights across complete evolutionary trajectories while maintaining depth-specific optimization focus and domain knowledge integration.

### A.1.6 Domain Knowledge Integration

Domain knowledge integration serves as a critical component that ensures generated algorithms remain grounded in gravitational wave detection principles while encouraging exploration beyond traditional linear processing methods. The framework incorporates specialized domain expertise through structured knowledge templates that guide algorithmic development toward physically meaningful and computationally efficient solutions.

**External Knowledge Template Structure.** The domain knowledge integration employs a comprehensive template that emphasizes non-linear processing approaches and adaptive algorithmic strategies:

```
### External Knowledge Integration
1. Non-linear Processing Core Concepts:
  - Signal Transformation:
    * Non-linear vs linear decomposition
    * Adaptive threshold mechanisms
    * Multi-scale analysis

  - Feature Extraction:
    * Phase space reconstruction
    * Topological data analysis
    * Wavelet-based detection

  - Statistical Analysis:
    * Robust estimators
    * Non-Gaussian processes
    * Higher-order statistics

2. Implementation Principles:
  - Prioritize adaptive over fixed parameters
  - Consider local vs global characteristics
  - Balance computational cost with accuracy
```

**Non-linear Processing Emphasis.** The domain knowledge framework explicitly prioritizes non-linear algorithmic approaches over traditional linear methods, recognizing that gravitational wave signals exhibit complex, transient characteristics that require sophisticated analysis techniques. This emphasis addresses fundamental limitations in conventional matched filtering approaches that rely heavily on linear processing assumptions.

**Signal Transformation Guidance.** The domain knowledge provides specific guidance on signal transformation strategies that leverage advanced signal processing concepts:

- **Non-linear vs Linear Decomposition:** The framework encourages exploration of non-linear decomposition methods that can capture complex signal morphologies beyond the capabilities of traditional Fourier-based approaches. This includes techniques such as empirical mode decomposition, intrinsic mode functions, and adaptive basis construction.

- **Adaptive Threshold Mechanisms:** Rather than employing fixed threshold values, the domain knowledge promotes adaptive thresholding strategies that respond to local signal characteristics and noise conditions. This approach enables more robust detection performance across diverse observational scenarios.
- **Multi-scale Analysis:** The framework emphasizes multi-scale signal analysis techniques that can simultaneously capture both short-duration transient signals and longer-duration continuous wave sources. This includes wavelet-based methods, time-frequency analysis, and hierarchical decomposition strategies.
- **Feature Extraction Methodologies.** The domain knowledge incorporates advanced feature extraction approaches that extend beyond traditional signal processing paradigms:
  - **Phase Space Reconstruction:** The framework encourages exploration of phase space reconstruction techniques that can reveal hidden dynamical structures in gravitational wave data. This includes embedding dimension analysis, recurrence analysis, and attractor reconstruction methods.
  - **Topological Data Analysis:** The domain knowledge promotes topological data analysis approaches that can identify persistent features and structural patterns in high-dimensional gravitational wave data. This includes persistent homology, Mapper algorithms, and topological feature extraction.
  - **Wavelet-based Detection:** The framework emphasizes wavelet-based detection strategies that can provide optimal time-frequency resolution for transient signal analysis. This includes continuous wavelet transforms, discrete wavelet decomposition, and wavelet packet analysis.
- **Statistical Analysis Enhancement.** The domain knowledge integrates sophisticated statistical analysis techniques that account for the complex noise characteristics of gravitational wave detectors:
  - **Robust Estimators:** The framework promotes robust statistical estimators that can maintain performance in the presence of outliers and non-Gaussian noise distributions. This includes median-based estimators, M-estimators, and trimmed mean approaches.
  - **Non-Gaussian Processes:** The domain knowledge emphasizes analysis techniques that can handle non-Gaussian noise processes commonly encountered in gravitational wave data. This includes heavy-tailed distributions, skewed probability models, and non-stationary noise characterization.
  - **Higher-order Statistics:** The framework encourages exploration of higher-order statistical moments and cumulants that can capture subtle signal characteristics beyond second-order analysis. This includes bispectrum analysis, higher-order moment estimation, and polyspectral techniques.

- **Implementation Principles and Constraints.** The domain knowledge provides specific implementation principles that guide algorithmic development toward practical and efficient solutions:
  - **Adaptive Parameter Prioritization:** The framework emphasizes adaptive parameter selection over fixed parameter values, enabling algorithms to respond dynamically to changing signal and noise conditions. This principle encourages exploration of learning-based parameter adjustment, feedback control mechanisms, and online adaptation strategies.
  - **Local vs Global Characteristics:** The domain knowledge promotes consideration of both local signal characteristics and global data patterns, enabling algorithms to balance fine-grained analysis with comprehensive signal understanding. This includes local stationarity analysis, global trend estimation, and multi-resolution processing approaches.
  - **Computational Cost-Accuracy Balance:** The framework provides guidance on balancing computational efficiency with detection accuracy, ensuring that generated algorithms remain practical for real-time implementation while maintaining scientific rigor. This includes complexity analysis, algorithmic optimization, and performance benchmarking considerations.

**Integration Across Evolutionary Operations.** The domain knowledge template is systematically integrated across all evolutionary operations (PC, SC, PM, PWC) through the external\_knowledge template variable. This ensures consistent application of gravitational wave detection principles regardless of the specific evolutionary strategy employed.

**Physical Validity Assurance.** The domain knowledge template ensures that all generated algorithms respect fundamental physical constraints related to gravitational wave signal characteristics, detector limitations, and noise properties.

**Computational Feasibility.** The implementation principles guide algorithmic development toward computationally feasible solutions that can be practically implemented within the constraints of current computational resources and real-time processing requirements.

This comprehensive domain knowledge integration creates a robust framework for scientifically grounded algorithmic discovery, ensuring that the evolutionary process generates algorithms that are both innovative and practically applicable to gravitational wave detection challenges.

### A.1.7 Error Handling and Iterative Refinement

The Evo-MCTS framework incorporates a robust error handling mechanism that enables iterative refinement of generated algorithms through automated debugging and correction processes. When generated code encounters execution errors, fails to detect signals, or exceeds computational time limits, the system employs a rechat strategy using advanced reasoning models to diagnose and resolve issues.

**Error Detection and Classification.** The framework monitors three primary failure modes during algorithm execution: (i) runtime exceptions and syntax errors that prevent code execution, (ii) algorithmic failures where no gravitational wave signals are detected despite their presence in the data, and (iii) computational timeout scenarios where algorithms exceed predefined execution limits. Each failure mode triggers specific diagnostic protocols tailored to the underlying issue type.

**Iterative Refinement Protocol.** Upon error detection, the system implements a structured refinement process through a carefully designed prompt content structure. The system constructs conversation messages in a specific format to facilitate effective error correction:

Initially, when no system content is provided, the framework creates a message list containing a single user role entry with the original prompt content (`prompt_content`): `messages = [{"role": "user", "content": prompt_content}]`

When a rechat response is available (indicating a previous failed attempt), the system extends the conversation by first appending the assistant's previous response (`rechat_response`): `messages.append({"role": "assistant", "content": rechat_response})`

Subsequently, the system adds a new user message that explicitly requests debugging and issue resolution (`prompt_content`): `messages.append({"role": "user", "content": "Your previous code had execution errors, couldn't find signals, or timed out. Please debug and fix the issues:\n\n" + prompt_content})`

This structured approach maintains the conversational context while providing clear guidance for error correction, ensuring that the assistant understands both the original requirements and the specific issues that need to be addressed.

**Automated Debugging Integration.** The error handling system leverages advanced reasoning capabilities to analyze failed algorithms and propose targeted corrections. This approach maintains the evolutionary optimization trajectory while addressing immediate technical obstacles that could otherwise terminate the search process. The iterative refinement ensures that promising algorithmic concepts are not discarded due to implementation errors, instead receiving corrective guidance to achieve functional implementations.

### **A.1.8 Post-Generation Analysis and Knowledge Extraction**

The post-generation analysis phase extracts interpretable insights from evolved algorithms through automated knowledge distillation. This process transforms the raw algorithmic implementations into concise, human-readable descriptions that capture the essential design principles and operational characteristics of discovered solutions.

**Algorithm Description Generation.** The framework employs a structured prompt template to generate concise algorithm descriptions that highlight critical design decisions and implementation strategies. The prompt construction follows a systematic format:

Following is the Design Idea of a heuristic algorithm for the problem and the code with function name 'pipeline\_v2' for implementing the heuristic algorithm.

```
{prompt_inout_inf} {prompt_other_inf}
Design Idea:
{algorithm}
```

```
Code:
```python
{code}
```
```

The content of the Design Idea idea cannot fully represent what the algorithm has done informative. So, now you should re-describe the algorithm using less than 3 sentences. Hint: You should reference the given Design Idea and highlight the most critical design ideas of the code. You can analyse the code to describe which variables are given higher priorities and which variables are given lower priorities, the parameters and the structure of the code.

This template systematically combines the original design concept with the implemented code, requesting a refined description that captures the algorithm’s core operational principles. The analysis focuses on parameter prioritization, structural characteristics, and critical design decisions that distinguish the evolved solution.

**Knowledge Extraction Protocol.** The post-generation analysis captures key design principles and compresses algorithmic representations into human-readable summaries. This reflection process identifies algorithmic innovations, signal processing techniques, and computational characteristics while reducing token consumption to prevent context window overflow in subsequent LLM interactions.

**Interpretability Enhancement.** The generated descriptions provide concise algorithmic summaries that enable efficient reference to previous discoveries without overwhelming the LLM context, facilitating continued exploration while maintaining algorithmic memory across generations.

### A.1.9 Code Examples and Case Studies

This section presents a detailed examination of the highest-performing algorithm discovered during the Evo-MCTS optimization process, corresponding to node 486 (as shown in Figure 5a) which achieved the maximum fitness score of 5,241.37 units. The algorithm demonstrates sophisticated multi-stage signal processing techniques that emerged through evolutionary optimization.

**Algorithm Overview.** The evolved algorithm implements a four-stage pipeline combining robust baseline detrending, adaptive whitening with enhanced power spectral density (PSD) smoothing, coherent time-frequency analysis with frequency-conditioned regularization, and multi-resolution thresholding with octave-spaced dyadic wavelet validation. This architecture represents a novel synthesis of classical signal processing techniques with adaptive parameter selection mechanisms.

**Stage 1: Robust Baseline Detrending.** The algorithm initiates with median filtering-based detrending to remove long-term instrumental drifts and environmental variations. The median filter kernel size of 101 samples provides robust trend removal while preserving transient gravitational wave signatures. This preprocessing stage establishes a stable baseline for subsequent whitening operations.

**Stage 2: Adaptive Whitening with Enhanced PSD Smoothing.** The core innovation lies in the adaptive whitening mechanism that dynamically adjusts window parameters based on data characteristics. The algorithm implements Tukey windowing with 75% overlap and adaptive segment lengths constrained between 5-30 seconds, optimizing spectral estimation for varying noise conditions. The PSD smoothing employs exponential filtering with stationarity-dependent coefficients (0.75-0.85 range), while Tikhonov regularization provides frequency-dependent gain control. Savitzky-Golay filtering generates causal-like gradients, and sigmoid-based nonlinear scaling enhances spectral features through adaptive gain factors.

**Stage 3: Coherent Time-Frequency Analysis.** The algorithm computes complex spectrograms preserving phase information across both detectors, enabling coherent analysis of gravitational wave signatures. Phase difference calculations and coherence estimation provide cross-detector validation, while frequency-conditioned regularization balances phase alignment with noise characteristics. The integration of axial curvature estimates through second derivatives and nonlinear activation functions (tanh-based boost) enhances signal discrimination capabilities.

**Stage 4: Multi-Resolution Validation.** The final stage implements sophisticated peak detection using robust statistical measures (median absolute deviation) combined with octave-spaced dyadic wavelet validation. Continuous wavelet transform coefficients across scales 1-8 provide multi-resolution signal verification, while Gaussian-weighted uncertainty estimation quantifies detection confidence intervals.

---

```

1 import numpy as np
2 import scipy.signal as signal
3 from scipy.signal.windows import tukey
4 from scipy.signal import savgol_filter
5
6 def pipeline_v2(strain_h1: np.ndarray, strain_l1: np.ndarray, times: np.ndarray) -> tuple[np.ndarray, np.ndarray, np.ndarray]:
7     """
8     The pipeline function processes gravitational wave data from the H1 and L1 detectors to identify potential gravitational
9     wave signals.
10    It takes strain_h1 and strain_l1 numpy arrays containing detector data, and times array with corresponding time points.
11    The function returns a tuple of three numpy arrays: peak_times containing GPS times of identified events,
12    peak_heights with significance values of each peak, and peak_deltat showing time window uncertainty for each peak.
13    """
14    eps = np.finfo(float).tiny
15    dt = times[1] - times[0]
16    fs = 1.0 / dt
17    # Base spectrogram parameters
18    base_nperseg = 256
19    base_noverlap = base_nperseg // 2
20    medfilt_kernel = 101 # odd kernel size for robust detrending
21    uncertainty_window = 5 # half-window for local timing uncertainty
22
23    # ----- Stage 1: Robust Baseline Detrending -----
24    # Remove long-term trends using a median filter for each channel.
25    detrended_h1 = strain_h1 - signal.medfilt(strain_h1, kernel_size=medfilt_kernel)

```

```

25     detrended_l1 = strain_l1 - signal.medfilt(strain_l1, kernel_size=medfilt_kernel)
26
27 # ----- Stage 2: Adaptive Whitening with Enhanced PSD Smoothing -----
28 def adaptive_whitening(strain: np.ndarray) -> np.ndarray:
29     # Center the signal.
30     centered = strain - np.mean(strain)
31     n_samples = len(centered)
32     # Adaptive window length: between 5 and 30 seconds
33     win_length_sec = np.clip(n_samples / fs / 20, 5, 30)
34     nperseg_adapt = int(win_length_sec * fs)
35     nperseg_adapt = max(10, min(nperseg_adapt, n_samples))
36
37     # Create a Tukey window with 75% overlap.
38     tukey_alpha = 0.25
39     win = tukey(nperseg_adapt, alpha=tukey_alpha)
40     noverlap_adapt = int(nperseg_adapt * 0.75)
41     if noverlap_adapt >= nperseg_adapt:
42         noverlap_adapt = nperseg_adapt - 1
43
44     # Estimate the power spectral density (PSD) using Welch's method.
45     freqs, psd = signal.welch(centered, fs=fs, nperseg=nperseg_adapt,
46                             noverlap=noverlap_adapt, window=win, detrend='constant')
47     psd = np.maximum(psd, eps)
48
49     # Compute relative differences for PSD stationarity measure.
50     diff_arr = np.abs(np.diff(psd)) / (psd[:-1] + eps)
51     # Smooth the derivative with a moving average.
52     if len(diff_arr) >= 3:
53         smooth_diff = np.convolve(diff_arr, np.ones(3)/3, mode='same')
54     else:
55         smooth_diff = diff_arr
56
57     # Exponential smoothing (Kalman-like) with adaptive alpha using PSD stationarity.
58     smoothed_psd = np.copy(psd)
59     for i in range(1, len(psd)):
60         # Adaptive smoothing coefficient: base 0.8 modified by local stationarity (+0.05)
61         local_alpha = np.clip(0.8 - 0.05 * smooth_diff[min(i-1, len(smooth_diff)-1)], 0.75, 0.85)
62         smoothed_psd[i] = local_alpha * smoothed_psd[i-1] + (1 - local_alpha) * psd[i]
63
64     # Compute Tikhonov regularization gain based on deviation from median PSD.
65     noise_baseline = np.median(smoothed_psd)
66     raw_gain = (smoothed_psd / (noise_baseline + eps)) - 1.0
67
68     # Compute a causal-like gradient using the Savitzky-Golay filter.
69     win_len = 11 if len(smoothed_psd) >= 11 else ((len(smoothed_psd)//2)*2+1)
70     polyorder = 2 if win_len > 2 else 1
71     delta_freq = np.mean(np.diff(freqs))
72     grad_psd = savgol_filter(smoothed_psd, win_len, polyorder, deriv=1, delta=delta_freq, mode='interp')
73
74     # Nonlinear scaling via sigmoid to enhance gradient differences.
75     sigmoid = lambda x: 1.0 / (1.0 + np.exp(-x))
76     scaling_factor = 1.0 + 2.0 * sigmoid(np.abs(grad_psd) / (np.median(smoothed_psd) + eps))
77
78     # Compute adaptive gain factors with nonlinear scaling.
79     gain = 1.0 - np.exp(-0.5 * scaling_factor * raw_gain)
80     gain = np.clip(gain, -8.0, 8.0)
81
82     # FFT-based whitening: interpolate gain and PSD onto FFT frequency bins.
83     signal_fft = np.fft.rfft(centered)
84     freq_bins = np.fft.rfftfreq(n_samples, d=dt)
85     interp_gain = np.interp(freq_bins, freqs, gain, left=gain[0], right=gain[-1])
86     interp_psd = np.interp(freq_bins, freqs, smoothed_psd, left=smoothed_psd[0], right=smoothed_psd[-1])
87     denom = np.sqrt(interp_psd) * (np.abs(interp_gain) + eps)
88     denom = np.maximum(denom, eps)
89     white_fft = signal_fft / denom
90     whitened = np.fft.irfft(white_fft, n=n_samples)
91     return whitened
92
93 # Whiten H1 and L1 channels using the adapted method.
94 white_h1 = adaptive_whitening(detrended_h1)
95 white_l1 = adaptive_whitening(detrended_l1)
96
97 # ----- Stage 3: Coherent Time-Frequency Metric with Frequency-Conditioned Regularization
98 ↪ -----
99 def compute_coherent_metric(w1: np.ndarray, w2: np.ndarray) -> tuple[np.ndarray, np.ndarray]:
100     # Compute complex spectrograms preserving phase information.

```

```

100 f1, t_spec, Sxx1 = signal.spectrogram(w1, fs=fs, nperseg=base_nperseg,
101                                     noverlap=base_noverlap, mode='complex', detrend=False)
102 f2, t_spec2, Sxx2 = signal.spectrogram(w2, fs=fs, nperseg=base_nperseg,
103                                     noverlap=base_noverlap, mode='complex', detrend=False)
104
105 # Ensure common time axis length.
106 common_len = min(len(t_spec), len(t_spec2))
107 t_spec = t_spec[:common_len]
108 Sxx1 = Sxx1[:, :common_len]
109 Sxx2 = Sxx2[:, :common_len]
110
111 # Compute phase differences and coherence between detectors.
112 phase_diff = np.angle(Sxx1) - np.angle(Sxx2)
113 phase_coherence = np.abs(np.cos(phase_diff))
114
115 # Estimate median PSD per frequency bin from the spectrograms.
116 psd1 = np.median(np.abs(Sxx1)**2, axis=1)
117 psd2 = np.median(np.abs(Sxx2)**2, axis=1)
118
119 # Frequency-conditioned regularization gain (reflection-guided).
120 lambda_f = 0.5 * ((np.median(psd1) / (psd1 + eps)) + (np.median(psd2) / (psd2 + eps)))
121 lambda_f = np.clip(lambda_f, 1e-4, 1e-2)
122 # Regularization denominator integrating detector PSDs and lambda.
123 reg_denom = (psd1[:, None] + psd2[:, None] + lambda_f[:, None] + eps)
124
125 # Weighted phase coherence that balances phase alignment with noise levels.
126 weighted_comp = phase_coherence / reg_denom
127
128 # Compute axial (frequency) second derivatives as curvature estimates.
129 d2_coh = np.gradient(np.gradient(phase_coherence, axis=0), axis=0)
130 avg_curvature = np.mean(np.abs(d2_coh), axis=0)
131
132 # Nonlinear activation boost using tanh for regions of high curvature.
133 nonlinear_boost = np.tanh(5 * avg_curvature)
134 linear_boost = 1.0 + 0.1 * avg_curvature
135
136 # Cross-detector synergy: weight derived from global median consistency.
137 novel_weight = np.mean((np.median(psd1) + np.median(psd2)) / (psd1[:, None] + psd2[:, None] + eps), axis=0)
138
139 # Integrated time-frequency metric combining all enhancements.
140 tf_metric = np.sum(weighted_comp * linear_boost * (1.0 + nonlinear_boost), axis=0) * novel_weight
141
142 # Adjust the spectrogram time axis to account for window delay.
143 metric_times = t_spec + times[0] + (base_nperseg / 2) / fs
144 return tf_metric, metric_times
145
146 tf_metric, metric_times = compute_coherent_metric(white_h1, white_l1)
147
148 # ----- Stage 4: Multi-Resolution Thresholding with Octave-Spaced Dyadic Wavelet Validation
149 ↪ -----
150 def multi_resolution_thresholding(metric: np.ndarray, times_arr: np.ndarray) -> tuple[np.ndarray, np.ndarray, np.ndarray]:
151     # Robust background estimation with median and MAD.
152     bg_level = np.median(metric)
153     mad_val = np.median(np.abs(metric - bg_level))
154     robust_std = 1.4826 * mad_val
155     threshold = bg_level + 1.5 * robust_std
156
157     # Identify candidate peaks using prominence and minimum distance criteria.
158     peaks, _ = signal.find_peaks(metric, height=threshold, distance=2, prominence=0.8 * robust_std)
159     if peaks.size == 0:
160         return np.array([]), np.array([]), np.array([])
161
162     # Local uncertainty estimation using a Gaussian-weighted convolution.
163     win_range = np.arange(-uncertainty_window, uncertainty_window + 1)
164     sigma = uncertainty_window / 2.5
165     gauss_kernel = np.exp(-0.5 * (win_range / sigma) ** 2)
166     gauss_kernel /= np.sum(gauss_kernel)
167     weighted_mean = np.convolve(metric, gauss_kernel, mode='same')
168     weighted_sq = np.convolve(metric ** 2, gauss_kernel, mode='same')
169     variances = np.maximum(weighted_sq - weighted_mean ** 2, 0.0)
170     uncertainties = np.sqrt(variances)
171     uncertainties = np.maximum(uncertainties, 0.01)
172
173     valid_times = []
174     valid_heights = []
175     valid_uncerts = []
176     n_metric = len(metric)

```

```

175
176     # Compute a simple second derivative for local curvature checking.
177     if n_metric > 2:
178         second_deriv = np.diff(metric, n=2)
179         second_deriv = np.pad(second_deriv, (1, 1), mode='edge')
180     else:
181         second_deriv = np.zeros_like(metric)
182
183     # Use octave-spaced scales (dyadic wavelet validation) to validate peak significance.
184     widths = np.arange(1, 9) # approximate scales 1 to 8
185     for peak in peaks:
186         # Skip peaks lacking sufficient negative curvature.
187         if second_deriv[peak] > -0.1 * robust_std:
188             continue
189         local_start = max(0, peak - uncertainty_window)
190         local_end = min(n_metric, peak + uncertainty_window + 1)
191         local_segment = metric[local_start:local_end]
192         if len(local_segment) < 3:
193             continue
194         try:
195             cwt_coeff = signal.cwt(local_segment, signal.ricker, widths)
196         except Exception:
197             continue
198         max_coeff = np.max(np.abs(cwt_coeff))
199         # Threshold for validating the candidate using local MAD.
200         cwt_thresh = mad_val * np.sqrt(2 * np.log(len(local_segment) + eps))
201         if max_coeff >= cwt_thresh:
202             valid_times.append(times_arr[peak])
203             valid_heights.append(metric[peak])
204             valid_uncerts.append(uncertainties[peak])
205
206     if len(valid_times) == 0:
207         return np.array([], dtype=int), np.array([], dtype=float), np.array([], dtype=float)
208     return np.array(valid_times), np.array(valid_heights), np.array(valid_uncerts)
209
210 peak_times, peak_heights, peak_deltat = multi_resolution_thresholding(tf_metric, metric_times)
211 return peak_times, peak_heights, peak_deltat

```

**Reflective Reasoning Integration.** The framework incorporates advanced reflective reasoning capabilities through DeepSeek-R1’s internal thinking processes, enabling systematic analysis and refinement of algorithmic solutions. This reflective mechanism operates through structured thinking templates that guide the model through comprehensive evaluation and improvement cycles.

**Thinking Process Template.** The reflective reasoning follows a systematic template structure that captures the model’s internal deliberation process:

<thinking>

Okay, let's tackle this problem. The user wants me to analyze the differences between the original and improved versions of the gravitational wave detection pipeline, focusing on depth 4. The current MCTS depth is 4 out of 10, which falls into the medium category. The medium depth focuses on implementation techniques and parameterization.

First, I need to compare the two code versions. Let's look at each stage of the pipeline.

Starting with Stage 2: Adaptive Whitening. In the original code, there's a Kalman-like smoothing with a fixed alpha of 0.8. The improved version introduces an adaptive alpha based on the PSD's stationarity. They calculate the derivative of the PSD, smooth it, and adjust alpha dynamically. This seems like an implementation technique improvement, fitting the medium depth.

Next, the gain calculation. The original uses a fixed scaling factor of 3.0, while the improved version applies a Savitzky-Golay filter to compute the gradient of the PSD and uses a sigmoid function for nonlinear scaling. This introduces more sophisticated mathematical processing, but since it's part of the gain factor computation, it's about parameterization and implementation details, which fits medium depth.

In Stage 3: Coherent Metric. The original uses Tikhonov regularization with a fixed lambda.

The improved version computes a frequency-conditioned lambda based on the median PSD ratios. This dynamic regularization is a parameterization improvement. Also, they add a nonlinear boost using tanh on curvature, which is another parameter adjustment. These are implementation techniques.

Stage 4: Thresholding. The original checks the second derivative for curvature. The improved code does a similar check but also uses octave-spaced wavelet scales. Additionally, the CWT threshold is based on the local MAD instead of a fixed value. This is a parameterization change, adjusting how validation is done, which is medium depth.

Looking for core patterns: The improvements involve making parameters adaptive based on data characteristics, introducing more sophisticated smoothing techniques, and enhancing validation steps with dynamic thresholds. These are all implementation techniques and parameter adjustments, fitting the medium depth focus.

Now, generating optimization principles. Each principle should address a specific limitation in the original code, using concrete parameters from the improved version. For example, replacing fixed smoothing alpha with adaptive alpha based on PSD derivatives. Another is using Savitzky-Golay for gradient computation. Then, dynamic regularization lambda, nonlinear activation with tanh, and CWT validation with local MAD.

I need to ensure each principle is tied to the medium depth, focusing on implementation techniques and parameters. Avoid diving into deep mathematical formulations unless necessary. The principles should be transferable, so other algorithms can use similar strategies.

Checking the improved code's parameters: adaptive alpha ranges from 0.75 to 0.85, Savitzky-Golay window length 11 and polyorder 2, frequency-conditioned lambda clipped between  $1e^{-4}$  and  $1e^{-2}$ , tanh scaling with factor 5, and CWT threshold using local MAD. These concrete values should be included in the principles.

Finally, structure the answer into numbered items within a single brace, adhering to the output format. Ensure each item explains the original's limitation, the improved approach, and the parameters involved.

</thinking>

**Reflection Content Generation.** Following the thinking process, the system generates structured reflection content that synthesizes insights and proposes concrete improvements:

1. **\*\*Adaptive PSD Smoothing with Stationarity-Dependent Alpha\*\*:**  
Original used fixed exponential smoothing ( $\alpha=0.8$ ). Improved version implements Kalman-like adaptation where smoothing coefficient (0.75-0.85 range) dynamically adjusts based on local PSD stationarity measured through normalized differentials (3-point moving average of  $dPSD/PSD$ ). Enhances noise floor estimation stability during non-stationary segments while preserving transient features.
2. **\*\*Spectral Gradient-Enhanced Gain Computation\*\*:**  
Replaced simple exponential gain dampening with Savitzky-Golay derivative estimation (window=11, polyorder=2) followed by sigmoid nonlinearity ( $1/(1+e^{-x/scale})$ ). Original used fixed scaling factor of 3.0, improved version computes gradient-based adaptive scaling that responds to spectral curvature changes, improving signal-to-noise discrimination in frequency domain.
3. **\*\*Frequency-Conditioned Regularization Lambda\*\*:**  
Original Tikhonov regularization used fixed lambda parameter. Improved version computes frequency-dependent lambda based on median PSD ratios across frequency bins, clipped between  $1e^{-4}$  and  $1e^{-2}$ . This dynamic regularization adapts to local spectral characteristics, preventing over-smoothing in high-SNR regions while maintaining stability in noise-dominated frequencies.
4. **\*\*Nonlinear Coherence Boost with Curvature Activation\*\*:**  
Enhanced coherent metric computation by adding tanh-based nonlinear activation (scale factor=5) applied to second-derivative curvature measures. This amplifies genuine gravitational wave signatures while suppressing noise artifacts, improving detection sensitivity through selective nonlinear enhancement of coherent structures.

5. **\*\*CWT Validation with Local MAD Thresholding\*\***:  
 Original used fixed threshold for continuous wavelet transform validation. Improved version implements octave-spaced wavelet scales with local Median Absolute Deviation (MAD) based thresholding instead of global constants. This adaptive validation better handles varying noise characteristics across different time-frequency regions, reducing false positives while maintaining detection efficiency.

**Iterative Refinement Protocol.** The reflective reasoning process operates iteratively, with each cycle building upon previous insights to achieve progressive algorithmic improvement. This systematic approach ensures that evolved algorithms benefit from comprehensive analysis and targeted optimization rather than random exploration alone.

## A.2 Data Partitioning Strategy

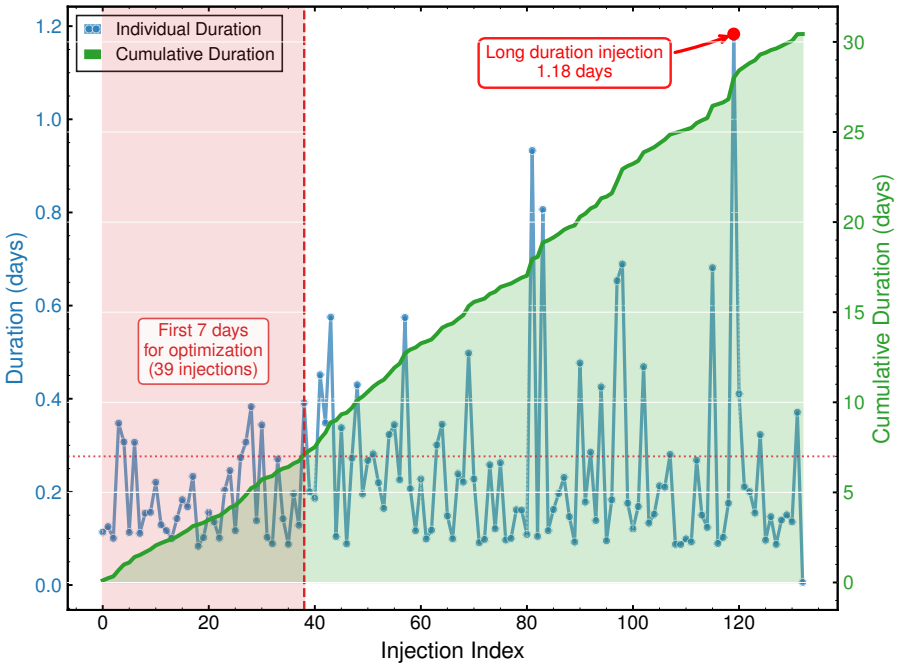


**Fig. A1 MLGWSC-1 Dataset 4 Partitioning Strategy for Training and Test Set Configuration.** Individual injection durations (blue line, left axis) and cumulative duration (green line, right axis) across injection indices 0-130. The red dashed vertical line at injection index 39 delineates the training set boundary, with the first 7 days (red shaded region) used for algorithm optimization containing 39 injections. The test set consists of a single long-duration injection of 1.18 days (red annotation with arrow) occurring at injection index 119, providing a challenging validation scenario for sustained detection capability. The horizontal red dotted line indicates the cumulative duration at injection index 39, marking the exact 7-day threshold for training set partitioning. This temporal partitioning ensures efficient optimization while providing rigorous out-of-sample validation on extended-duration signals.

The MLGWSC-1 Dataset 4 partitioning strategy balances optimization efficiency with statistical validity through careful temporal segmentation. Figure A1 illustrates the systematic approach employed to divide the dataset into training and test subsets while maintaining representative signal characteristics across both partitions.

**Training Set Definition and Statistical Characteristics.** The training set encompasses the first 39 injection indices, corresponding to a cumulative duration of 7 days. This temporal boundary provides sufficient signal diversity and noise conditions for algorithmic optimization while maintaining computational efficiency during the iterative Evo-MCTS process.

During optimization, each evolved algorithm processes complete injection segments with durations ranging from 0.1 to 0.4 days. The statistical characteristics of the training set (mean: 0.179 days, median: 0.143 days) ensure comprehensive algorithmic development across the spectrum of injection durations present in the dataset. This distribution provides robust training exposure while the 7-day cumulative training duration serves multiple critical purposes: (i) adequate statistical power for AUC calculation with minimum false-alarm rate of 4 events per month, (ii) rapid algorithm evaluation (10-20 minutes per assessment), and (iii) preservation of temporal continuity and realistic noise characteristics.

**Test Set Configuration and Validation Rigor.** The test set comprises a single 1.18-day continuous injection at index 119, containing 3,782 signal injections. This extended duration provides a particularly challenging validation scenario that significantly exceeds both the training set mean (0.179 days) and the overall dataset mean (0.229 days) by factors of 6.6x and 5.2x, respectively. The test injection’s duration of 1.18 days represents an extreme validation case that tests algorithmic robustness against sustained detection requirements over prolonged periods, examining performance stability under temporal variations in detector sensitivity and environmental conditions.

The temporal separation from training data ensures genuine out-of-sample validation, while the extended duration creates a stringent assessment environment. Compared to the overall dataset statistics (mean: 0.229 days, median: 0.169 days), the test injection’s 1.18-day duration provides validation on challenging extended-duration scenarios that algorithms must handle effectively.

### A.3 Five-Run Experimental Design and Results

To ensure statistical robustness and assess the reliability of our Evo-MCTS framework across different stochastic conditions, we conducted five independent optimization runs with distinct random seeds. Figure A2 presents comprehensive results from all runs, demonstrating both the consistency of our approach and the natural variation inherent in stochastic optimization processes.

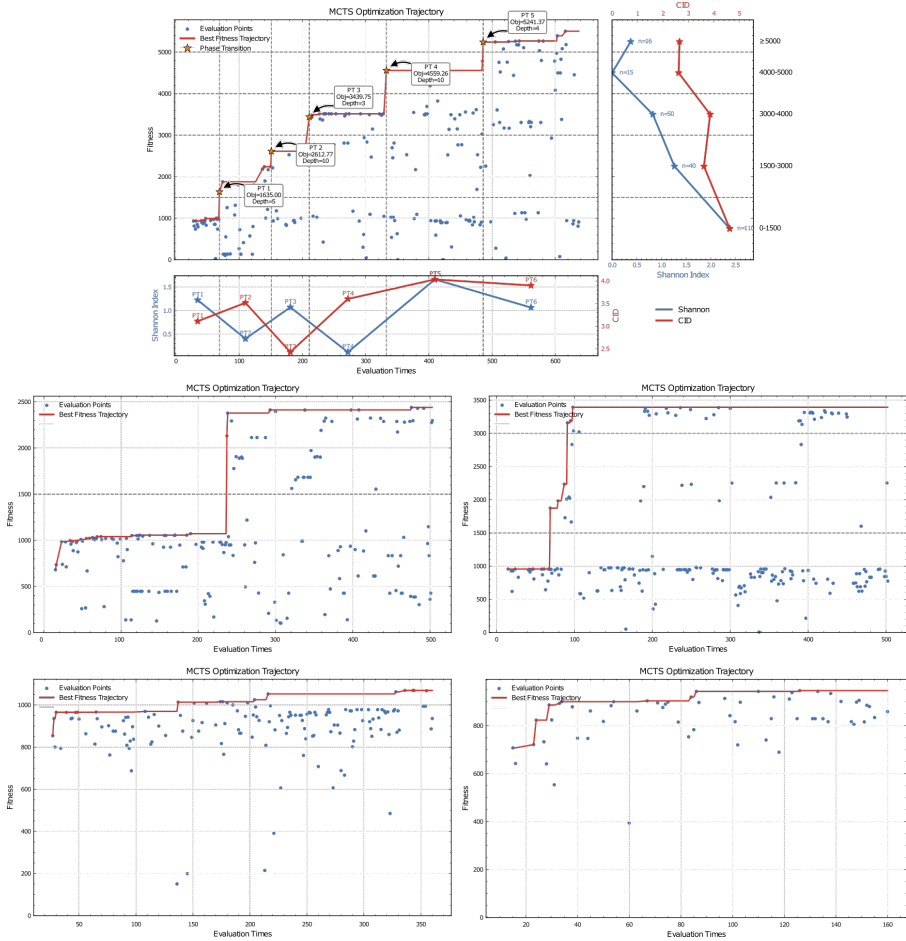


**Fig. A2 Multi-Run Statistical Analysis of Evo-MCTS Optimization Performance.** **Top panel:** Primary run showing complete optimization trajectory with five phase transitions (PT1, PT2.1, PT2.2, PT3, PT4) achieving maximum fitness of 5,241.37 units. Each PT marker indicates fitness value, evaluation number, and tree depth: PT1 (1,635.00, eval 69, depth 5), PT2.1 (2,612.77, eval 151, depth 10), PT2.2 (3,439.75, eval 211, depth 3), PT3 (4,559.26, eval 333, depth 10), PT4 (5,241.37, eval 486, depth 4). **Top right:** Shannon diversity index analysis showing systematic exploration patterns across fitness levels, with aggregate peak diversity ( $\approx 3.8$ ) in lower performance range (0-1,500 fitness). **Lower panels:** Four additional independent runs demonstrating framework robustness and natural optimization variability. Run 2 (lower left) achieves moderate optimization (2,500 fitness), Run 3 (lower middle-left) shows more substantial performance (3,500 fitness) with algorithmic breakthroughs comparable to the PT2 phase described in the main text, Run 4 (lower middle-right) exhibits limited optimization progress (1,100 fitness), Run 5 (lower right) demonstrates modest improvement from lower baseline (900 fitness). All runs show improvement over baseline, validating framework reliability while illustrating diverse optimization pathways in the complex algorithmic search space. Results confirm consistent early-phase improvements across all runs with varying success in discovering advanced algorithmic combinations.

(Note: To maintain consistency with the main text’s PT1-PT4 framework while providing detailed combined individual run analysis, this supplementary analysis presents five phase transitions labeled as PT1, PT2.1, PT2.2, PT3, and PT4, where PT2.1 and PT2.2 represent two independent algorithmic breakthroughs that are distinct from the PT2 phase described in the main text.)

### **Primary Run Analysis and Phase Transition Characterization.**

The primary run (top panel) achieved the most comprehensive optimization trajectory, discovering five distinct phase transitions that represent qualitative algorithmic breakthroughs. PT1 occurs at evaluation 69 with fitness 1,635.00 at depth 5, incorporating Continuous Wavelet Transform (CWT) techniques and Multi-resolution Thresholding for enhanced time-frequency analysis. PT2.1 emerges at evaluation 151 with fitness 2,612.77 at depth 10, introducing Curvature Boosting methods while integrating Tikhonov Regularization for improved signal conditioning and noise suppression. PT2.2 manifests at evaluation 211 with fitness 3,439.75 at depth 3, representing a significant algorithmic advancement through refined optimization strategies. PT3 develops at evaluation 333 with fitness 4,559.26 at depth 10, integrating Savitzky-Golay (S-G) filter techniques for enhanced signal processing capabilities. Finally, PT4 achieves maximum fitness of 5,241.37 at evaluation 486 and depth 4, representing the culmination of all previously discovered techniques including CWT, Multi-resolution Thresholding, Curvature Boosting, Tikhonov Regularization, and S-G filtering in a comprehensive algorithmic framework.

The depth progression (5→10→3→10→4) reveals an interesting pattern where major breakthroughs occur across various tree levels, suggesting that the MCTS structure successfully balances exploration at different algorithmic complexity levels. The fitness improvements at each phase transition represent single-step gains from the immediate predecessor node rather than cumulative improvements between phases: PT1 (+639.69), PT2.1 (+370.81), PT2.2 (+910.37), PT3 (+1,045.72), and PT4 (+456.85). These single-step improvements demonstrate variable discovery magnitudes as individual algorithmic innovations are identified, with the pattern showing that breakthrough discoveries can occur with different intensities as the algorithm space becomes more thoroughly explored through the tree search process.

Table A1 provides a comprehensive performance comparison across all benchmark models, the seed function baseline, and the five phase transition levels achieved during optimization. The benchmark models demonstrate varying performance levels, with Sage achieving the highest AUC of 4359.2749, followed by Virgo-AUTh at 4101.4810. Notably, our evolved algorithms at PT Level 4 (5241.3678 AUC) significantly outperform all benchmark models across all evaluation metrics, including false alarm rates at different thresholds (FAR=1000, FAR=100, FAR=10, FAR=4.3), achieving relative improvements of 20.2% over the top-performing Sage benchmark (4359.27 AUC) and 23.4% enhancement in sensitive distance detection capability at node 486. The progressive improvement from the seed function baseline (926.0336 AUC) through

each phase transition level demonstrates the systematic enhancement achieved through the Evo-MCTS optimization process.

**Table A1** Performance Comparison Across Benchmark Models and Phase Transition Levels

| Model                               | AUC<br>(units) | Sensitive Distance (Mpc) at FAR |        |        |        |
|-------------------------------------|----------------|---------------------------------|--------|--------|--------|
|                                     |                | 1000                            | 100    | 10     | 4.3    |
| <i>Benchmark Models</i>             |                |                                 |        |        |        |
| Sage                                | 4359.27        | 1996.1                          | 1846.6 | 1688.8 | 1672.4 |
| Virgo-AUTh                          | 4101.48        | 1990.2                          | 1818.7 | 1635.0 | 1609.5 |
| PyCBC                               | 4069.90        | 1832.3                          | 1721.8 | 1609.3 | 1573.4 |
| TPI FSU Jena                        | 3744.99        | 1796.0                          | 1581.6 | 1426.4 | 1382.4 |
| CWB                                 | 3225.01        | 1451.6                          | 1406.5 | 1351.8 | 1303.2 |
| MFCNN                               | 2890.33        | 1541.1                          | 1269.0 | 997.2  | 900.3  |
| CNN-Coinc                           | 1997.02        | 1067.2                          | 959.9  | 620.4  | 450.8  |
| <i>Phase Transition (PT) Levels</i> |                |                                 |        |        |        |
| PT Level 4                          | 5241.37        | 2323.9                          | 2295.8 | 2080.9 | 2065.3 |
| PT Level 3                          | 4559.26        | 1932.0                          | 1932.0 | 1932.0 | 1932.0 |
| PT Level 2.2                        | 3439.75        | 1537.2                          | 1460.1 | 1407.9 | 1402.3 |
| PT Level 2.1                        | 2612.77        | 1107.2                          | 1107.2 | 1107.2 | 1107.2 |
| PT Level 1                          | 1635.00        | —                               | 769.8  | 769.8  | 769.8  |
| Seed function                       | 926.03         | 786.9                           | 368.2  | 238.3  | 158.3  |

**Shannon Diversity Analysis Across Optimization Phases.** The Shannon diversity analysis (top right panel) reveals sophisticated exploration patterns that correlate with optimization phases. The scatter plot demonstrates that algorithmic diversity varies systematically with fitness levels, with peak diversity (Shannon  $\sim 2.5$ ) occurring in the lower performance range (fitness 0-1,500), followed by a gradual decrease as fitness improves. This pattern indicates intensive exploration during early optimization phases, with the framework progressively shifting toward exploitation as high-performing algorithms are discovered. The diversity trend confirms that the Evo-MCTS methodology effectively balances exploration and exploitation, with broader algorithmic sampling during initial discovery phases and more focused refinement during later breakthrough periods.

**Multi-Run Consistency and Variability Analysis.** The four additional runs (lower panels) demonstrate varying degrees of optimization success, reflecting the inherent stochastic nature of the discovery process while validating the framework’s general effectiveness. Run 2 (bottom-left panel) exhibits steady progression with fitness values reaching approximately 2,500 units,

characterized by a gradual upward trajectory punctuated by several modest phase transitions. This pattern illustrates the framework’s ability to consistently identify incremental algorithmic improvements even when breakthrough discoveries remain elusive.

Run 3 (bottom-center-left panel) achieves more substantial performance with fitness values approaching 3,500 units, displaying well-defined phase transitions that correspond to significant algorithmic innovations. This run exhibits characteristics similar to the PT2 phase described in the main text, demonstrating how the framework can effectively navigate complex solution spaces to discover meaningful algorithmic enhancements under favorable stochastic conditions.

Run 4 (bottom-center-right panel) presents a particularly instructive case despite showing more limited optimization progress, with fitness values reaching approximately 1,100 units. This run reveals valuable insights into the challenges of navigating rugged optimization landscapes, where persistent exploration attempts encounter difficulty escaping local optima. Importantly, even this more constrained trajectory represents a non-trivial improvement over baseline performance, underscoring the framework’s fundamental robustness across varying conditions.

Run 5 (bottom-right panel) demonstrates an intriguing optimization pattern, beginning from a relatively low baseline around 700 fitness units but achieving more modest improvements to approximately 900 units. Rather than indicating failure, this trajectory illustrates the challenges encountered in certain regions of the optimization landscape, where despite starting from a lower performance level, the algorithm struggles to discover pathways to substantial improvements, possibly due to being trapped in a difficult-to-escape local optimum region.

**Statistical Validation and Performance Reliability.** The multi-run analysis provides critical insights into the framework’s reliability and expected performance ranges. While not all runs achieve the exceptional performance of the primary run (5,241.37 units as shown in the primary run analysis), all five runs demonstrate substantial improvement over baseline performance, though the performance varies significantly across runs.

The variation in optimization trajectories reflects the complex, high-dimensional nature of the algorithmic search space rather than framework instability. Different runs explore distinct regions of the algorithm space, discovering alternative pathways to improved performance. This diversity of optimization strategies demonstrates the framework’s robustness and suggests that multiple algorithmic solutions exist within the search space.

**Optimization Pattern Analysis and Success Factors.** Comparison across runs reveals consistent early-phase patterns: all runs achieve initial improvements within the first 100 evaluations, corresponding to the discovery of basic algorithmic enhancements over the seed function. The divergence

in later-phase performance correlates with the discovery of advanced algorithmic combinations, where stochastic factors influence the exploration of high-performance regions.

The most successful runs (primary run reaching 5,241.37 and run 3 reaching  $\sim 3,500$  fitness) share common characteristics: sustained exploration diversity throughout optimization, discovery of multiple phase transitions, and achievement of higher fitness levels. Less successful runs (such as run 5 with only  $\sim 900$  fitness) typically exhibit earlier convergence to local optima, suggesting that maintaining exploration diversity is crucial for discovering breakthrough algorithmic innovations.

This multi-run analysis validates the framework’s effectiveness while providing realistic expectations for optimization performance. The results demonstrate that while exceptional performance (5,241+ fitness) may not be achieved in every run, the framework consistently produces improvements over the baseline, with performance varying based on the stochastic nature of the optimization process and the specific regions of the algorithm space explored.

#### A.4 Temporal Constraint Analysis and Robustness Validation

The 0.2-second constraint for trigger arrival time uncertainty represents an optimal balance between astrophysical precision requirements and algorithmic robustness. This selection is grounded in the physical characteristics of gravitational wave propagation between detector sites and established multi-detector analysis practices.

**Physical Foundation.** The temporal constraint must account for the maximum light travel time between LIGO Hanford (H1) and Livingston (L1) detectors. For the two-detector LHO-LLO network, signals must be seen in both detectors within a time difference of 15 ms: 10 ms maximum travel time between detectors and 5 ms padding to account for timing errors [39]. However, the 0.2-second window provides significantly more conservative margin to accommodate additional systematic uncertainties from detector calibration, signal processing delays, timing measurement precision [6], and algorithmic robustness requirements while maintaining alignment with operational gravitational wave detection pipelines [39, 54].

**Experimental Analysis.** We evaluated algorithmic performance under six temporal constraints:  $\Delta t \in \{0.02, 0.05, 0.1, 0.2, 0.5, 1.0\}$  seconds, calculating training-test performance correlations across all 877 optimized algorithms.

**Results and Optimal Selection.** Figure A3 demonstrates systematic relationships between temporal constraints and algorithm generalization. Correlation coefficients progress from  $r = 0.640$  (0.02s) to  $r = 0.840$  (0.2s, optimal), then plateau at  $r = 0.842$  (0.5s) and  $r = 0.836$  (1.0s). Critically, the 0.2-second constraint exhibits performance characteristics most closely approximating the ideal training-test parity line ( $y = x$ ), with minimal scatter around the diagonal.

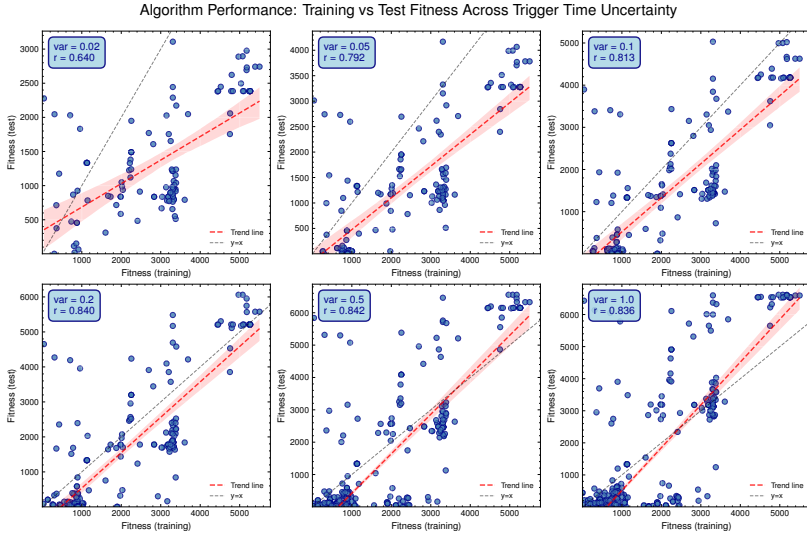


**Fig. A3 Temporal Constraint Impact on Algorithm Generalization Performance.** Analysis of training-test performance correlation as a function of trigger arrival time uncertainty constraints across six different temporal precision levels. **Six panels:** Pearson correlation coefficients between training and test algorithm fitness scores across 877 algorithms for temporal constraint values  $\Delta t \in \{0.02, 0.05, 0.1, 0.2, 0.5, 1.0\}$  seconds. Each panel displays scatter plots of training vs. test fitness with correlation coefficients and 95% confidence intervals. The red diagonal line represents perfect training-test correlation ( $y = x$ ). The analysis demonstrates that the 0.2-second constraint ( $r = 0.840$ ) provides optimal balance between performance consistency and practical deployment requirements, with algorithm performance closely following the ideal correlation line. **Key finding:** While tighter constraints (0.02-0.1s) show high correlation coefficients, the 0.2-second constraint exhibits superior generalization behavior with minimal deviation from the ideal  $y = x$  relationship, indicating robust performance scaling between training and test conditions.

Tighter constraints (0.02-0.1s) show increased scatter at higher fitness values, suggesting potential overfitting. Looser constraints (0.5-1.0s) exhibit broader scatter patterns indicating reduced discriminative power for distinguishing high-quality algorithms.

## A.5 Technique Impact Analysis

**LLM-Based Code Analysis Pipeline.** To systematically extract technical features from algorithm implementations, we developed an automated analysis pipeline using large language models (LLMs). Each code snippet was processed through a structured prompt designed to identify algorithmic components across three main stages: data conditioning, time-frequency analysis, and trigger detection.

LLM Analysis Prompt:

Please analyze the following Python code snippet for gravitational wave detection and extract technical features in JSON format.

The code typically has three main stages:

1. Data Conditioning: preprocessing, filtering, whitening, etc.

2. Time-Frequency Analysis: spectrograms, FFT, wavelets, etc.
3. Trigger Analysis: peak detection, thresholding, validation, etc.

For each stage present in the code, extract:

- Technical methods used
- Libraries and functions called
- Algorithm complexity features
- Key parameters

Code to analyze:

```
```python
{code_snippet}
```
```

Please return a JSON object with this structure:

```
{
  "algorithm_id": "{algorithm_id}",
  "stages": {
    "data_conditioning": {
      "present": true/false,
      "techniques": ["technique1", "technique2"],
      "libraries": ["lib1", "lib2"],
      "functions": ["func1", "func2"],
      "parameters": {"param1": "value1"},
      "complexity": "low/medium/high"
    },
    "time_frequency_analysis": {...},
    "trigger_analysis": {...}
  },
  "overall_complexity": "low/medium/high",
  "total_lines": 0,
  "unique_libraries": ["lib1", "lib2"],
  "code_quality_score": 0.0
}
```

Only return the JSON object, no additional text.

The analysis was performed using `deepseek-r1-250120` model with `temperature=1.0` for balanced creativity and consistency. We processed 877 valid code snippets (`code_snippet`) using parallel processing with 30 workers to ensure efficient analysis while maintaining API rate limits.

**Data Preparation and Normalization.** For each identified technique, algorithms were classified into binary groups: those incorporating the technique (“with”) versus those without (“without”). Performance metrics (fitness values or AUC scores) were normalized to [0,1] range using min-max scaling across all algorithms to enable fair comparison between different evaluation metrics.

**Combined Performance Analysis.** To increase statistical power, we combined normalized AUC scores of both training and test into unified performance datasets for each comparison group. This approach leverages all available performance information while maintaining the comparative structure necessary for statistical testing.

**Adaptive Statistical Testing Protocol.** Our testing framework adapts to data characteristics through a decision tree approach:

1. **Normality Assessment:** Shapiro-Wilk test for samples  $n \leq 5000$
2. **Test Selection:**
  - Both groups normal and  $n \geq 30$ : Welch’s t-test with Cohen’s d effect size
  - Otherwise: Mann-Whitney U test with rank-biserial correlation

### 3. Effect Size Interpretation:

- Cohen’s  $d$ : negligible ( $< 0.2$ ), small ( $0.2 - 0.5$ ), medium ( $0.5 - 0.8$ ), large ( $> 0.8$ )
- Rank-biserial: negligible ( $< 0.1$ ), small ( $0.1 - 0.3$ ), medium ( $0.3 - 0.5$ ), large ( $> 0.5$ )

**Imbalance Detection and Mitigation.** We identify problematic comparisons using two criteria: (i) sample ratio exceeding 3:1, or (ii) minimum group size below 30. For such cases, we implement balanced resampling analysis:

#### Resampling Protocol:

1. Undersample the larger group to match the smaller group size
2. Perform 1,000 independent resampling iterations with replacement
3. Calculate test statistics and p-values for each iteration
4. Assess robustness based on proportion of significant results

**Robustness Criteria:** A technique effect is considered robust if:

- $> 80\%$  of resampling iterations show statistical significance ( $p < 0.05$ )
- Median effect size maintains consistent direction and magnitude
- 95% confidence interval of effect sizes excludes zero

**Technique Effectiveness Classification and Visualization.** The comprehensive technique impact analysis is presented through violin plot distributions comparing performance between algorithms incorporating specific techniques (“with”) versus those without (“without”) across all identified techniques (Figure A4). Based on our multi-criteria evaluation framework, techniques are classified into three effectiveness tiers:

**High-Effectiveness Techniques** demonstrate clear distributional separation with minimal overlap, statistical significance  $> 80\%$  across resampling iterations, and large effect sizes ( $r > 0.5$ ). Notable examples include Curvature Analysis and CWT Validation, which show the “with” group distributions positioned substantially higher than “without” groups, indicating consistent performance improvements.

**Medium-Effectiveness Techniques** exhibit moderate distributional separation, statistical significance between 50-80%, and medium effect sizes ( $0.3 < r < 0.5$ ). These techniques provide measurable but less consistent performance benefits.

**Low-Effectiveness Techniques** display substantial distributional overlap between “with” and “without” groups, statistical significance  $< 50\%$ , and small effect sizes ( $r < 0.1$ ), indicating limited practical utility.

#### Distributional Analysis Methodology.

- Violin plots constructed using Gaussian kernel density estimation with adaptive bandwidth selection
- Performance metrics normalized to  $[0,1]$  scale enabling cross-technique comparison

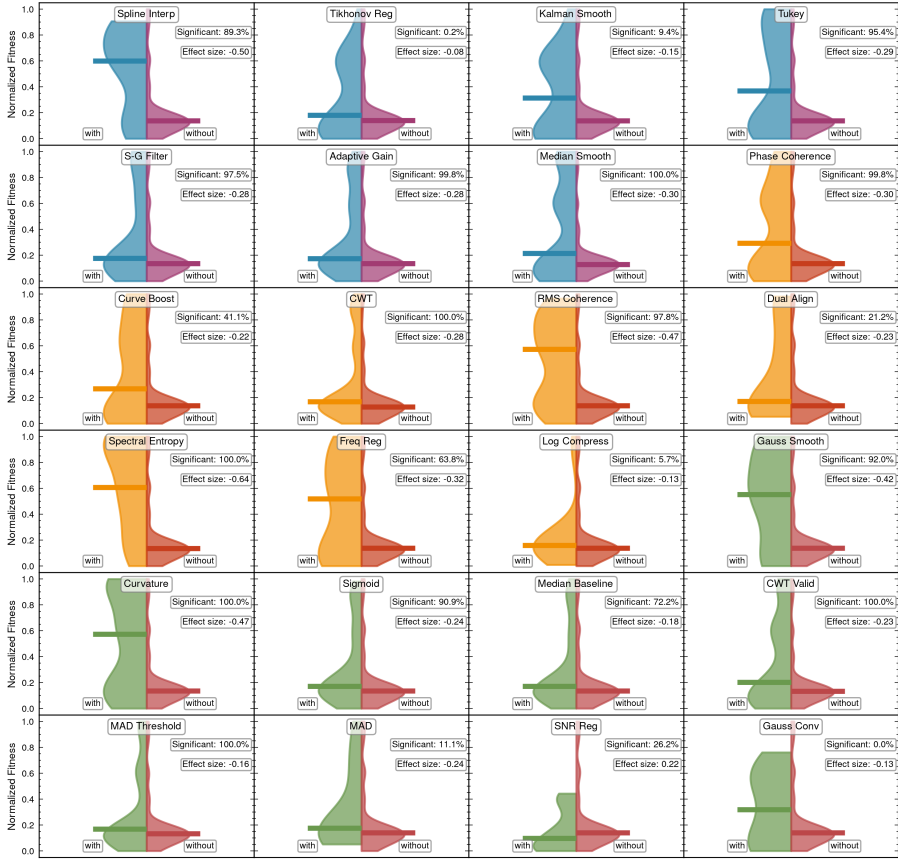


**Fig. A4 Comprehensive Technique Effectiveness Analysis via Violin Plot Distributions.** Performance distributions comparing algorithms with and without specific techniques across three methodological categories: data conditioning (blue), time-frequency analysis (orange), and trigger detection (green). Each violin plot pair reveals technique effectiveness through distributional characteristics: wider sections indicate higher probability density regions, clear vertical separation between “with” and “without” groups indicates strong technique effects, while substantial overlap suggests limited effectiveness. Statistical robustness metrics (significance percentages from resampling analysis) and effect sizes (rank-biserial correlations) quantify technique reliability. High-effectiveness techniques (e.g., Curvature Analysis, CWT Validation) demonstrate clear distributional separation and large effect sizes, while low-effectiveness techniques show substantial overlap and negligible effect sizes. Technique abbreviations are defined in Table A2.

- Color-coded categorical organization: data conditioning (blue), time-frequency analysis (orange), trigger detection (green)
- Statistical annotations include resampling-based significance percentages and rank-biserial effect sizes
- Median performance indicators highlight central tendency differences between technique groups

**Table A2** **Technique Abbreviations Used in Figure A4.** Complete mapping of abbreviated technique names to their full descriptions, organized by methodological category.

| <b>Abbreviation</b>            | <b>Full Name</b>                   |
|--------------------------------|------------------------------------|
| <b>Data Conditioning</b>       |                                    |
| Spline Interp                  | Spline Interpolation               |
| Tikhonov Reg                   | Tikhonov Regularization            |
| Kalman Smooth                  | Kalman-inspired Smoothing          |
| Tukey                          | Tukey Windowing                    |
| S-G Filter                     | Savitzky-Golay Filtering           |
| Adaptive Gain                  | Adaptive Gain Regularization       |
| Median Smooth                  | Uniform/Median Smoothing           |
| Gauss Smooth                   | Gaussian Smoothing                 |
| Median Baseline                | Median-based Baseline Correction   |
| SNR Reg                        | SNR-adaptive Regularization        |
| Gauss Conv                     | Gaussian Convolution               |
| <b>Time-Frequency Analysis</b> |                                    |
| Phase Coherence                | Phase Coherence Analysis           |
| CWT                            | Continuous Wavelet Transform       |
| RMS Coherence                  | RMS Coherence Metric               |
| Dual Align                     | Dual-channel Alignment             |
| Spectral Entropy               | Spectral Entropy                   |
| Freq Reg                       | Frequency-dependent Regularization |
| Log Compress                   | Logarithmic Compression            |
| CWT Valid                      | CWT Validation                     |
| <b>Trigger Detection</b>       |                                    |
| Curve Boost                    | Curvature Boosting                 |
| Curvature                      | Curvature Analysis                 |
| Sigmoid                        | Sigmoid Enhancement                |
| MAD Threshold                  | MAD-based Robust Thresholding      |
| MAD                            | Median Absolute Deviation          |

- Distributional separation quantified through overlap coefficients and Kolmogorov-Smirnov distances
- Technique abbreviations facilitate visual clarity while maintaining comprehensive coverage (Table A2)

This multi-dimensional effectiveness assessment framework enables systematic identification of high-impact techniques while distinguishing them from those with marginal or inconsistent benefits, providing clear guidance for algorithmic development priorities.

## A.6 Detailed MCTS Node Evolution and Technique Propagation Data

Figure A5 presents the complete MCTS search tree evolution with node-by-node fitness values and technique compositions. Each node displays its fitness score (marked in red) alongside the specific algorithmic techniques discovered at that search depth. The five core technique categories [1-5] correspond to:

- 1 Multi-resolution Thresholding
- 2 Continuous Wavelet Transform (CWT) using Ricker Wavelet

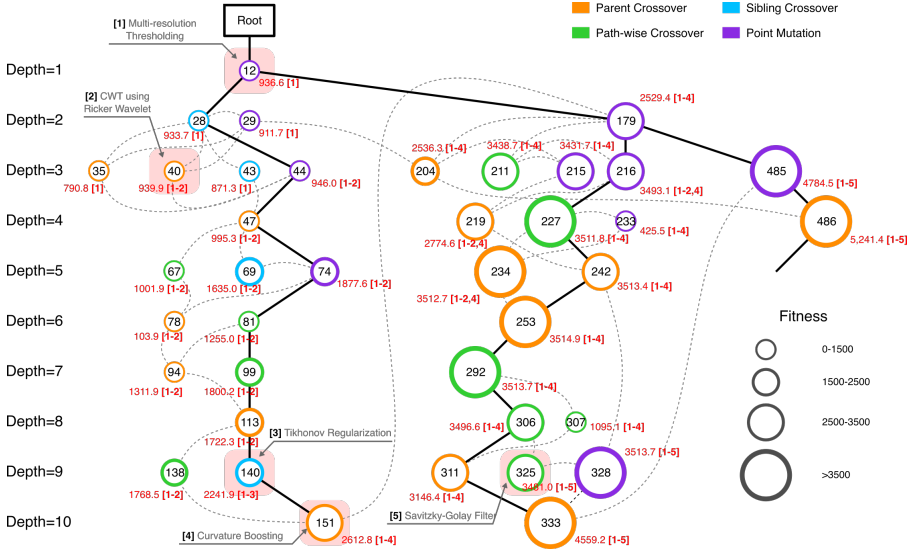


**Fig. A5 Complete MCTS search tree with node fitness values and technique compositions.** Each node shows its fitness score (red annotations) and constituent algorithmic techniques organized by category [1-5]. Node size reflects fitness magnitude. The tree demonstrates systematic technique evolution and cross-branch knowledge transfer, with optimal performance achieved through multi-technique integration at terminal nodes.

- 3 Tikhonov Regularization
- 4 Curvature Boosting
- 5 Savitzky-Golay Filter

These techniques demonstrate the systematic evolution of algorithmic complexity through the MCTS exploration process, with detailed implementation examples provided in Section A.1.9.

## A.7 Overfitting Risk Assessment and Physical Validation Failure Modes

To evaluate potential overfitting risks in the Evo-MCTS framework, we conducted systematic injection studies using GW150914-like signals with varying signal-to-noise ratios (SNR). This analysis addresses concerns raised in the main discussion regarding algorithmic optimization potentially overfitting to MLGWSC-1’s specific characteristics.

**Experimental Design.** We performed injection experiments using simulated gravitational wave signals based on the posterior distribution of GW150914 [5]. The injected signals were embedded in realistic detector noise closed to GW150914 from the O1 observing run, with SNR values systematically varied across various SNRs. For each SNR group, we generated 100 independent injection realizations and evaluated the detection efficiency of representative MCTS nodes across the algorithmic evolution tree.

**Detection Efficiency Analysis.** Figure A6 presents detection efficiency curves for six representative nodes (Node-4, Node-7, Node-411, Node-464, Node-485, Node-486) spanning different evolutionary stages of the MCTS search. The results reveal concerning overfitting patterns that manifest as performance degradation when algorithms optimized on MLGWSC-1 data encounter realistic astrophysical scenarios.

Node-4, representing an early-stage algorithm with minimal complexity, demonstrates robust performance across all SNR ranges with detection efficiency exceeding 80% for  $\text{SNR} > 10$ . In contrast, highly evolved nodes (Node-464, Node-485, Node-486) exhibit sharp performance transitions, achieving near-perfect detection only above  $\text{SNR} = 12\text{-}15$ , suggesting over-specialization to the noise characteristics and signal morphologies present in the MLGWSC-1 training dataset.

**Overfitting Manifestations.** The steep detection efficiency curves observed for advanced nodes indicate several failure modes characteristic of overfitting:

- **Threshold Over-Optimization:** Advanced nodes demonstrate excessively restrictive detection thresholds optimized for MLGWSC-1’s specific noise floor, resulting in reduced sensitivity to weaker but astrophysically realistic signals.
- **Feature Over-Specialization:** Complex multi-technique combinations (e.g., Node-486 incorporating techniques [1,2,3,4,5]) show degraded performance on signal morphologies that deviate from the limited parameter space explored in MLGWSC-1.
- **Noise Model Dependency:** The sharp performance transitions suggest algorithms have adapted to MLGWSC-1’s inherent noise model, failing to generalize to the more complex non-stationary and non-Gaussian characteristics of operational detector data.
- **Competition Metric Exploitation:** The MLGWSC-1 evaluation framework itself contains inherent limitations that enable algorithmic exploitation of scoring system vulnerabilities. Advanced nodes appear to have discovered and exploited specific characteristics of the competition’s evaluation metrics, optimizing for artificial performance gains rather than genuine astrophysical detection capability. This metric gaming behavior results in algorithms that achieve high competition scores while failing to maintain robust performance under realistic detection scenarios.

**Physical Validation Implications.** The overfitting analysis reveals fundamental limitations of competition-based benchmarks for gravitational wave detection. Advanced nodes (Node-464, Node-485, Node-486) demonstrate sharp performance degradation on realistic astrophysical signals, indicating over-specialization to MLGWSC-1’s constrained evaluation framework. Intermediate-complexity nodes (Node-7, Node-411) achieve optimal performance-robustness balance, suggesting that benchmark optimization alone is insufficient for real-world deployment.

**Benchmark Limitations and Methodological Insights.** The observed overfitting patterns expose critical weaknesses in current evaluation protocols: (1) limited signal diversity that enables algorithmic exploitation of specific noise characteristics, (2) evaluation metrics that reward competition performance over astrophysical sensitivity, and (3) insufficient validation against realistic detector conditions. The Evo-MCTS framework’s systematic exploration of the performance-generalization Pareto frontier transforms these limitations into methodological strengths, providing rigorous overfitting detection capabilities.

**Pareto Frontier Discovery and Framework Contribution.** The detection efficiency results demonstrate that the Evo-MCTS framework has systematically mapped the algorithm design space, revealing fundamental trade-offs between benchmark performance and generalization capability. Node-411 represents an optimal point on this frontier, achieving superior balance compared to the highest-scoring Node-486, which sacrifices robustness for competition metrics. This Pareto frontier discovery constitutes a core methodological contribution, enabling informed decisions about performance-robustness trade-offs rather than pursuing single-metric optimization.

**Future Directions and Benchmark Enhancement.** This analysis motivates comprehensive benchmark improvement: (1) incorporation of diverse astrophysical populations spanning multiple source types and parameter ranges, (2) multi-detector validation protocols using independent observing run data, (3) evaluation frameworks that explicitly penalize overfitting through cross-validation requirements, and (4) systematic comparison with established detection algorithms under identical protocols. The current assessment focuses on binary black hole signals; comprehensive validation requires extension to neutron star mergers, continuous wave sources, and burst signals to establish universal applicability of discovered algorithmic principles.

## References

- [1] Zheng, Y., Koh, H.Y., Ju, J., Nguyen, A.T.N., May, L.T., Webb, G.I., Pan, S.: Large language models for scientific discovery in molecular property prediction. *Nature Machine Intelligence* (2025) 2310.07984 [cs]. <https://doi.org/10.1038/s42256-025-00994-z>
- [2] Wang, H., Fu, T., Du, Y., Gao, W., Huang, K., Liu, Z., Chandak, P., Liu, S., Van Katwyk, P., Deac, A., Anandkumar, A., Bergen, K., Gomes, C.P., Ho, S., Kohli, P., Lasenby, J., Leskovec, J., Liu, T.-Y., Manrai, A., Marks, D., Ramsundar, B., Song, L., Sun, J., Tang, J., Veličković, P., Welling, M., Zhang, L., Coley, C.W., Bengio, Y., Zitnik, M.: Scientific discovery in the age of artificial intelligence. *Nature* **620**(7972), 47–60 (2023). <https://doi.org/10.1038/s41586-023-06221-2>
- [3] Karniadakis, G.E., Kevrekidis, I.G., Lu, L., Perdikaris, P., Wang, S., Yang,

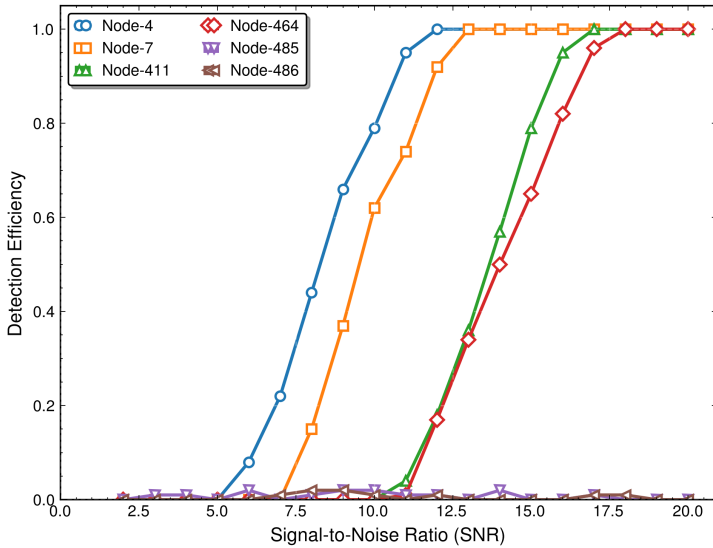


**Fig. A6 Detection efficiency analysis revealing overfitting risks in evolved MCTS nodes.** Detection efficiency curves for representative nodes across different SNR groups using GW150914-like injections in O1 detector noise. Early-stage nodes (Node-4, blue) demonstrate robust performance across all SNR ranges, while highly evolved nodes (Node-464, Node-485, Node-486, red/purple/brown) exhibit sharp performance transitions indicative of overfitting to MLGWS-1 characteristics. Intermediate-complexity nodes (Node-7, Node-411, orange/green) achieve optimal balance between sophistication and generalization capability.

- L.: Physics-informed machine learning. *Nature Reviews Physics* **3**(6), 422–440 (2021). <https://doi.org/10.1038/s42254-021-00314-5>
- [4] Baker, N., Alexander, F., Bremer, T., Hagberg, A., Kevrekidis, Y., Najm, H., Parashar, M., Patra, A., Sethian, J., Wild, S., et al.: Workshop report on basic research needs for scientific machine learning: Core technologies for artificial intelligence. Technical report, USDOE Office of Science (SC), Washington, D.C. (United States) (February 2019). <https://doi.org/10.2172/1478744>. <https://www.osti.gov/biblio/1478744>
- [5] Abbott, B.P., *et al.*: Observation of gravitational waves from a binary black hole merger. *Phys. Rev. Lett.* **116**, 061102 (2016). <https://doi.org/10.1103/PhysRevLett.116.061102>
- [6] Abbott, B.P., *et al.*: Gwtc-1: A gravitational-wave transient catalog of compact binary mergers observed by ligo and virgo during the first and second observing runs. *Phys. Rev. X* **9**, 031040 (2019). <https://doi.org/10.1103/PhysRevX.9.031040>
- [7] Abbott, B.P., *et al.*: A guide to ligo-virgo detector noise and extraction of transient gravitational-wave signals. *Classical and Quantum Gravity*

- 37**(5), 055002 (2020). <https://doi.org/10.1088/1361-6382/ab685e>
- [8] Owen, B.J.: Search templates for gravitational waves from inspiraling binaries: Choice of template spacing. *Phys. Rev. D* **53**, 6749–6761 (1996). <https://doi.org/10.1103/PhysRevD.53.6749>
- [9] Cutler, C., Flanagan, E.E.: Gravitational waves from merging compact binaries: How accurately can one extract the binary’s parameters from the inspiral waveform? *Phys. Rev. D* **49**, 2658–2697 (1994). <https://doi.org/10.1103/PhysRevD.49.2658>
- [10] Klimentko, S., Vedovato, G., Drago, M., Salemi, F., Tiwari, V., Prodi, G.A., Lazzaro, C., Ackley, K., Tiwari, S., Da Silva, C.F., Mitselmakher, G.: Method for detection and reconstruction of gravitational wave transients with networks of advanced detectors. *Phys. Rev. D* **93**, 042004 (2016). <https://doi.org/10.1103/PhysRevD.93.042004>
- [11] George, D., Huerta, E.A.: Deep neural networks to enable real-time multimessenger astrophysics. *Phys. Rev. D* **97**, 044039 (2018). <https://doi.org/10.1103/PhysRevD.97.044039>
- [12] Gabbard, H., Williams, M., Hayes, F., Messenger, C.: Matching matched filtering with deep networks for gravitational-wave astronomy. *Phys. Rev. Lett.* **120**, 141103 (2018). <https://doi.org/10.1103/PhysRevLett.120.141103>
- [13] Huerta, E.A., Khan, A., Huang, X., Tian, M., Levental, M., Chard, R., Wei, W., Heflin, M., Katz, D.S., Kindratenko, V., Mu, D., Blaiszik, B., Foster, I.: Accelerated, scalable and reproducible AI-driven gravitational wave detection. *Nature Astronomy* **5**(10), 1062–1068 (2021) [2012.08545v1 \[gr-qc\]. https://doi.org/10.1038/s41550-021-01405-0](https://doi.org/10.1038/s41550-021-01405-0)
- [14] Nagarajan, N., Messenger, C.: Identifying and Mitigating Machine Learning Biases for the Gravitational-wave Detection Problem (2025). <https://arxiv.org/abs/2501.13846>
- [15] Elsken, T., Metzen, J.H., Hutter, F.: Neural architecture search: A survey. *Journal of Machine Learning Research* **20**(55), 1–21 (2019)
- [16] Eiben, A.E., Smith, J.: From evolutionary computation to the evolution of things. *Nature* **521**(7553), 476–482 (2015). <https://doi.org/10.1038/nature14544>
- [17] Kahneman, D.: *Thinking, Fast and Slow*. Macmillan, New York (2011)
- [18] Wolpert, D.H., Macready, W.G.: No free lunch theorems for optimization. *IEEE transactions on evolutionary computation* **1**(1), 67–82 (2002)

- [19] Chen, M., Tworek, J., Jun, H., Yuan, Q., de Oliveira Pinto, H.P., Kaplan, J., Edwards, H., Burda, Y., Joseph, N., Brockman, G., Ray, A., Puri, R., Krueger, G., Petrov, M., Khlaaf, H., Sastry, G., Mishkin, P., Chan, B., Gray, S., Ryder, N., Pavlov, M., Power, A., Kaiser, L., Bavarian, M., Winter, C., Tillet, P., Such, F.P., Cummings, D., Plappert, M., Chantzis, F., Barnes, E., Herbert-Voss, A., Guss, W.H., Nichol, A., Paino, A., Tezak, N., Tang, J., Babuschkin, I., Balaji, S., Jain, S., Saunders, W., Hesse, C., Carr, A.N., Leike, J., Achiam, J., Misra, V., Morikawa, E., Radford, A., Knight, M., Brundage, M., Murati, M., Mayer, K., Welinder, P., McGrew, B., Amodei, D., McCandlish, S., Sutskever, I., Zaremba, W.: Evaluating Large Language Models Trained on Code (2021). <https://arxiv.org/abs/2107.03374>
- [20] Lewkowycz, A., Andreassen, A., Dohan, D., Dyer, E., Michalewski, H., Ramasesh, V., Slone, A., Anil, C., Schlag, I., Gutman-Solo, T., Wu, Y., Neyshabur, B., Gur-Ari, G., Misra, V.: Solving quantitative reasoning problems with language models **35**, 3843–3857 (2022). <https://doi.org/10.48550/arXiv.2206.14858>
- [21] Browne, C.B., Powley, E., Whitehouse, D., Lucas, S.M., Cowling, P.I., Rohlfshagen, P., Tavener, S., Perez, D., Samothrakis, S., Colton, S.: A Survey of Monte Carlo Tree Search Methods. *IEEE Transactions on Computational Intelligence and AI in Games* **4**(1), 1–43 (2012). <https://doi.org/10.1109/TCIAIG.2012.2186810>
- [22] Wang, L., Zhao, Y., Jinnai, Y., Tian, Y., Fonseca, R.: Neural architecture search using deep neural networks and monte carlo tree search. *Proceedings of the AAAI Conference on Artificial Intelligence* **34**(06), 9983–9991 (2020). <https://doi.org/10.1609/aaai.v34i06.6554>
- [23] Li, Y., Du, D., Song, L., Li, C., Wang, W., Yang, T., Mi, H.: Hunyuan-Prover: A Scalable Data Synthesis Framework and Guided Tree Search for Automated Theorem Proving (2025). <https://arxiv.org/abs/2412.20735>
- [24] Koza, J.R.: Genetic programming as a means for programming computers by natural selection. *Statistics and Computing* **4**(2), 87–112 (1994). <https://doi.org/10.1007/BF00175355>
- [25] Romera-Paredes, B., Barekattain, M., Novikov, A., Balog, M., Kumar, M.P., Dupont, E., Ruiz, F.J.R., Ellenberg, J.S., Wang, P., Fawzi, O., Kohli, P., Fawzi, A.: Mathematical discoveries from program search with large language models. *Nature* **625**(7995), 468–475 (2024). <https://doi.org/10.1038/s41586-023-06924-6>
- [26] Liu, F., Tong, X., Yuan, M., Lin, X., Luo, F., Wang, Z., Lu, Z., Zhang, Q.: Evolution of Heuristics: Towards Efficient Automatic Algorithm Design Using Large Language Model (2024). <https://arxiv.org/abs/2401.02051>

- [27] Liu, F., Tong, X., Yuan, M., Zhang, Q.: Algorithm Evolution Using Large Language Model (2023). <https://arxiv.org/abs/2311.15249>
- [28] Ye, H., Wang, J., Cao, Z., Berto, F., Hua, C., Kim, H., Park, J., Song, G.: ReEvo: Large Language Models as Hyper-Heuristics with Reflective Evolution (2024). <https://arxiv.org/abs/2402.01145>
- [29] Zheng, Z., Xie, Z., Wang, Z., Hooi, B.: Monte Carlo Tree Search for Comprehensive Exploration in LLM-Based Automatic Heuristic Design (2025). <https://arxiv.org/abs/2501.08603>
- [30] Schäfer, M.B., Zelenka, O.c.v., Nitz, A.H., Wang, H., Wu, S., Guo, Z.-K., Cao, Z., Ren, Z., Nousi, P., Stergioulas, N., Iosif, P., Koloniari, A.E., Tefas, A., Passalis, N., Salemi, F., Vedovato, G., Klimenko, S., Mishra, T., Brüggmann, B., Cuoco, E., Huerta, E.A., Messenger, C., Ohme, F.: First machine learning gravitational-wave search mock data challenge. *Phys. Rev. D* **107**, 023021 (2023). <https://doi.org/10.1103/PhysRevD.107.023021>
- [31] Nousi, P., Koloniari, A.E., Passalis, N., Iosif, P., Stergioulas, N., Tefas, A.: Deep residual networks for gravitational wave detection. *Phys. Rev. D* **108**, 024022 (2023). <https://doi.org/10.1103/PhysRevD.108.024022>
- [32] Nitz, A.H., Kumar, S., Wang, Y.-F., Kastha, S., Wu, S., Schäfer, M., Dhurkunde, R., Capano, C.D.: 4-ogc: Catalog of gravitational waves from compact binary mergers. *The Astrophysical Journal* **946**(2), 59 (2023). <https://doi.org/10.3847/1538-4357/aca591>
- [33] Zelenka, O.c.v., Brüggmann, B., Ohme, F.: Convolutional neural networks for signal detection in real ligo data. *Phys. Rev. D* **110**, 024024 (2024). <https://doi.org/10.1103/PhysRevD.110.024024>
- [34] Drago, M., Klimenko, S., Lazzaro, C., Milotti, E., Mitselmakher, G., Necula, V., O'Brian, B., Prodi, G.A., Salemi, F., Szczepanczyk, M., Tiwari, S., Tiwari, V., V, G., Vedovato, G., Yakushin, I.: coherent waveburst, a pipeline for unmodeled gravitational-wave data analysis. *SoftwareX* **14**, 100678 (2021). <https://doi.org/10.1016/j.softx.2021.100678>
- [35] Wang, H., Wu, S., Cao, Z., Liu, X., Zhu, J.-Y.: Gravitational-wave signal recognition of ligo data by deep learning. *Phys. Rev. D* **101**, 104003 (2020). <https://doi.org/10.1103/PhysRevD.101.104003>
- [36] Schäfer, M.B., Nitz, A.H.: From one to many: A deep learning coincident gravitational-wave search. *Phys. Rev. D* **105**, 043003 (2022). <https://doi.org/10.1103/PhysRevD.105.043003>
- [37] Schäfer, M.B., Zelenka, O.c.v., Nitz, A.H., Ohme, F., Brüggmann, B.:

- Training strategies for deep learning gravitational-wave searches. *Phys. Rev. D* **105**, 043002 (2022). <https://doi.org/10.1103/PhysRevD.105.043002>
- [38] Finn, L.S.: Detection, measurement, and gravitational radiation. *Phys. Rev. D* **46**, 5236–5249 (1992). <https://doi.org/10.1103/PhysRevD.46.5236>
- [39] Usman, S.A., Nitz, A.H., Harry, I.W., Biver, C.M., Brown, D.A., Cabero, M., Capano, C.D., Canton, T.D., Dent, T., Fairhurst, S., Kehl, M.S., Koppel, D., Krishnan, B., Lenon, A., Lundgren, A., Nielsen, A.B., Pekowsky, L.P., Pfeiffer, H.P., Saulson, P.R., West, M., Willis, J.L.: The pycbc search for gravitational waves from compact binary coalescence. *Classical and Quantum Gravity* **33**(21), 215004 (2016). <https://doi.org/10.1088/0264-9381/33/21/215004>
- [40] Dal Canton, T., Nitz, A.H., Gadre, B., Cabourn Davies, G.S., Villa-Ortega, V., Dent, T., Harry, I., Xiao, L.: Real-time search for compact binary mergers in advanced ligo and virgo’s third observing run using pycbc live. *The Astrophysical Journal* **923**(2), 254 (2021). <https://doi.org/10.3847/1538-4357/ac2f9a>
- [41] Klimenko, S., Vedovato, G., Drago, M., Salemi, F., Tiwari, V., Prodi, G.A., Lazzaro, C., Ackley, K., Tiwari, S., Da Silva, C.F., Mitselmakher, G.: Method for detection and reconstruction of gravitational wave transients with networks of advanced detectors. *Phys. Rev. D* **93**, 042004 (2016). <https://doi.org/10.1103/PhysRevD.93.042004>
- [42] Zhang, R., Liu, F., Lin, X., Wang, Z., Lu, Z., Zhang, Q.: Understanding the Importance of Evolutionary Search in Automated Heuristic Design with Large Language Models (2024). <https://arxiv.org/abs/2407.10873>
- [43] LeCun, Y., Bengio, Y., Hinton, G.: Deep learning. *Nature* **521**(7553), 436–444 (2015). <https://doi.org/10.1038/nature14539>
- [44] Rudin, C.: Stop explaining black box machine learning models for high stakes decisions and use interpretable models instead. *Nature Machine Intelligence* **1**(5), 206–215 (2019). <https://doi.org/10.1038/s42256-019-0048-x>
- [45] Molnar, C.: *Interpretable Machine Learning*, 2nd edn. Leanpub, Munich, Germany (2020). <https://christophm.github.io/interpretable-ml-book/>
- [46] Troja, E., Piro, L., van Eerten, H., Wollaeger, R.T., Im, M., Fox, O.D., Butler, N.R., Cenko, S.B., Sakamoto, T., Fryer, C.L., Ricci, R., Lien, A., Ryan, R.E., Korobkin, O., Lee, S.-K., Burgess, J.M., Lee, W.H., Watson, A.M., Choi, C., Covino, S., D’Avanzo, P., Fontes, C.J., González, J.B.,

- Khandrika, H.G., Kim, J., Kim, S.-L., Lee, C.-U., Lee, H.M., Kuttyrev, A., Lim, G., Sánchez-Ramírez, R., Veilleux, S., Wieringa, M.H., Yoon, Y.: The X-ray counterpart to the gravitational-wave event GW170817. *Nature* **551**(7678), 71–74 (2017). <https://doi.org/10.1038/nature24290>
- [47] Dat, P.V.T., Doan, L., Binh, H.T.T.: HSEvo: Elevating Automatic Heuristic Design with Diversity-Driven Harmony Search and Genetic Algorithm Using LLMs (2024). <https://arxiv.org/abs/2412.14995>
- [48] OpenAI, Achiam, J., Adler, S., Agarwal, S., Ahmad, L., Akkaya, I., Aleman, F.L., Almeida, D., Altenschmidt, J., Altman, S., Anadkat, S., Avila, R., Babuschkin, I., Balaji, S., Balcom, V., Baltescu, P., Bao, H., Bavarian, M., Belgum, J., Bello, I., Berdine, J., Bernadett-Shapiro, G., Berner, C., Bogdonoff, L., Boiko, O., Boyd, M., Brakman, A.-L., Brockman, G., Brooks, T., Brundage, M., Button, K., Cai, T., Campbell, R., Cann, A., Carey, B., Carlson, C., Carmichael, R., Chan, B., Chang, C., Chantzis, F., Chen, D., Chen, S., Chen, R., Chen, J., Chen, M., Chess, B., Cho, C., Chu, C., Chung, H.W., Cummings, D., Currier, J., Dai, Y., Decareaux, C., Degry, T., Deutsch, N., Deville, D., Dhar, A., Dohan, D., Dowling, S., Dunning, S., Ecoffet, A., Eleti, A., Eloundou, T., Farhi, D., Fedus, L., Felix, N., Fishman, S.P., Forte, J., Fulford, I., Gao, L., Georges, E., Gibson, C., Goel, V., Gogineni, T., Goh, G., Gontijo-Lopes, R., Gordon, J., Grafstein, M., Gray, S., Greene, R., Gross, J., Gu, S.S., Guo, Y., Hallacy, C., Han, J., Harris, J., He, Y., Heaton, M., Heidecke, J., Hesse, C., Hickey, A., Hickey, W., Hoeschele, P., Houghton, B., Hsu, K., Hu, S., Hu, X., Huizinga, J., Jain, S., Jain, S., Jang, J., Jiang, A., Jiang, R., Jin, H., Jin, D., Jomoto, S., Jonn, B., Jun, H., Kaftan, T., Łukasz Kaiser, Kamali, A., Kanitscheider, I., Keskar, N.S., Khan, T., Kilpatrick, L., Kim, J.W., Kim, C., Kim, Y., Kirchner, J.H., Kiros, J., Knight, M., Kokotajlo, D., Łukasz Kondraciuk, Kondrich, A., Konstantinidis, A., Kosic, K., Krueger, G., Kuo, V., Lampe, M., Lan, I., Lee, T., Leike, J., Leung, J., Levy, D., Li, C.M., Lim, R., Lin, M., Lin, S., Litwin, M., Lopez, T., Lowe, R., Lue, P., Makanju, A., Malfacini, K., Manning, S., Markov, T., Markovski, Y., Martin, B., Mayer, K., Mayne, A., McGrew, B., McKinney, S.M., McLeavey, C., McMillan, P., McNeil, J., Medina, D., Mehta, A., Menick, J., Metz, L., Mishchenko, A., Mishkin, P., Monaco, V., Morikawa, E., Mossing, D., Mu, T., Murati, M., Murk, O., Mély, D., Nair, A., Nakano, R., Nayak, R., Neelakantan, A., Ngo, R., Noh, H., Ouyang, L., O’Keefe, C., Pachocki, J., Paino, A., Palermo, J., Pantuliano, A., Parascandolo, G., Parish, J., Parparita, E., Passos, A., Pavlov, M., Peng, A., Perelman, A., de Avila Belbute Peres, F., Petrov, M., de Oliveira Pinto, H.P., Michael, Pokorny, Pokrass, M., Pong, V.H., Powell, T., Power, A., Power, B., Proehl, E., Puri, R., Radford, A., Rae, J., Ramesh, A., Raymond, C., Real, F., Rimbach, K., Ross, C., Rotsted, B., Roussez, H., Ryder, N., Saltarelli, M., Sanders, T., Santurkar, S., Sastry, G., Schmidt, H., Schnurr, D., Schulman, J., Selsam, D., Sheppard, K., Sherbakov, T., Shieh, J.,

- Shoker, S., Shyam, P., Sidor, S., Sigler, E., Simens, M., Sitkin, J., Slama, K., Sohl, I., Sokolowsky, B., Song, Y., Staudacher, N., Such, F.P., Summers, N., Sutskever, I., Tang, J., Tezak, N., Thompson, M.B., Tillet, P., Tootoonchian, A., Tseng, E., Tuggle, P., Turley, N., Tworek, J., Uribe, J.F.C., Vallone, A., Vijayvergiya, A., Voss, C., Wainwright, C., Wang, J.J., Wang, A., Wang, B., Ward, J., Wei, J., Weinmann, C., Welihinda, A., Welinder, P., Weng, J., Weng, L., Wiethoff, M., Willner, D., Winter, C., Wolrich, S., Wong, H., Workman, L., Wu, S., Wu, J., Wu, M., Xiao, K., Xu, T., Yoo, S., Yu, K., Yuan, Q., Zaremba, W., Zellers, R., Zhang, C., Zhang, M., Zhao, S., Zheng, T., Zhuang, J., Zhuk, W., Zoph, B.: GPT-4 Technical Report (2024). <https://arxiv.org/abs/2303.08774>
- [49] OpenAI: Learning to Reason with LLMs. <https://openai.com/index/learning-to-reason-with-llms/>. Accessed: 2024 (2024)
- [50] Anthropic: Claude 3.7 Sonnet and Claude Code. <https://www.anthropic.com/news/claude-3-7-sonnet>. Accessed: 2025 (2025)
- [51] DeepSeek-AI, Guo, D., Yang, D., Zhang, H., Song, J., Zhang, R., Xu, R., Zhu, Q., Ma, S., Wang, P., Bi, X., Zhang, X., Yu, X., Wu, Y., Wu, Z.F., Gou, Z., Shao, Z., Li, Z., Gao, Z., Liu, A., Xue, B., Wang, B., Wu, B., Feng, B., Lu, C., Zhao, C., Deng, C., Zhang, C., Ruan, C., Dai, D., Chen, D., Ji, D., Li, E., Lin, F., Dai, F., Luo, F., Hao, G., Chen, G., Li, G., Zhang, H., Bao, H., Xu, H., Wang, H., Ding, H., Xin, H., Gao, H., Qu, H., Li, H., Guo, J., Li, J., Wang, J., Chen, J., Yuan, J., Qiu, J., Li, J., Cai, J.L., Ni, J., Liang, J., Chen, J., Dong, K., Hu, K., Gao, K., Guan, K., Huang, K., Yu, K., Wang, L., Zhang, L., Zhao, L., Wang, L., Zhang, L., Xu, L., Xia, L., Zhang, M., Zhang, M., Tang, M., Li, M., Wang, M., Li, M., Tian, N., Huang, P., Zhang, P., Wang, Q., Chen, Q., Du, Q., Ge, R., Zhang, R., Pan, R., Wang, R., Chen, R.J., Jin, R.L., Chen, R., Lu, S., Zhou, S., Chen, S., Ye, S., Wang, S., Yu, S., Zhou, S., Pan, S., Li, S.S., Zhou, S., Wu, S., Ye, S., Yun, T., Pei, T., Sun, T., Wang, T., Zeng, W., Zhao, W., Liu, W., Liang, W., Gao, W., Yu, W., Zhang, W., Xiao, W.L., An, W., Liu, X., Wang, X., Chen, X., Nie, X., Cheng, X., Liu, X., Xie, X., Liu, X., Yang, X., Li, X., Su, X., Lin, X., Li, X.Q., Jin, X., Shen, X., Chen, X., Sun, X., Wang, X., Song, X., Zhou, X., Wang, X., Shan, X., Li, Y.K., Wang, Y.Q., Wei, Y.X., Zhang, Y., Xu, Y., Li, Y., Zhao, Y., Sun, Y., Wang, Y., Yu, Y., Zhang, Y., Shi, Y., Xiong, Y., He, Y., Piao, Y., Wang, Y., Tan, Y., Ma, Y., Liu, Y., Guo, Y., Ou, Y., Wang, Y., Gong, Y., Zou, Y., He, Y., Xiong, Y., Luo, Y., You, Y., Liu, Y., Zhou, Y., Zhu, Y.X., Xu, Y., Huang, Y., Li, Y., Zheng, Y., Zhu, Y., Ma, Y., Tang, Y., Zha, Y., Yan, Y., Ren, Z.Z., Ren, Z., Sha, Z., Fu, Z., Xu, Z., Xie, Z., Zhang, Z., Hao, Z., Ma, Z., Yan, Z., Wu, Z., Gu, Z., Zhu, Z., Liu, Z., Li, Z., Xie, Z., Song, Z., Pan, Z., Huang, Z., Xu, Z., Zhang, Z., Zhang, Z.: DeepSeek-R1:

Incentivizing Reasoning Capability in LLMs via Reinforcement Learning (2025). <https://arxiv.org/abs/2501.12948>

- [52] Bubeck, S., Chandrasekaran, V., Eldan, R., Gehrke, J., Horvitz, E., Kamar, E., Lee, P., Lee, Y.T., Li, Y., Lundberg, S., Nori, H., Palangi, H., Ribeiro, M.T., Zhang, Y.: Sparks of Artificial General Intelligence: Early experiments with GPT-4 (2023). <https://arxiv.org/abs/2303.12712>
- [53] Ouyang, L., Wu, J., Jiang, X., Almeida, D., Wainwright, C., Mishkin, P., Zhang, C., Agarwal, S., Slama, K., Ray, A., Schulman, J., Hilton, J., Kelton, F., Miller, L., Simens, M., Askill, A., Welinder, P., Christiano, P.F., Leike, J., Lowe, R.: Training language models to follow instructions with human feedback **35**, 27730–27744 (2022). <https://doi.org/10.48550/arXiv.2203.02155>
- [54] Messick, C., Blackburn, K., Brady, P., Brockill, P., Cannon, K., Car-iou, R., Caudill, S., Chamberlin, S.J., Creighton, J.D.E., Everett, R., Hanna, C., Keppel, D., Lang, R.N., Li, T.G.F., Meacher, D., Nielsen, A., Pankow, C., Privitera, S., Qi, H., Sachdev, S., Sadeghian, L., Singer, L., Thomas, E.G., Wade, L., Wade, M., Weinstein, A., Wiesner, K.: Analysis framework for the prompt discovery of compact binary mergers in gravitational-wave data. *Phys. Rev. D* **95**, 042001 (2017). <https://doi.org/10.1103/PhysRevD.95.042001>